Simulation and Optimization of Wet Double Clutch Transmission (DCT)

Von der Fakultät für Maschinenbau
der Technischen Universität Carolo-Wilhelmina zu Braunschweig
zur Erlangung der Würde
eines Doktor-Ingenieurs (Dr.-Ing.)
genehmigte Dissertation

von:	Mohammad Adhitya
aus (Geburtsort):	Jakarta, Indonesien

eingereicht am:	22. Februar 2016
mündliche Prüfung am:	14. November 2016

Gutachter:	Prof. Dr.-Ing. F. Küçükay
	Prof. Dr.-Ing. P. Eilts

2016

Schriftenreihe des Instituts für Fahrzeugtechnik
TU Braunschweig

Band 48

Mohammad Adhitya

Simulation and Optimization of Wet Double Clutch Transmission (DCT)

Shaker Verlag
Aachen 2016

Bibliographic information published by the Deutsche Nationalbibliothek
The Deutsche Nationalbibliothek lists this publication in the Deutsche Nationalbibliografie; detailed bibliographic data are available in the Internet at http://dnb.d-nb.de.

Zugl.: Braunschweig, Techn. Univ., Diss., 2016

Printed in Germany.

ISBN 978-3-8440-4938-1
ISSN 1619-6325

Shaker Verlag GmbH • P.O. BOX 101818 • D-52018 Aachen
Phone: 0049/2407/9596-0 • Telefax: 0049/2407/9596-9
Internet: www.shaker.de • e-mail: info@shaker.de

Vorwort

Diese Arbeit entstand während meiner Zeit als Gastwissenschaftlicher am Institut für Fahrzeugtechnik (IfF) der Technischen Universität Braunschweig mit einem Stipendium von Indonesische Regierung (beasiswa DIKTI).

Die Arbeit wurde von Herrn Prof. Dr.-Ing. F. Küçükay, Leiter des Instituts für Fahrzeugtechnik der Technischen Universität Braunschweig betreut. Für die engagierte Betreuung und Unterstützung danke ich ihm sehr herzlich. Weiterhin gilt mein Dank Herrn Prof. Dr.-Ing. P. Eilts, Leiter des Instituts für Verbrennungskraftmaschinen der Technischen Universität Braunschweig, für die Übernahme der Gutachter sowie Herrn Prof. Dr.-Ing. J. Köhler, Leiter des Instituts für Thermodynamik der Technischen Universität Braunschweig, für die Übernahme des Vorsitzes im Promotionsausschuss.

Bei den Mitarbeitern des Instituts für Fahrzeugtechnik möchte ich mich für die gute Zusammenarbeit und ihre außerordentliche Hilfsbereitschaft bedanken. Insbesondere geht mein Dank an Dr.-Ing. T. Kassel, Dr.-Ing. A. Plötner, Dr.-Ing. R. Mustafa für die vielen anregenden Gespräche sowie Herrn Dr.-Ing. G. Alvermann und Frau S. Engelhardt, M.A., für das hohe Engagement beim Korrekturlesen dieser Arbeit und Dr.-Ing. B. Weiler für die tatkräftige Unterstützung.

Bei dem Dozenten des Maschinenbau Departemen Universitas Indonesia möchte ich mich für die unterstutzung bedanken. Insbesondere geht mein Dank an Prof. Dr. Budiarso, Prof. Dr. M. I. Alhamid, Prof. Dr. R. A. Koestoer, Prof. Dr. R. Danardono, Prof. Dr. B. Sugiarto, Prof. Dr. Yanuar, Prof. Dr. Y. S. Nugroho, Prof. Dr. Harinaldi, Prof. Dr.-Ing. N. S. Putra, Dr. W. Nirbito, Dr. H. D. S. Budiono, Dr.-Ing. Nasruddin, Dr. G. Kiswanto, Dr. A. S. Baskoro, Dr. Y. Whulanza, Herr H. T. Wibowo, M.T. und Herr R. Irwansyah, M.T..

Bei der Indonesischen Familie in Braunschweig möchte ich mich für die unterstutzung bedanken. Insbesondere geht mein Dank an Dr.-Ing. H. S. Wasisto, Herrn. R. Brahmana, Herrn Grohmann und Herrn. A. Y. Putera.

Ein großer Anteil am Erfolg dieser Arbeit gebührt meinem privaten Umfeld. Hierbei richte ich einen besonderen Dank an meine Eltern, die mich stets unterstütz und seit meiner Kindheit das Interesse an der Fahrzeugtechnik gefördert haben. Abschließend danke ich meiner liebe Frau Dilla und meine alle Kinder Salsabiila, Assyifa und Faza dafür, dass sie mich immer motiviert und mir somit für den nächsten Arbeitstag das nötige Kraftgegeben hat.

Braunschweig, November 2016 Mohammad Adhitya

Simulation and Optimization of Wet Double Clutch Transmission (DCT)

by Mohammad Adhitya

Abstract

This work focused on the longitudinal 7-speed wet DCT that is used by some high performance sport cars due to its capability to handle high rpm and torque output engine. This capability is coming from the use of wet friction clutch which able to dissipate more heat generated by high torque engine in slipping clutch during engagement process. Although the wet DCT has many advantages, it still needs further development to increase its efficiency and use ability. One of inefficiency comes from the use of clutch fluid which tends to stick the clutch pairs, causing the drag torque when the fluid sheared by the clutch pair that rotates with different speed after the gear preselects action. The other drawback is occurred in the manual shift mode when the next gear that automatically preselected by the TCU before the gear shift is unmatched to the next gear as wished by the driver. As explained, these both drawback is strongly related with the conventional strategy of gear preselect action in wet DCT.

The research was done to overcome the explained wet DCT drawback by improving the gear preselect action strategy so-called the seamless gear preselect strategy. This new strategy is achieved by improving the software of control algorithm rather than the DCT hardware for cost efficiency through software in the loop (SiL) method. This new strategy was achieved by simultaneously activate the gear preselect action during the fast filling phase of the ongoing clutch hydraulic system. In manual shift mode, the gear preselect is done after the driver perform the gear shift by pull/push the shift stick or paddle to eliminate the possibility of wrong gear being preselected or prepared. By this strategy, the TCU does not have to exercise the algorithm to predict the driver's wish for up/down shift. Furthermore, the new gear preselect strategy make the reduction of unnecessary drag torque that normally occurs in wet DCT after gear preselect action in steady condition.

The state of the art focusing on the subject of DCT construction, empiric system modeling, objectification and optimization method that were presented using a simulation environment to prepare the virtual gear shift optimization. Afterward, the full vehicle drivetrain model is developed using Matlab-Simulink and –Simscape. The model includes the engine, dual clutch, synchronizer, vehicle's resistance and transmission mechatronic module. The complete model simulation including the shift quality was compared with the measurement data from the real vehicle for validation and to guarantee the model fidelity. After the model is fully confirmed, the optimization of wet DCT gear shift using genetic algorithm method was explained to meet the optimization objectives including the shift qualities, the uninterrupted torque during gear shifting and the limited heat generated as a losses energy. Ten control parameters were given as an input to model to control the power shift in dual clutch. Furthermore, the vehicle acceleration during gear shifting as a simulation results was assessed to get the shift spontaneity and shift comfort score through objectification method. Moreover, the model simulation for optimization has one more addition input to activate the dog clutch synchronizer engagement as a gear preselect action beside the previous ten input control parameter.

The new gear preselect strategy is superior particularly for manual gear shift mode. The proposed strategy was carefully prepared in regards to the capability of the particular wet DCT construction particularly the hydraulic valve and gear shift actuator structure, while this optimization was done on the software basis alone without any further modification on the hardware. The optimization result confirmed the new gear preselect strategy is possible to be adapted in the particular seven speed wet DCT.

Simulation und Optimierung die nassen Doppelkupplungsgetriebe (DKG)

von Mohammad Adhitya

Kurzfassung Die Arbeit hatte ihren Schwerpunkt auf dem 7-Gang-nassen-DKG für Längsmotoren, welches von einigen Hochleistungssportwagen genutzt wird aufgrund dessen Fähigkeit, hochdrehenden und drehmomentstarken Motoren standhalten zu können. Diese Fähigkeit liegt begründet in der Verwendung einer nass Doppelkupplung, die mehr Hitze abführen kann, welche in einem drehmomentstarken Motor durch Rutschkupplung beim Einkuppeln entsteht. Obwohl der Nass-DKG viele Vorteile hat, sind weitere Entwicklungen nötig, um dessen Effizienz und Nutzungsmöglichkeiten zu steigern. Eine der Ineffizienzen beruht auf der Nutzung von Kupplungsflüssigkeit. Diese neigt dazu, die Kupplungspaare zusammenzukleben, welches ein Schleppmoment verursacht, weil das gescherte Öl des Kupplungspaares nach der Gangvorwahl mit einer veränderten Geschwindigkeit rotiert. Der weitere Nachteil liegt im manuellen Schalten, wenn der Gang, welcher automatisch von der TCU vorgewählt wurde, nicht dem vom Fahrer gewünschten Gang entspricht.

Die Forschung wurde durchgeführt, um den geschilderten Nachteil der Nass-DKG zu eliminieren durch den Gangvorwahl Strategie verbessert die nahtlose-Gangvorwahl Strategie sogenannte. Diese neue Strategie wird dadurch erreicht, indem lediglich der Kontrollalgorithmus verbessert werden musste, und nicht etwa die DKG-Hardware, zum kosteneffizienten Zweck durch die Software in the loop (SiL)-Methode. Diese neue Strategie wurde durch gleichzeitig erreicht das Gangvorwahl während der schnellen Füllphase der laufenden Kupplung Hydrauliksystem aktivieren. Im manuellen Schaltbetrieb wird die Gangvorwahl vorgenommen, sobald der Fahrer den Schaltknüppel entsprechend bedient, um die Möglichkeit zu beseitigen, das ein falscher Gang vorgewählt oder wird. Durch diese Strategie muss die TCU nicht den Algorithmus durchlaufen, der zur Vorhersage des nächsten Schaltwunsches des Fahrers nötig ist. Darüber hinaus machen die neue Gangvorwahl Strategie, um die Reduzierung unnötiger Schleppmoment, das in nassen DKG erfolgt in der Regel nach dem Gangvorwahl Aktion im stationären Zustand

Der Stand der Technik in Bezug auf Fokussierung auf die Themen DKG-Konstruktion, empirisches Modellierungssystem, Versachlichung und Optimierung wurde während einer Simulation vorgestellt, um die virtuelle Gang-Auswahl vorzubereiten. Im Anschluss wird der gesamte Antriebsstrang mit Matlab-Simulink und –Simscape entwickelt. Nachdem das Modell vollständig bestätigt war, wurde die Optimierung des Schaltvorgangs vom nassen DKG durch genetische Algorithmus-Verfahren erläutert, um die Optimierungsziele einschließlich Schaltqualitäten, ununterbrochenem Drehmoment beim Gangwechsel und begrenzter Wärmeerzeugung als Energieverlust zu erreichen. Zehn Kontrollparameter dienten dem Modell als Input, um die Lastschaltung in einer Doppelkupplung zu kontrollieren. Weiterhin wurde die Fahrzeugbeschleunigung während der Gangwechsel als Simulationsergebnis bewertet, um die Spontanitäts- und Schaltkomfortwerte durch eine Objektivierungsmethode zu erhalten. Darüber hinaus Die Modellsimulation für die Optimierung hat neben den zehn Kontrollparametern einen weiteren zur Aktivierung der Klauenkupplung Synchronisierer Einkupplung als Getriebevorwahl.

Das neue Gangvorwahl-Strategie überlegen ist besonders für den manuellen Gangschaltmodus. Die vorgeschlagene Strategie wurde im Hinblick auf die Fähigkeit der Sieben-Gang-nassen-DKG-Konstruktion, insbesondere des Hydraulikventils und der Gangschaltungsaktuator-Struktur, gewählt, während die Optimierung allein auf Softwarebasis ohne jegliche weitere Änderung an der Hardware durchgeführt wurde. Das Optimierungsergebnis hat bestätigt, dass die neue Gangvorwahl-Strategie geeignet ist zur Anwendung in der Sieben-Gang-nassen-DKG.

Contents

Variable, Parameter and Abbreviation Lists

Latin Alphabet

Symbol	Unit	Remarks
A_C	[m^2]	Clutch surface area
A_{cl}	[m^2]	Port/orifice closing area
A_{op}	[m^2]	Port/orifice opening area
A_P	[m^2]	Effective clutch piston area
A_S	[m^2]	Cylinder area
$A_{Vehicle}$	[m^2]	Vehicle frontal area
b	[m]	Width of the synchronizer cone contact surface
C_D	[-]	Discharge coefficient
c_D	[-]	Vehicle aerodynamic drag coefficient
c_{RS}	[m]	Radial clearance
c_v	[-]	Discharge coefficient of the valve orifices
D_{CV}	[m]	Orifice diameter
D_S	[m]	Cylinder diameter
d_P	[$N.s/m$]	Damping coefficient of piston
d_s	[$N.s/m$]	Damping coefficient
d_s	[$N.s/m$]	Damping coefficient of valve spool
E	[N/m^2]	Fluid bulk modulus
F_A	[N]	Synchronizer axial force
$F_{Air\ Drag}$	[N]	Vehicle air resistance
$F_{Centrifugal}$	[N]	Centrifugal force
$F_{Clutch\ Disc}$	[N]	Drag force due to the clutch disc stiffness
$F_{Damping}$	[N]	Damping force
$F_{Friction}$	[N]	Friction force
$F_{Initial}$	[N]	Initial mechanical spring force caused by the spool spring preload
$F_{magnetic}$	[N]	Magnetic force
F_N	[N]	Clutch normal force
F_{Piston}	[N]	Clutch piston force
F_R	[N]	Clutch friction force
$F_{Road\ Gradient}$	[N]	Road gradient resistance force
$F_{Rolling}$	[N]	Rolling resistance
F_{Spring}	[N]	Spring force
f_R	[-]	Rolling resistance coefficient
g	[m/s^2]	Gravitation acceleration
I	[A]	Electric current
I_{FW}	[kgm^2]	Synchronizer freewheeling inertia
$I_{Vehicle}$	[kgm^2]	Vehicle inertia
$i_{magnetic}$	[A]	Electric current

Symbol	Unit	Remarks
k_p	[N/m]	Spring stiffness of clutch piston
k_s	[N/m]	Spool spring stiffness constant
m_p	[Kg]	Clutch piston mass
m_s	[Kg]	Valve spool mass
$m_{Vehicle}$	[Kg]	Vehicle mass
P_{CV}	[N/m^2]	Hydraulic pressure in control volume
P_{EX}	[N/m^2]	Exhaust pressure
P_P	[N/m^2]	Clutch piston pressure
P_S	[N/m^2]	Solenoid pressure
p_C	[N/m^2]	Clutch pressure
p_s	[N/m^2]	Supply pressure
p_t	[N/m^2]	Oil sump tank pressure
p_v	[N/m^2]	Output pressure
Q_{con}	[m^3/s]	Volume flow rate losses through the seals and hydraulic lines
Q_{ct}	[m^3/s]	Volume flow rate out of the system through a small discharge orifice
Q_{net}	[m^3/s]	Hydraulic flow rate
Q_{ov}	[m^3/s]	Volume flow rate out of the system when reaching the max pressure
Q_{pm}	[m^3/s]	Volume flow rate caused by the piston movement
R	[M]	Orifice radius
R^2	[-]	Coefficient of determination
R^2_{adj}	[-]	Adjusted coefficient of determination
R_C	[M]	Effective clutch radius
R_C	[M]	Synchronizer cone mean radius
R_I	[M]	Synchronizer chamfer pitch radius
R^2_{new}	[-]	New coefficient of determination
$R^2_{y\|x_1,x_2,\ldots.}$	[-]	Coefficient of determination
r_{c1o}	[M]	Clutch outer radius
r_{c1i}	[M]	Clutch inner radius
r_i	[M]	Friction lining outer radius
r_m	[M]	Friction lining mean radius
r_o	[M]	Friction lining inner radius
r_{Tire}	[M]	Tyre radius
r_{xy}	[-]	Correlation coefficient
T_B	[$N.m$]	Synchronizer chamfer torque
T_C	[$N.m$]	Synchronizer cone torque
T_C	[$N.m$]	Clutch torque
T_D	[$N.m$]	Synchronizer drag torque
T_F	[$N.m$]	Synchronizer gear tooth friction torque
T_{SF}	[$N.m$]	Synchronizer shaft drag torque
T_W	[$N.m$]	Synchronizer gear windage torque

Symbol	Unit	Remarks
$V_{Air\ Relative}$	[*m/s*]	Relative velocity surrounding air movement
V_0	[m^3]	Initial hydraulic volume
X_0	[*M*]	Minimum sleeve displacement for synchronizer cone contact
x_S	[*M*]	Synchronizer sleeve displacement
x_j	[-]	Independent variables
x_s	[*M*]	Valve spool displacement
$x_{s\,min}$	[*M*]	Valve spool rest position
$x_{s\,max}$	[*M*]	Valve spool maximum displacement position
$\dot{x}_s$	[*M*]	Valve spool speed
$\ddot{x}_s$	[*m/s*]	Valve spool acceleration
x_{sl}	[*M*]	Sleeve displacement
x_P	[*M*]	Travel distance of clutch piston
$\dot{x}_P$	[*m/s*]	Speed of clutch piston
$\ddot{x}_P$	[m/s^2]	Acceleration of clutch piston
y_i	[-]	Endogenous variables
$\widehat{y_i}$	[-]	Multiple linear regression
z	[-]	Number of clutch pairings

Greek Alphabet

Symbol	Unit	Remarks
α	[-]	Road gradient angle
α_{FW}	[rad/s^2]	Angular acceleration of freewheeling component
β	[-]	Synchronizer chamfer angle
β	[N/m^2]	Bulk modulus
β	[-]	Regression coefficients
δ	[-]	Decay constant
ε	[-]	Deviation
μ_f	[-]	Clutch coefficient of friction
μ_I	[-]	Friction coefficient of the synchronizer chamfer
ρ_{oil}	[kg/m^3]	Oil density
$\sigma^2_{\hat{y}}$	[-]	Explained model variance
σ^2_y	[-]	Total variance
$\sigma^2_{\hat{\varepsilon}}$	[-]	Residual variance
$\varphi_{magnetic}$	[*volt.sec.*]	Magnetic flux
ω_e	[*rad/s*]	Engine rotational speed
ω_{CL}	[*rad/s*]	Synchronizer clutch slip speed
ω_0	[*rad/s*]	Natural angular frequency
ω_S	[*rad/s*]	Synchronizer cone slip speed

Abbreviation

Abreviation	Remarks
ABS	Anti-Lock Braking System
ACC	Adaptive Cruise Control
AMG	Aufrecht, Melcher and Großaspach (High Performance Division of Mercedes-Benz)
AMT	Automated Manual Transmission
AP	Automotive Product
AT	Automatic Transmission
ATZ	Automobiltechnische Zeitschrift (English: Automobile Technical Magazine)
BMW M	Bayerische Motoren Werke Motorsport
BTL	Break Through the Load
CAD	Computer Aided Design
CAE	Computer Aided Engineering
CAN	Controller Area Network
CVT	Continuously Variable Transmission
CV-C1	Control Valve Clutch 1
CV-G1	Control Valve Gear 1
DCI	Double Clutch Inline
DCT	Double Clutch Transmission
DoE	Design of Experiment
DSG	Direct Shift Gearbox
ECU	Engine Electronic Controller
ESP	Electronic Stability Programme
ETI	Engine Torque Intervention
FF	Fast Filling
GV1	Gear Valve 1
HiL	Hardware in the Loop
MV	Manifold Valve
MT	Manual Transmission
PRV-C1	Pressure Regulator Valve Clutch 1
PRV-G1	Pressure Regulator Valve Gear 1
RBF	Radial Basis Function
RMS	Root Mean Square
RMSE	Root Mean Square Error
SiL	Software-in-the-Loop
SQ	Shift Quality
TCU	Transmission Electronic Controller
VDV	Vibration Dose Value
VW	Volkswagen

1 Introduction

Global warming and constantly increasing gas price have created new trends in the automotive industry towards low emissions and low fuel consumption by downsizing and down-speeding the engine using boost technology and automatic transmission for both hybrid and non-hybrid vehicles [30]. Automatic transmissions play since they make sure that the engines work in an economical engine speed range in any driving situation, which can be achieved by automatically selecting the suitable gear ratio. Moreover, this strategy even obtains better results with high, wide spread-gear ratios, which can be provided by using either stepless transmissions (i.e. continuously variable transmission (CVT)) or step transmissions (i.e. automatic transmissions (AT), automated manual transmissions (AMT), and double-clutch transmissions (DCT)). They make shifting more comfortable. In addition, automatic transmissions for full hybrid vehicles also ensure smooth shifting from electric motor to combustion engine and vice versa. This is almost impossible to be done even by the most talented driver with manual transmission. For a driver assistance system (e.g. cruise control system), gear shifting has to be independent in order to work without driver involvement, which can be achieved by using automatic transmissions. Due to those reasons, automatic transmissions will undoubtedly become more important in the future [132].

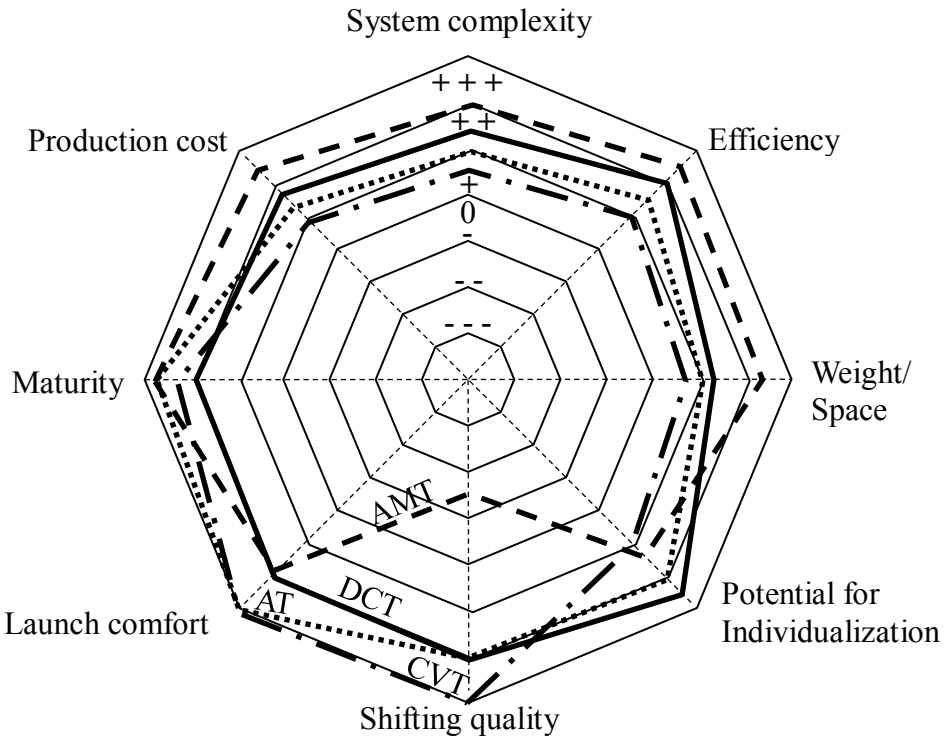

Figure 1.1: Comparison of AT, AMT, CVT and DCT [107].

The automatic transmissions was at first meant to reduce the tasks for the driver rather than to increase the fuel efficiency [97] by automatically selecting the suitable gear ratios in any driving situation, providing a high level of comfort and using a torque converter that makes it possible to stop the vehicle while the engine is still running. Due to its practical use, the automatic transmission is even recommended for older people with regard to safe driving and the quality of their mobility [113, 123]. The shift comfort is achieved by a planetary gear set up with several friction clutches to control the speed of the planetary gear set. Nowadays, however, when the efficiency also has to be considered in the system design, the later generation of automatic transmission systems (i.e. AMT and DCT) based on robust constructions of MT due to the fact that a friction clutch has a higher efficiency than a torque converter [98]. Moreover, the number of engaged gears for those AMT and DCT systems is lower than that for ATs, which may lead to an increase in mechanical efficiency. In this case, the CVT is not included because it does not use gears as a transmission mechanism. Regardless of the higher efficiency produced by the friction clutch, this method still needs a complicated control strategy to provide the same level of comfort in launch and creep as naturally found in a torque converter. Nevertheless, this drawback mechanism of the friction clutch can be considered as an advantage for its manufacturers. Therefore, the torque converter in AT is replaced with a friction clutch to have several launch options[1].

The DCT, which is the latest automatic transmission technology entering the modern vehicle market, has several advantages compared to other automatic transmission systems as shown in Figure 1.1. In general, the DCT exhibits good mechanical efficiency. In terms of efficiency, only the AMT that is outperformed the DCT. Moreover, by having a double clutch design which provides power shifts from odd to even gears or vice versa, the DCT can obtain gear shifting as smooth as the AT. Regardless of its superiority in performance, the DCT can still be further improved because the technology is relatively new compared to the other transmission systems, particularly in terms of stop-go, launch, creep and gear shifting.

1.1 Background and Objectives

DCTs have become more popular over the years due to their advantages (i.e. no torque interruption during gear shifting, low fuel consumption, high comfort, and possible combination with a driver assistance system for improved driving safety) as shown in Figure 1.2. The global DCT market is expected to reach 7.15 million units by 2018, with Europe being the market leader followed by Asia-Pacific and North America [94].

[1] Daimler-AMG have replaced the torque converter in their automatic transmission with friction clutch to have several launch options for their Mercedes AMG [98].

Despite the competition with other transmission systems including AT and the MT, the DCT promises growth potential in the near future. Major automotive manufacturers have adapted the DCT to their products to produce high performance and eco-friendly vehicle models. Some transmission and vehicle manufacturers have invested a lot in the respective research, development and production facilities to meet the growing demand for transmission technologies in the global automotive market [99].

Furthermore, all those advantages of DCTs are supported by the robust construction design, which is very similar to that of MTs. Due to the integrated transmission control unit (TCU), the DCT system can not only enhance the car's efficiency (i.e. fuel consumption and emissions), but also dynamics, shift spontaneity and comfort. DCTs have not only been used in entry-level cars, but also in several high-end sports cars.

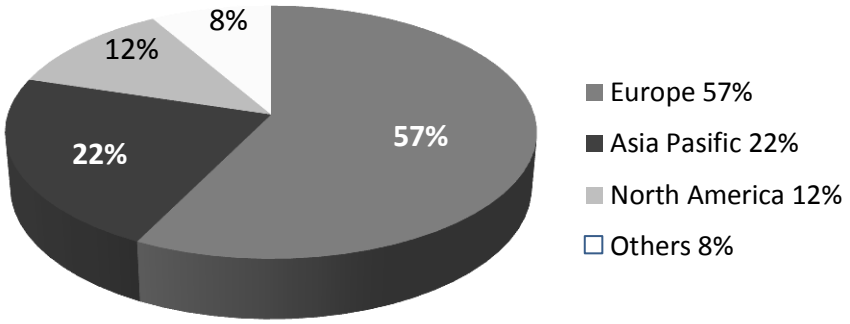

Figure 1.2: Market share prediction of DCT by Geography in 2018 [94].

Even though the DCT is similar in design to the MT, it has different method in term of gear shifting. DCT uses its double clutch to change the gear ratio through clutch-to-clutch power shiftting from odd to even gears or vice versa, which is similar to the AT which make no torque interruption during gear shifting. Before gear shifting takes place (i.e. torque transmission changes from closed to open clutch), the intended next gear should be engaged with the open clutch first through the synchronizer system (i.e. gear preselection, which is done automatically in most DCT systems). This preselection gives inefficiency in wet DCTs since the open clutch rotates faster/slower than the clutch pack casing, shearing the clutch oil causing the clutch viscous drag. The preselection shows another weakness in terms of manual shift mode when the transmission control unit (TCU) preselect the next gear which not desired by the driver. To overcome this issue, some DCT manufacturers provide manual gear preselect, where the next gear is selected manually by the driver before gear shifting (i.e. Pre-cog system) [95].

DCT has a modular design for reasons of cost effeciency and assembly. It has three separated hardware units consisting of a double clutch pack, a mechatronics unit and a gearbox. As a complex system, an improvement of the DCT efficiency can be achieved by either improving the software system as a relatively easy and low-cost method or by changing the DCT hardware component that is considerably expensive. Therefore, this work attempts to increase the DCT efficiency by improving the software control through model simulation as a low-cost method.

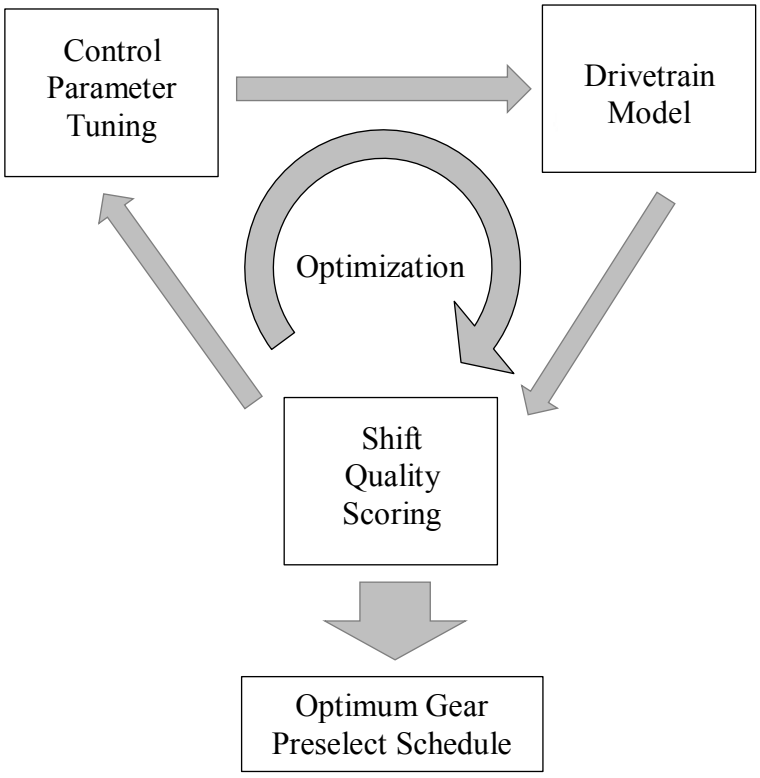

Figure 1.3: Optimization of gear preselection during gear shifting to increase wet DCT efficiency with the help of objective scoring and model simulation.

The quality of DCT gear shifting can be adjusted in the same manner as that of the AT by assuming that the gear is preselected just before the gears are shifted. Although its synchronizer system is also a friction clutch system with build-in dog clutch, the TCU cannot control the synchronizer in the same way as the double clutch due to the lack of sensor (i.e. the sensor of the synchronizer system is only for its engagement status). However, in this research, an alternative approach for gear shifts in wet DCTs and simultaneous gear preselection through model simulation is introduced, as shown in Figure 1.3. This method is used to maintain an acceptable level of uninterrupted torque during gear shift as well as spontaneity and comfort. Therefore, the objectives of this research are as follows:

1. Developing a drivetrain model for the software-in-the-loop (SiL) environment,
2. Optimizing the gear preselection during gear shift to increase wet DCT efficiency and use ability,
3. Implementing the objective scoring of gear shift quality.

1.2 Outline

First chapter explains briefly how the objective will be achieved. The focus of this research is mainly on the quality of wet DCT gear shifting, which is done simultaneously with the gear preselection. The chapter ends with ideas on how to improve the gear shifting strategy in the automatic shift mode as well as in manual shift mode with regard to gear preselection.

Chapter Two describes the state of the art of DCT systems including design and working principle (i.e. gear preselection with clutch-to-clutch gear shift) followed by system modelling and objective scoring. Furthermore, the optimization methods using a genetic algorithm will be explained in this section. In addition, the previous researches in the area of automatic transmissions that are used as references in this thessis are acknowledged.

Chapter Three explains the concept of wet DCTs, particularly focusing on the longitudinal seven-speed wet DCT analyzed in this thesis, covering clutch, shaft arrangement, synchronizer system for gear engagement and mechatronic module including sensors, actuators and electro-hydraulic valve.

Chapter Four illustrates the drivetrain model used in the SiL environment, which consists of engine, gearbox, synchronizer, vehicle resistance and electro-hydraulic system including the shift element. Moreover, a verification of the model concludes this section.

Chapter Five focuses on the objective evaluations of the shift quality, including shift comfort, gear shift event, calculation of characteristic parameters, subjective evaluation, determination of objective scores as well as shift spontaneity and calculation of weighting function. The chapter ends with the description of the influence of clutch friction on shift quality.

Chapter Six will discuss the optimization of DCT gearshifts through SiL simulation in detail on the optimization of gear preselection activation time, which includes the influence of clutch friction on the shift quality using the genetic algorithm method. Finally, the results will be summarized in chapter Seven.

2 State of the Art

This chapter illustrates the state of the art of double clutch transmission (DCT), including the history and the concept of DCTs. First, the structure, function and operation of dual clutch transmissions are described, particularly in the uninterrupted torque during gear shifting regarding to the clutch-to-clutch shifting and gear preselection concerning the design of DCT. Afterward, the modelling method is explained followed by the objectification process to quantify the shift quality including shift comfort and shift spontaneity and, finally, the results of literature research.

The history of the double clutch transmission (DCT) started when Adolphe Kégresse introduced the concept in 1940. In 1980, an automotive company named Automotive Products (AP) developed the first DCT prototype, which was installed in Ford Fiesta Mk1, Ford Ranger and Peugeot 205. The gearshift control system was completely based on an analogue/discrete digital circuit. The DCT concept was further explored in motorsports by Porsche and Audi in the eighties. Porsche introduced the “Porsche Doppelkupplungsgetriebe” (abbreviated as PDK or DCT in English), which was used in the Porsche 956 and 962 Le Mans race cars, while Audi used the DCT in their Audi Sport Quattro S1 rally car. The DCT has a significant advantage in motorsports due to its ability to up-shift at full throttle without interruption of traction, therefore resulting in very fast gear shifting. That advantage was achieved by further development of the electronic transmission control and improvements in hydraulics and mechanical systems. Although the DCT had been used in motorsports since the eighties, it did not enter the global automotive market before 2003. Volkswagen was the first manufacturer to introduce a DCT in that year, the “Direct Shift Gearbox” (DSG) DQ250, which was installed in the VW Golf Mk4 R32.

2.1 Double Clutch Transmission

In terms of the structure, the DCT is a merging of two manual transmissions which are well known for their robust design, as shown in Figure 2.1. The DCT uses two separate clutches for the different gears. The first clutch is for the odd gears (i.e. 1^{st}, 3^{rd}, 5^{th} and 7^{th} gear) and the second for the even gears (i.e. 2^{nd}, 4^{th}, and 6^{th} gear). The DCT clutches are connected to their respective gears through a synchronizer system that is similar to the one used by manual transmission (MT). In order to work properly, DCTs use an intelligence system to control the actuator mechanism through the electro-hydraulic system. Therefore, the gears in a DCT can be shifted automatically. However, most of the DCTs still provide a manual gear shift mode, which is preferred by the enthusiast drivers.

Based on the shaft layout, there are two types of DCT available: the first type uses two countershafts (as shown in Figure 2.1) and the second one only one countershaft. DCTs with two countershafts are usually used for front wheel drive vehicles with transverse engine. The DCT with one countershaft, is usually used for rear wheel drive vehicles with a longitudinal engine layout.

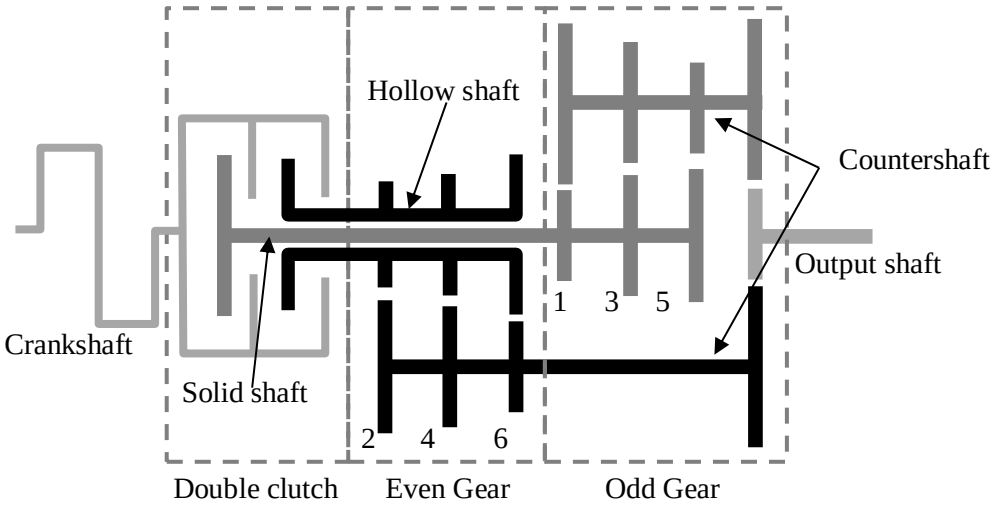

Figure 2.1: DCT design with two countershafts.

DCT can be further classified based on the type of clutch used: dry clutch and wet clutch. A wet clutch is designed for high engine torque (i.e. engine torque above 350 Nm) since a clutch immersed in oil can dissipate more of the heat generated during the clutch engaging process to minimize the clutch pad wear and therefore extend the gearbox lifetime. However, a wet clutch DCT also has some disadvantages compared to the dry clutch DCTs, e.g. it needs more energy to pump the clutch lubrication oil.

Based on the clutch installation, there are two different DCT clutch arrangements. The first type shows side-by-side clutches when viewed from the perpendicular side, with both clutches having a similar size (as shown in Figure 2.1). This arrangement is uasually used for dry DCTs with two single-plate dry clutches. The second arrangement type is a concentric clutch type, with both clutches posisitioned at the same plane. This makes one clutch noticeably larger than the other. This concentric clutch arrangement is usually used for wet DCTs.

2.1.1 Clutch-to-Clutch Shift

The DCT gear shifting is perform by transferring the engine torque from one engaged clutch (off-going clutch) to the other, disengage clutch (on-going clutch) while simultaneously creating uninterrupted engine torque shift similar to those in planetary gear automatic transmission (AT), which is known as clutch-to-clutch shifting or overlap shift. Basically,

there are four shift modes to the load torque on the clutch. The first and second modes are the traction-up and traction-down shifts, where the torque on the engine-side clutch is larger than that on the output-side clutch. Furthermore, the third and fourth modes are the trailing mode-up and trailing mode-down shifts, where the torque on the engine-side clutch is lower than that on the output-side clutch. The tractions up-shift, however, is the most difficult situation among the modes, particularly from the 1st to the 2nd gear due to higher engine torque transfer from one clutch to other.

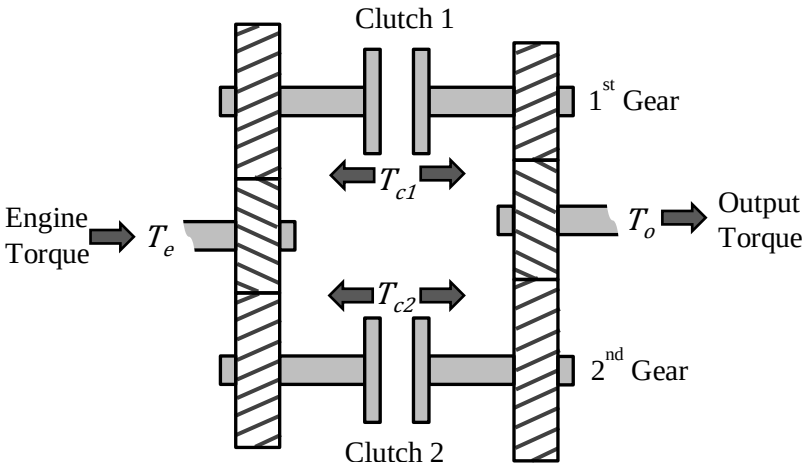

Figure 2.2: Diagram of a DCT.

Basically, the TCU is programmed for two groups of four gear shifting modes due to the similarities of the sequences. The first group consists of the tractions-up and trailing mode-down shift, which is also known as active shifting, indicated by the reduction of the engine torque during gear ratio changes to the new synchronized to final speed. The second group, i.e. trailing mode-up and tractions-down shift, on the other hand, the engine runs independently to the new synchronous speed and referred to a passive gear shifting. The comparison of overlap phases and the gear ratio changes between passive and active gear shifting are in the reverse order.

Figure 2.2 represents a simple DCT design to explain the overlap shift by using the simple traction upshift from 1st to 2nd gear as an example. Furthermore, Figure 2.3 illustrates the overlap shift phase, showing engine speed, output shaft torque as well as torque and pressure of both double clutches [10]. The transmission control unit (TCU) tries to implement these curves in Figure 2.3 using the clutch pressure and transmission shaft sensors. In order to create the torque curve as shown in Figure 2.3, the clutch pressure control valves must be controlled by the transmission control unit. Furthermore, the clutch-to-clutch shift is explained as follows:

The first phase is a stationary phase where the 1st gear is fully connected to the engine and the engine torque is transferred from the engine through this off-going clutch 1 (clutch torque T_{C1}) to the output shaft.

The second phase is a fast fill phase where the up-shift process is started at t_1, characterized by the rise of the gearshift signal, which results in the TCU controling the electric hydraulic valve and therefore the double clutch. Moreover, the clutch pressure of the on-going clutch 2 increases to prepare for the overlap phase while the clutch pressure on the off-going clutch 1 starts to decrease.

The third phase is an overlap phase where the load from the off-going clutch 1 is transferred to the on-going clutch 2, which is characterized by a constant increase in the pressure on the clutch 2 while at the same time the pressure on clutch 1 decreases to a minimum level. Furthermore, the engine torque is only transmitted to clutch 2 (clutch torque T_{C2}) at the end of the phase.

The fourth phase is a gear ratio change phase, characterized by the sliding of clutch 2 while it has different speed with the engine speed. The pressure on the clutch 2 is now increased to reduce the speed difference. From t_3, the engine speed is brought to the level of the 2nd gear ratio (lower engine rpm). In this phase, the energy of the rotational inertia stored in the engine is released as additional torque, resulting in a significant increase in the output torque. To compensate the increase in the output torque, the engine control unit (ECU) reduces the engine torque (i.e. by adjusting the ignition timing) to avoid an increase in the transmission output torque. Since this phase has a significant influence on the shift quality, the shift quality is measured in this phase.

To determine the necessity of the clutch pressure (p_C) for the gear shifting, the TCU uses the following simplified formula [130]:

$$T_C = p_C . A_C . \mu_f . R_C . z \tag{2.1}$$

Where the torque transmitted by the clutch T_C basically depends on the clutch pressure (p_C) only since the other clutch parameters are known quantities. (i.e. clutch surface area (A_C), effective clutch radius (R_C), number of clutch pairings (z) and the coefficient of friction (μ_f)). A map of the change in the speed dependent of the friction coefficient (μ_f) of the clutch pad disc as shown in Figure 3.4 is also taken into account by the control unit. Therefore, after the gear ratio change phase, the clutch pressure (p_C) has to be at least as high as the transmitted engine torque to guarantee that the clutch is fully engaged without any slip.

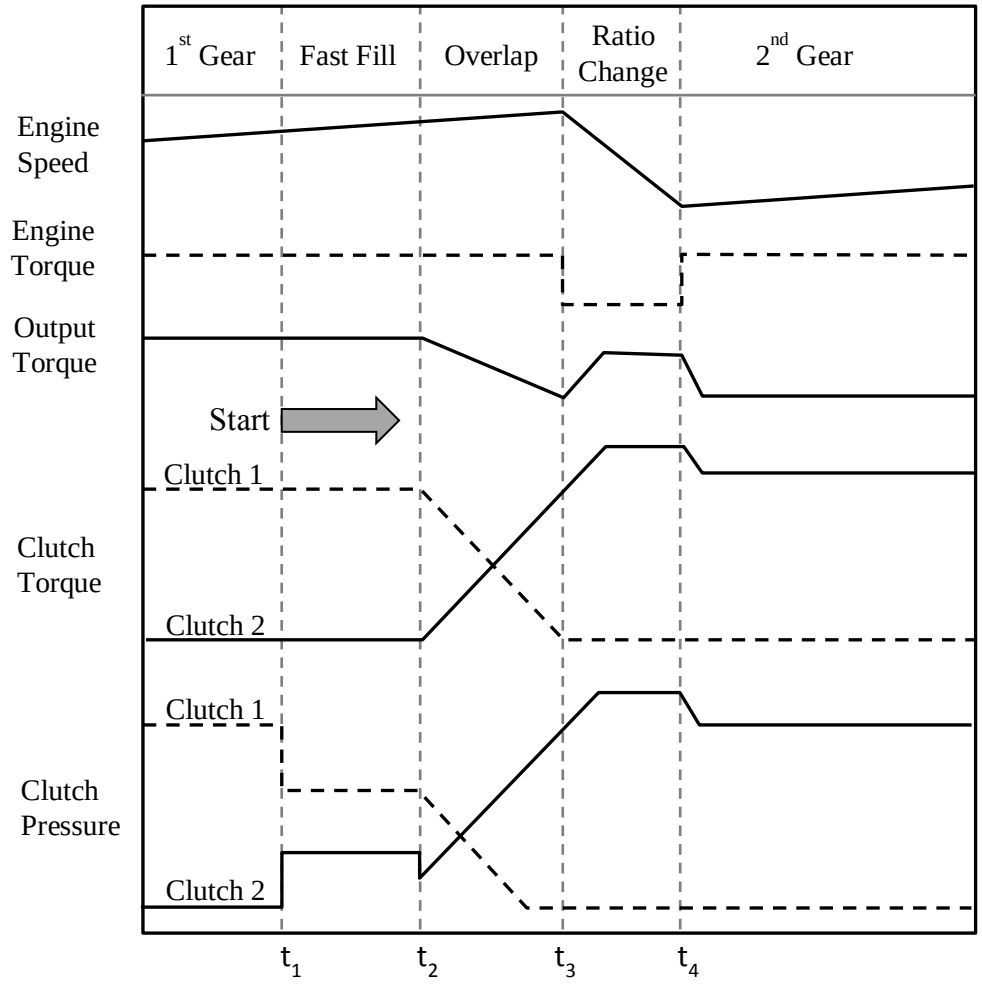

Figure 2.3: The tractions-up shift process [10].

At t_4, the 2nd gear is now fully connected, denoted by the match of the engine speed with the 2nd gear. Furthermore, the engine torque intervention ends and the pressure on clutch 2 is further increased. Moreover, the pressure on the clutch 1 is reduced to the pressure level in the fluid reservoir. When this phase is completed, the transmission control switches again to the stationary mode, in which the pressures are set to the torque, depending on the load that carried by the engaging clutch as specified in Equation 2.1.

2.1.2 Gear Preselection

Gear preselection can be defined as the gear engagement process of one constant mesh gear pairs to the on-going clutch through the synchronizer system before gear shifting. This method guarantees that the on-going clutch is ready to receive the engine torque from the off-going clutch and to simultaneously transmitting it to the wheel with the new gear ratio. Each clutch can only be engaged with just one gear at a time. Furthermore, only one of the double

clutches can be engaged to the engine in order to avoid serious gearbox damage. In most DCTs, gears are automatically preselected before the gears are shifted by the DCT system without the driver being involved. However, automatic gear preselection could cause some problems in the manual shift mode if the gear automatically preselected by the DCT system does not match the next gear desired by the driver, which results in longer shifting time. To overcome this problem, some DCTs use manual gear preselection or pre-cog method, in a manual shift mode. Manual gear preselection means that the driver manually preselects the next gear before gear shifting to guarantee the correct gear has been preselected. This method, however, increase the driver task load.

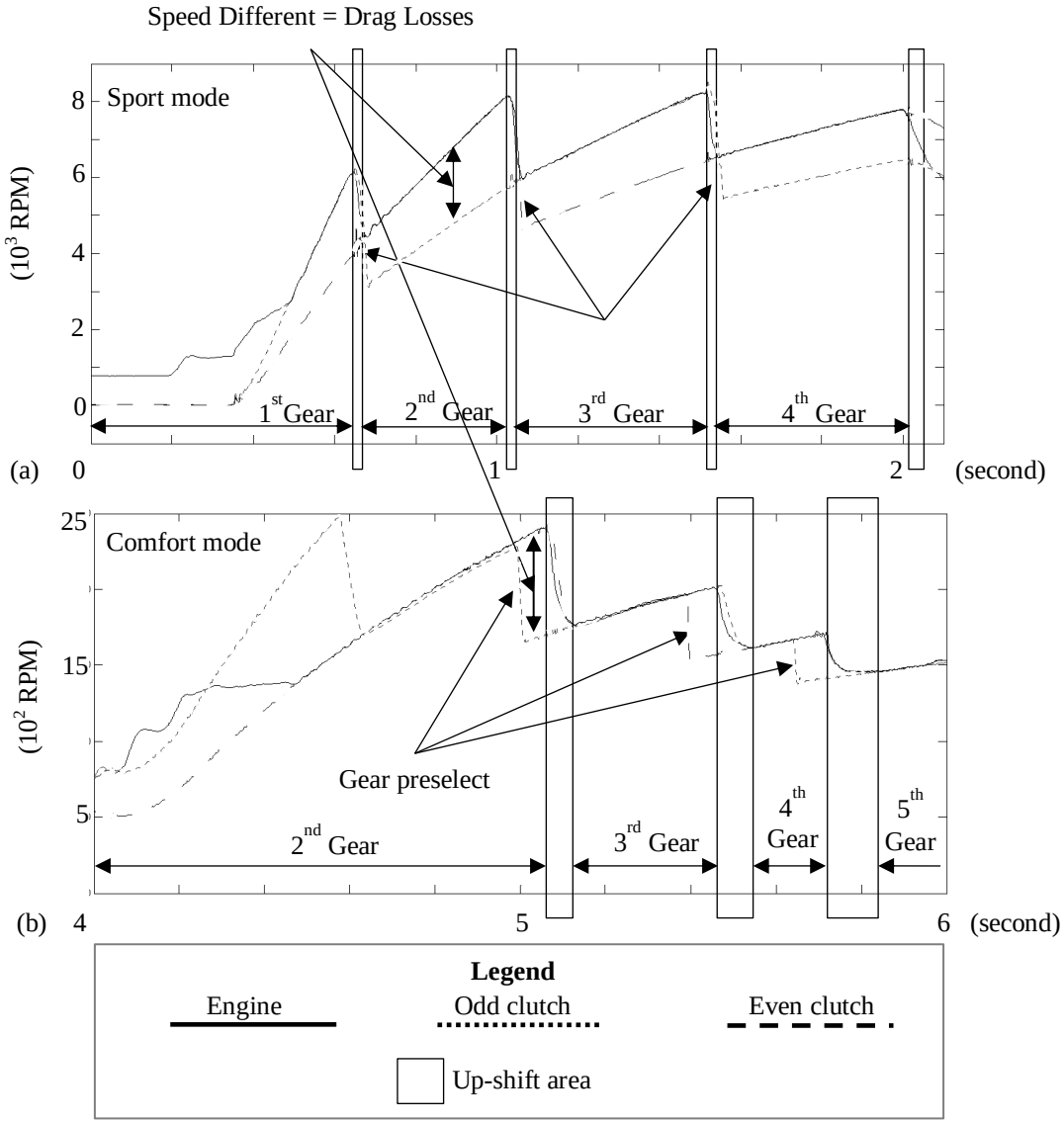

Figure 2.4: Measured rotational speeds of engine, odd clutch, and even clutch for (a) sporty driving mode and (b) comfort driving mode.

Figure 2.4 shows the measured results of the rotational speeds of the engine, odd and even clutch in a sporty and comfort driving modes. The figure clearly shows that gear shifting in the sporty mode occurs with higher engine rpm and a shorter shifting time than that in the comfort mode. The different gear shifting times are intended to be used for different purposes. The shorter shifting time is well suited for the sporty mode due to the quick response of the gear shifting. In the comfort mode, on the other hand, the longer shift time in reduces the shift jerk. Moreover, the open clutch will stick and rotate together with clutch pack before the gear is preselected in the comfort driving mode, as shown in Figure 2.4(b). After the preselection, the open clutch will rapidly change its rotational speed to be either higher or lower than that of the clutch pack to prepare for the upcoming shift, i.e. upshift or downshift. The different gear preselection strategies for both the sporty and the comfort driving mode are also depicted in Figure 2.4. In the sporty mode, the gear is preselected only after the gear shifting has been finished to reduce the next gear shift time. This is different to the comfort mode where the gear preselection takes place before the gear shifting. Comparing these two methods reveals that the drag losses occurring in the sporty driving mode in terms of the strategy for gear preselect are higher than in the comfort driving mode due to the extended sliding clutch time.

2.1.3 Electronic Transmission Control System

The modern automatic transmission consists of sensors and electro-hydraulic valves the electronic control unit needs to accomplish its function. Modern electronic control systems are able to control complex systems such as modern automatic transmissions including DCTs. The DCT uses a mechatronics module consisting of the transmission control unit (TCU), sensors and electro-hydraulic valves to actuate the gear fork selector and double clutch piston in order to control the shifting process as shown in Figure 2.5.

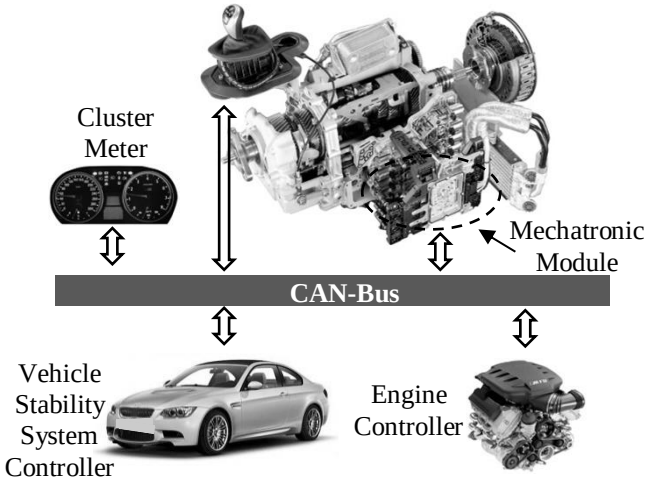

Figure 2.5: The structure of DCT electronic control system.

For cost savings in manufacturing and assembly, a modular system (i.e. gearbox module, double clutch module and mechatronics module) is used in DCTs since it is more compact and more reliable when compared to the previous design of the electro-hydraulic system usually found in planetary gear automatic transmissions (AT).

The TCU communicates with the other control unit systems via a Controller Area Network (CAN) bus. The interaction to the other control unit is for example to the Engine Control Unit (ECU) to control the engine torque during active gear shift. The other control unit connected to the TCU is the vehicle stability control unit (Electronic Stability Program or ESP), which controls the wheel traction to avoid sudden load changes in critical driving situations - particularly in an active mode of the Adaptive Cruise Control (ACC). The TCU is also connected to the peripheral system or cluster meter, which provides the driver with information about the current vehicle condition, and also to the shift stick or shift paddles module used by the driver to select the driving mode or to manually shift the gears.

The information exchange between TCU and other control unit is as a measured signal found in the transmission and vehicle system (i.e. vehicle speed, wheel speed, etc.) to decide which actions should be executed. The TCU furthermore controls the electro-hydraulic valve which in turn actuates the fork gear selector to preselect the gear and also the double clutch piston to ensure all the required double clutch pressures are set.

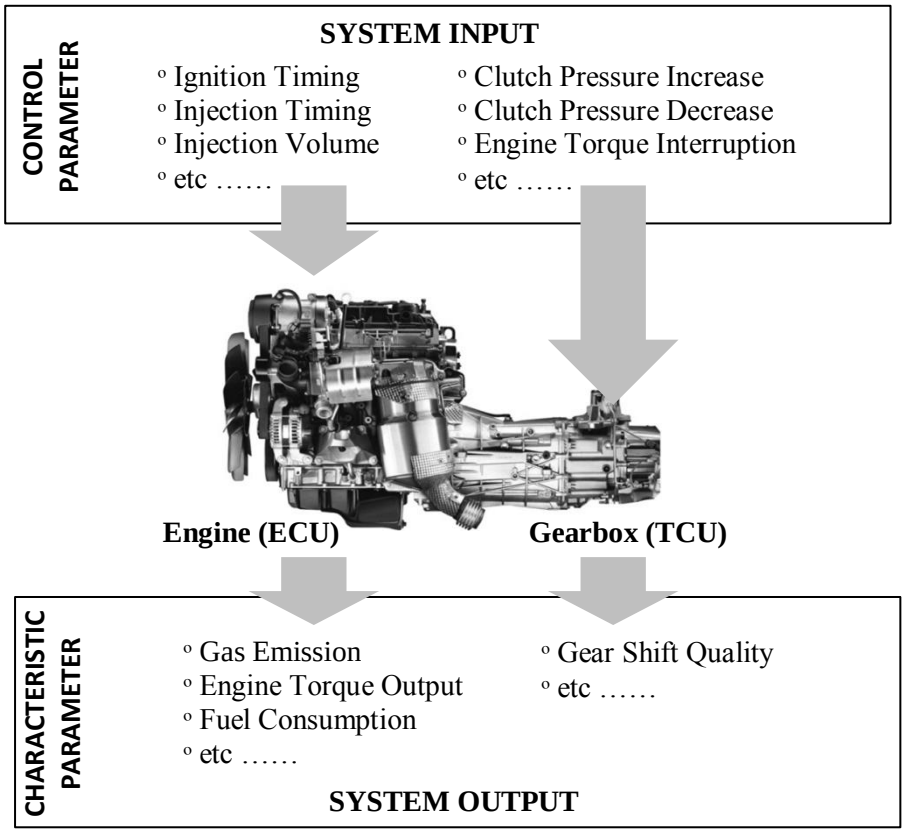

Figure 2.6: Interaction between ECU and TCU in vehicle drivetrain system [10].

Furthermore, the vehicle drivetrain performance (i.e. wheel traction, shifting quality, fuel consumption, etc.) is as an output of the control parameter input given by ECU and TCU. The control parameter input for the engine, including the ignition timing, injection timing, fuel volume, etc., affects the engine torque, fuel consumption and gas emission. On the other hand, the control parameter input for the transmission consisting of shifting schedule and clutch pressure also affects the performance of the transmission system (e.g. shifting quality and driveability) as shown in Figure 2.6. The system performance can be modified depending on the control parameters provided by ECU and TCU. This means, the tuned or improved control parameter will improve the system performance.

By using transmission control parameters for automatic transmissions, those parameters can be tuned or adjusted with regard to the 3D-parameter space, which consist of “driver”, “driving environs” and “driven vehicle”. In automatics transmissions there are at least two aspects can be further improved: First, the improvement of the gearshift schedule strategy which primarily concerns the optimization of the engine operating point selection in terms of fuel consumption, exhaust emission characteristics and output power demanded by the driver. Second, the improvement that concerns to the shifting process by adjusting the gear shifting control parameter related to the shifting quality parameters.

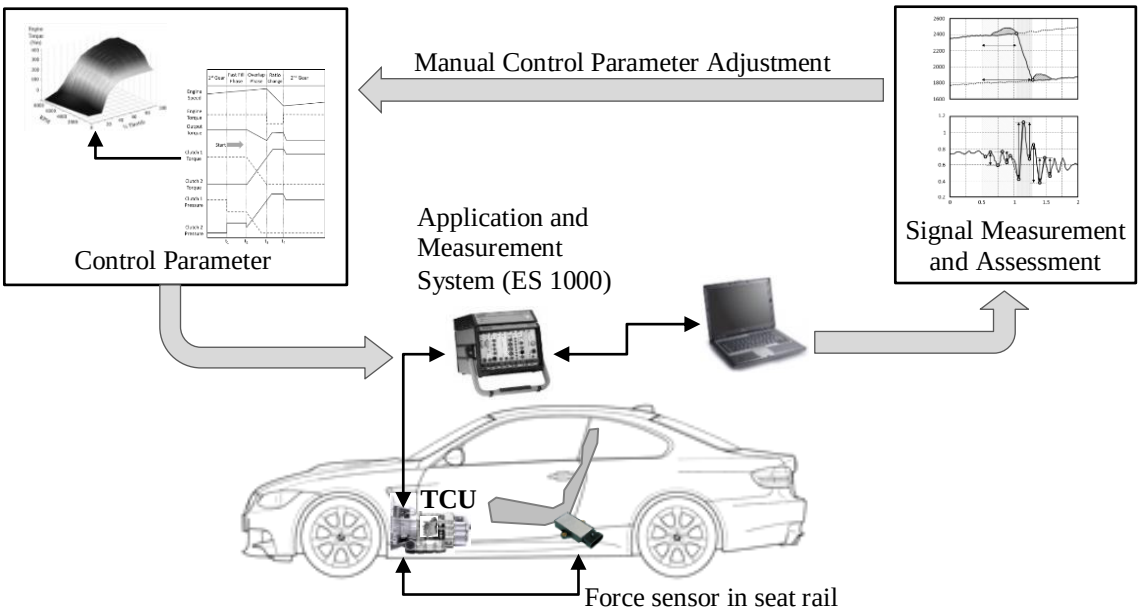

Figure 2.7: Tuning process of control software to improve the gear shifting.

One of the common procedures for transmission tuning process in general is done manually during tests on the public roads or test tracks as shown in Figure 2.7. The test driver drives the vehicle to reach the operating points and adjusts the gear shifting. The measurement system records all relevant signals (i.e. vehicle speed and acceleration) during gear shifting and the calibration system evaluates the results, including speeds, torques, control of the involved

shifting elements and also internal transmission calculation and longitudinal vehicle acceleration. Based on the measured signals and a subjective assessment of the acceleration curve, the test driver makes a subjective evaluation of the gearshift. He adjusts it to comply with the specifications provided by rating tables, such as the ATZ[2]-rating scale (see Table 5.2).

2.2 Modelling

A model is an image of reality - usually in form of a mathematical or physical model - which is used to better understand a system in order to be able to make some predictions about the system. There are three types of modelling approaches, depending on the prior knowledge of the system: white- box, black- box and grey- box modelling. The white- box model is used if the main influencing factors and the internal structure of the system are well known and the modelling is built through logical deterministic models. The black- box model, on the other hand, is used when the system performance is largely unknown or difficult to identify. The gray- box model, however, is combination of white and black- box models to represent systems where only certain parts of the systems are known.

The choice of the model type depends on several factors, such as [10]:

- cost of model creation,
- time and effort required for the parameterization,
- required accuracy and the model error
- need for traceability and
- required computation time.

The empirical modelling based on a statistical experimental design is a tool that is often used in the industry. In the field of vehicle technology, it has become the standard to calibrate the software program. The application of transmission control parameters in the past few years is an area of research that carried out and this type of modelling, in combination with an optimization process, is used to increase the efficiency.

After the model has been created, the further step is validating the model simulation result with experimental data. Due to the highly nonlinear performance, that task is very challenging. If the physical system is well known (i.e. white- box modelling), the validation process is normally used to find the constant value of the model. The process that can be used to optimize the model validation is a genetic algorithm that is discussed in the Chapter 2.4.

[2] ATZ is an acronym of “Automobiltechnische Zeitschrift” or ‘automobile technical magazine’ in English. It is a German specialist journal for technology-oriented management in the automotive industry.

2.3 Objectification

Objectification is a mathematical correlation between the subjective feeling of the driver or passenger and objective characteristic parameters. Therefore, it is important to know the customer expectations on the shifting quality based on the rating of the customer's subjective feeling (see, [18, 43, 51, 58]). The goal of objectification is to find a mathematical correlation between the subjective assessment of the vehicle occupants with respect to events occurring during driving (vibrations, noise, acceleration, etc.) and measureable physical conditions in order to derive objective, measurable parameters.

The objectification process is shown in Figure 2.8. The evaluation of the input and output parameters felt by the customer or test driver lead to a subjective score. In the automotive industry, a scale of 1 to 10 is often used as a subjective score, where each grade describes the perception (see Table 5.2). Furthermore, the measurement on the vehicle is also attempting to determine the characteristic parameters that seem potentially useful to establish a basis for an objective assessment. Moreover, the relationship between the measured characteristic parameters and the given subjective score are derived from various mathematical procedures. This process ends with a model which is based on measurements to perform an objective evaluation. The main advantages of the objectification model are a constant assessment quality and increased availability. Since the model is not necessarily dependent on measurements, it is particularly used in simulation calculations.

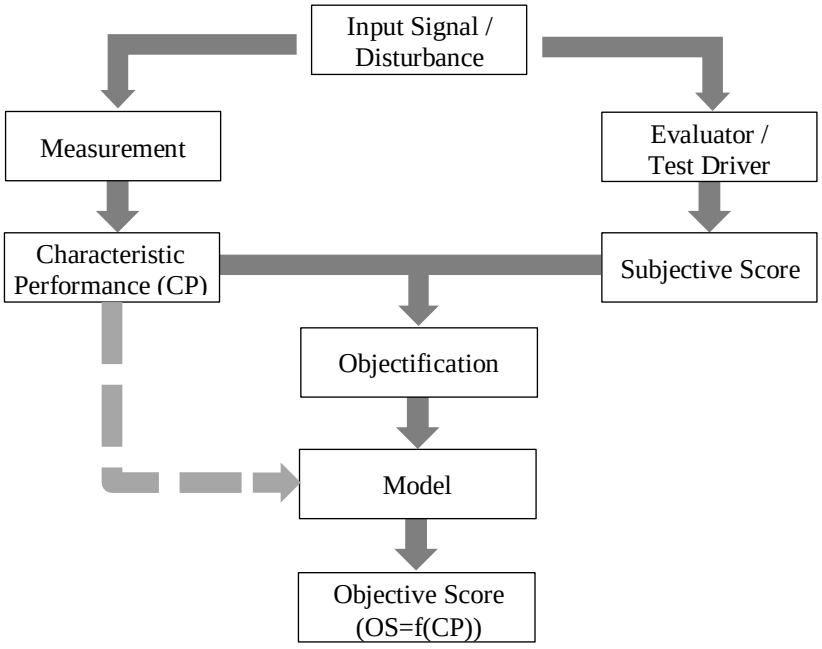

Figure 2.8: The objectification process [10].

Furthermore, the model is evaluated by how well it can reproduce the relationships between characteristic parameters and subjective score. In order to obtain a larger validity range of the model, a sufficient spread of the characteristic parameter values must be provided. At the same time, a uniform distribution is also important, otherwise the connection of higher order cannot be mapped. After performing the subjective scoring, statistical analysis and processing of the data is generally required. The correlation and regression analysis are important tools that provide information about the degree of a linear relationship between characteristic parameters and subjective score.

2.3.1 Correlation Analysis

The correlation analysis measures the relationship between pairs of items. The correlation coefficient (r_{xy}) as a resulting value has a range value between minus one and plus one ($-1 \leq r_{xy} \leq 1$). The linear relationship is achieved if the value of the correlation coefficient (r_{xy}) is equal to 1 which means that changes in the independent item will result in an identical change in the dependent item. On the other side, the linear relationship is in the opposite direction if (r_{xy}) is equal to -1, which means that changes in the independent item will result in -an identical change in the dependent item, but the change will be in the opposite direction. Furthermore, a correlation coefficient (r_{xy}) of zero means there is no relationship between both items and that a change in the independent item will have no effect on the dependent item.

In a two-dimensional data analysis, the correlation coefficient is calculated for a normally distributed population (x, y) of the sample with n feature pairs (x, y) [69] as follow:

$$r_{xy} = \frac{cov(x,y)}{\sigma_x . \sigma_y} = \frac{\sum_{i=1}^{n}(x_i - \bar{x}) . (y_i - \bar{y})}{\sqrt{\sum_{i=1}^{n}(x_i - \bar{x})^2 . \sum_{i=1}^{n}(y_i - \bar{y})^2}} \tag{2.2}$$

$\bar{x}, \bar{y}$ = average of the characteristics

x_i, y_i = series of value for i = 1, 2, ..., n

n = number of pairings

In the objectification, the feature combinations consist of the objective (as measurable characteristic parameters) and the subjective score. It evaluates several subjects in the same events, assuming a normal distribution of the correlation analysis before averaging the characteristic parameters to generate the subjective scores.

2.3.2 Multiple Linear Regression Analysis

The correlation analysis described above is used to identify a linear relationship. In general, we need to objectify more than just an explanatory variable for an adequate description of the functional relationship with the subjective score. Here, we use the multiple linear regression analysis, looking for a functional relationship between a dependent variable ($y_i \; and \; k$) and independent variables (x_j). Generally, a linear model is assumed as the following equation:

$$\hat{y}_i = \beta_0 + 1 \sum_{j=1}^{k} \beta_j . x_{ij} + \varepsilon_i \tag{2.3}$$

The aim of a multiple linear regression analysis is to estimate the regression coefficients (β), so that the deviation (ε) between the observed endogenous variables (y_i) and the calculated values from the model ($\hat{y}_i$) is as small as possible. The minimization of least squares method is used for this task.

Furthermore, the quality of the model is described using the coefficient of determination ($R^2_{y|x_1,x_2,\ldots.}$) that indicates the ratio of the explained model variance ($\sigma^2_{\hat{y}}$) to the total variance (σ^2_y) as the following equation [69, 78]:

$$R^2_{y|x_1,x_2,\ldots.} = \frac{\sigma^2_{\hat{y}}}{\sigma^2_y} \tag{2.4}$$

While the total variance (σ^2_y) is the sum of the modes by the explained model variance ($\sigma^2_{\hat{y}}$) and the variance of the residual ($\sigma^2_{\hat{\varepsilon}}$) as following equation:

$$\sigma^2_y = \sigma^2_{\hat{y}} + \sigma^2_{\hat{\varepsilon}} \tag{2.5}$$

$$\underbrace{\frac{1}{n}\sum_{i=1}^{n}(y_i - \bar{y})^2}_{\text{total variance}} = \underbrace{\frac{1}{n}\sum_{i=1}^{n}(\hat{y}_i - \bar{y})^2}_{\text{explained variance}} + \underbrace{\frac{1}{n}\sum_{i=1}^{n}(y_i - \hat{y})^2}_{\text{residual variance}} \tag{2.6}$$

If the value of $R^2_{y|x_1,x_2,\ldots.}$ = 1, all values lie on the regression line. However, if value of $R^2_{y|x_1,x_2,\ldots.}$ is not significantly different from zero, the model does not provide a sufficient explanation for the investigated context.

The regression coefficients are determined from a certain system of equations. The more explanatory variables are included in the system of equations will result in the less data material represents their estimate at the disposal. Finally, if the number of coefficients equals the number of observations, there will be no statistical estimation, but a calculation. Regardless of the explanatory variables, the coefficients may be determined so that an accurate solution of the equation system is present. In such a case, the coefficient of determination has the value of 1. Therefore, it is useful to include the number of explanatory

variables in the calculation of the adjusted coefficient of determination. The adjusted coefficient of determination (R^2_{adj}) is calculated by:

$$R^2_{adj} = 1 - \frac{\sigma^2_{\hat{\varepsilon}}/(n-p-1)}{\sigma^2_y/(n-1)} = 1 - \frac{(n-1)}{(n-p-1)}.(1-R^2) \tag{2.7}$$

The adjusted coefficient of determination (R^2_{adj}) continues for a coefficient of determination (R^2) to the value of 1. However, it carries out the fact that fewer observations and degrees of freedom for estimating the coefficients of determination will be removed, if the number of degrees of freedom due to the parameters used in the model is lower, and the adjusted coefficient of determination tends to be worse. The adjusted coefficient of determination (R^2_{adj}) therefore increases only when the new coefficient of determination (R^2_{new}) rises accordingly by the addition of a further declarant parameter as follow:

$$R^2_{new} \overset{!}{>} \frac{1-(n-p_{new}-1).R^2_{old}}{(n-p_{new})} \tag{2.8}$$

R^2_{old} = the coefficient of determination without the additional model parameters

p_{new} = the number of new model parameters

For further explanations, please see [69] and [79].

2.4 Genetic Algorithm for Optimization

The genetic algorithm is a method for solving both constrained and unconstrained optimization problems that are based on natural selection that drives biological evolution. Genetic algorithms can be applied to solve a variety of optimization problems that are not well suited for standard optimization algorithms, including problems in which the objective function is discontinuous, non-differentiable, stochastic, or highly nonlinear. The genetic algorithm can address problems of mixed integer programming, where some components are restricted to be integer-valued.

While based on natural selection as in biological evolution, the genetic algorithm uses three main types of rules at each calculation step to create the next generation from the current population. The first rule is the selection rule which selects the individuals, called parents, that contribute to the population for the next generation. Typically, the algorithm is more likely to select parents that have better fitness values. The second rule is the crossover rule, which combines two parents to form children for the next generation, enabling the algorithm to extract the best genes from different individuals and recombine them into potentially superior children. The third rule is the mutation rule, which applies random changes to individual

parents to form children, adding to the diversity of a population and thereby increasing the likelihood that the algorithm will generate individuals with better fitness values.

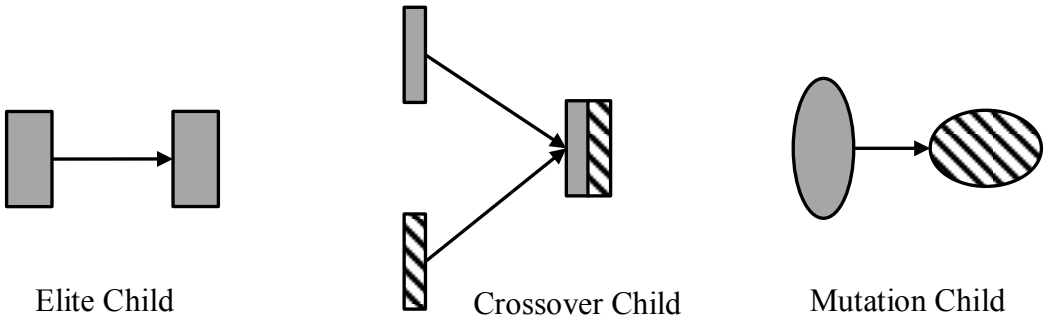

Figure 2.9: Schematic diagram illustrating the three types of children [104].

There are three types of children that are created by the genetic algorithm for the next generation as shown in Figure 2.9. The first type is called elite children, individuals in the current generation with the best fitness values. These individuals automatically survive to the next generation. The second type is called crossover children which are created by selecting vector entries, or genes, from a pair of individuals in the current generation and combining them to form a child. The last type is called mutation children, which are created by applying random changes to a single individual in the current generation to create a child.

2.5 Results of Literature Research

Based on the literature research, the studies of DCTs generally focus on four aspects: DCT modelling and simulation used for further optimization of the system, optimization of the DCT shifting quality with regard to the clutch design (i.e. dry or wet clutch), DCT efficiency improvement regarding its components (i.e. synchronizer system and oil pump) and DCT control strategy. However, due to the similarity between DCT and planetary gear automatic transmission (AT) in terms of clutch-to-clutch shift performance and evaluation of the shift quality, the literature related to the AT is also taken into account in this work. Basically, the research related to this work is the method to improve the shift quality that started with the introduction of an objective evaluation of comfort and spontaneity as relevant characteristics of the gear shifting process based on the characteristic parameter calculations in the time and frequency domain. Furthermore, the DCT is similar in design to the manual transmission (MT) as well as to the automated manual transmission (AMT). Therefore, the literature dealing with both types of transmission (MT and AMT) is also taken into account in this work. Furthermore, Table 2.1 lists the relevant studies vehicle transmissions.

DCT system modelling is known as an effective and cost efficient method for further DCT development and optimization of the relatively new technology of dry as well as wet DCTs [33]. Furthermore, the study and optimization of DCTs to increase the mechanical efficiency are also done on DCT components, particularly on the oil pump system in [5] and [6]. Additionally, the synchronizer system as a critical component in DCTs is analyzed in detail in order to learn about the limits of the system in [42], [116] and [142].

The longitudinal acceleration during gear shifting is known as a crucial signal for the comfort rating and as a target for optimization in [10, 37, 43]. In practice, the driver's seat rail is the best position to measure the vehicle acceleration [19] besides the other method introduced by [159] using a driver dummy with strain sensors in the neck to measure vehicle jerk during gear shifting.

The principle set up on the basis of a regression analysis between characteristic parameters and subjective scoring delivered an evaluation function was initially introduced for automatic transmissions. The procedure has also been found as a target in the objectification of other gear types such as AMT, DCT and CVT (in manual mode) [17, 20, 21, 22], as well as in the evaluation of load-change reactions [44]. In [37], the feasibility of an adaptive parameter optimization for fast filling of the coupling is first detected, due to non-map-able interactions of empirical modelling for a larger number of parameters with a linear objective function does not provide a sufficient good model for optimization.

An online optimization with the same twelve free parameters is first presented in [43]. It is conducted on a chassis dynamometer equipped with the operating points which are used as often as reproducible approachable. A fuzzy controller, which was built on the basis of a sensitivity analysis, is used as an optimization tool. The system shows the potential for shift comfort optimization, but remains limited by the time-consuming manual controller design a high effort when changing the free parameters.

The advantage of using a chassis dynamometer for system identification in order to connecting an experimental design to data input for a model of higher order is explained in [19]. An offline optimization based on polynomial -model and neural network is first shown, driven by the success of the model-truncated optimization methods that used in engine application. A new, improved model is used to reduce the effort significantly. To reduce the test costs, the first performance is identified precisely at an operating point. It is assumed, that the system performance changes only in terms of quantity, but not quality if the operating points are changed. The performance at adjacent operating points can therefore be identified with much less effort.

Table 2.1: Literature dealing with automatic transmissions (AT, AMT, CVT and DCT).

Topic	References
New automatic transmission concepts	[25], [29], [30], [39], [52], [82], [92] [95], [96], [97], [98], [99], [100], [101] [102], [103], [105], [117], [118], [120] [132]
Automatic transmission system modelling	[9], [24], [28], [33], [38], [45], [55] [56], [60], [61], [65], [66], [67], [68] [70], [86], [90], [91], [128], [130] [140], [143], [146], [147], [148], [149] [150], [151], [154], [158], [160], [163]
Automatic transmission control systems	[2], [11], [12], [13], [14], [15], [27] [31], [32], [34], [35], [36], [46], [47] [48], [50], [54], [57], [59], [62], [64] [71], [72], [76], [80], [85], [88], [89] [93], [112], [114], [115], [119], [124] [125], [126], [131], [133], [135], [136] [137], [139], [141], [144], [145], [155] [157], [161], [162]
Automatic transmissions - gear shifting optimization	[3], [4], [10], [17], [18], [19], [20], [21] [22], [37], [40], [41], [43], [44], [45] [58], [78], [87], [111], [159]
Automatic transmissions - efficiency improvement	[5], [6], [81], [127], [134]
Synchronizer system	[1], [23], [42], [83], [84], [116], [121] [142]
Simulation environment, SiL and HiL	[8], [16], [24], [28], [53], [63], [70] [77], [129], [152], [153], [156]

The branch with regard to improving the gear switch sequence control for an increased shift quality and less effort in the application is strongly influenced by the simulation. A pioneer takes here the work of [47], which extensively with the simulation of the powertrain itself - including a consideration of the hydraulics and detailed models for the transmission capability of the multi-plate clutches. The gear switch is improved in a backward recursion through the

optimization of the control parameters using a simplified model of the drivetrain. The objective function contains both the parameters work losses during the gearshift, which is essential for the durability, as well as comfort-related individual parameters from acceleration and speed characteristics.

The shifting performance has also performed in [40] studies using a multi-body simulation program. It combines models of vehicle chassis, suspension, drive axle and engine-gearbox unit to identify the influence of critical vehicle-specific parameters. The following conclusion can be drawn from the simulation: An excellent shifting quality results from the combination of optimized engine and transmission control unit and the vehicle sensitivity. The vehicle sensitivity can be changed by combining experimental and analytical techniques to identify problematic areas. The control of the drive train and the vehicle sensitivity in most cases, are the two areas to be considered to achieve the desired shift quality.

Furthermore, many researchers have worked on the DCT for a better understanding of the system. Alvermann proposed the off-line method for clutch control in gear shifting for improved comfort [10], whereas the synchronizer working load due to the drag torque in the transmission was investigated by Walker et al. [140-142]. Furthermore, the electro-hydraulic system for gear shift actuators and the shift schedule to increase drivability and DCT quality were analyzed and optimized by Mustafa et al. and Liu et al. [90-91, 81]. Contrary to previous research, an enhancement of the wet DCT efficiency is proposed and described in this work by improving the gear preselection based on the limits of the DCT design and the electro-hydraulic system. The results obtained with the proposed method are also compared to those of the conventional sport mode gear preselection strategy.

3 Concept of a Wet DCT

The DCT analyzed in this work is a longitudinal seven-speed wet DCT used in a sports car[3]. This particular wet DCT is the first DCT for a longitudinal high-revving engine up to 9000 RPM. The capability to cope with high engine RPM is a true advantage of this DCT in comparison with other automatic transmissions (i.e. AT and CVT), while high engine RPM is not feasible for the transmission which use a torque converter as its coupling system. The other advantage of the DCT is its capability to shift gears without interruption of traction and therefore supports both a sporty driving performance as well as the shifting comfort. Moreover, this wet DCT has a flexible design that can be used not only for sports cars, but also for comfort-oriented vehicles, without any major changes. Further information on this particular wet DCT transmission can be found in [25, 105, 117 and 118].

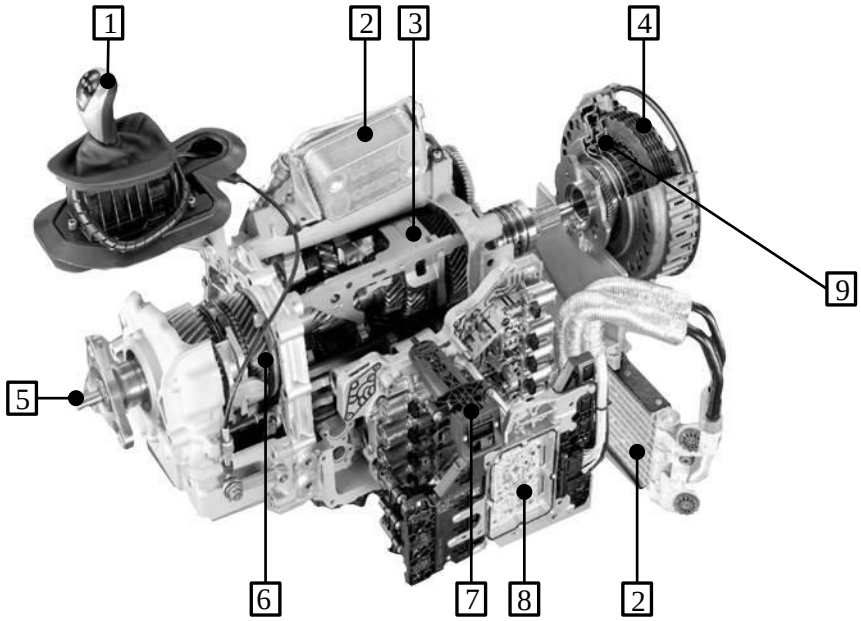

Figure 3.1: Exploded view of the longitudinal seven-speed wet DCT with its major components [105].

The longitudinal seven-speed wet DCT has a compact design and employ the mature design of the manual transmission to ensure the robust performance yet easy to maintain. The major

[3] The particular seven-speed wet DCT transmission was developed by Getrag together with BMW to be used in the high-powered BMW M-Series.

components of the DCT are the mechanical transmission system, which contains the double clutch, synchronizer and gears, the mechatronics module containing the transmission control unit, electro-hydraulic valve, hydraulic body valve, sensors, synchronizer actuator and the hydraulic cooling system as shown in Figure 3.1.

3.1 Double Wet Clutch Transmission

The double clutch is the central component of DCT transmissions due to their strong influence in the shifting processes. The longitudinal seven-speed wet DCT uses a concentric double clutch layout as shown in Figure 3.2. The outer multi-disc clutch (larger diameter clutch as an odd clutch) is connected to the odd gear set (i.e. 1^{st}, 3^{rd}, 5^{th} and 7^{th} gear) and the reverse gear through an solid input shaft, while the inner multi-disc clutch (smaller diameter clutch as an even clutch) is connected to the even gear set (i.e. 2^{nd}, 4^{th} and 6^{th} gear) through a hollow input shaft. Both of those double clutches have six outer disc plates that are connected to the engine crankshaft through the clutch casing and the double mass flywheel. Furthermore, they have five inner steel discs with friction linings that are connected to the transmission input shaft. All of the clutch discs are able to slide axially for engagement and disengagement process. The first and the reverse gear are connected to the larger diameter of the odd clutch rather than to the smaller diameter of the even clutch to ensure the high engine torque can be transmitted safely that needed by a car when starting from full stop condition. This is due to the larger diameter clutch will require less clutch pressing force compared to the smaller diameter clutch in transferring the same amount of engine torque.

This particular wet DCT uses a wet clutch system with a pressurized oil circulation system. In this system, the clutch disc is immersed in the oil for cooling purposes to increase their thermal resistance particularly during the clutch engagement process. The wet clutch also guarantees that high engine torque (up to 600 Nm) can be transmitted safely with a relatively small clutch diameter and compact design compared to the dry clutch. Moreover, the clutches are designed with a normally open state by a return coil spring to assure the clutch controlling process can be done positively by an electro-hydraulic system.

As shown in Figure 3.2, the cooling fluid oil is pumped in a radial direction from the centre to the outside to flow through the clutch disc. The oil flow direction is designed to align with the oil centrifugal force direction for efficiency. At a high rotational speed, the centrifugal force causes a dynamic pressure build-up on the clutch piston. This dynamic pressure build-up is not desirable as it increases the contact pressure and unnecessarily complicates the defined pressure increase and reduction in the clutch cylinder. To overcome this undesired

phenomenon, the compensation chamber was designed to equalize and balance the centrifugal pressure build-up in the clutch piston.

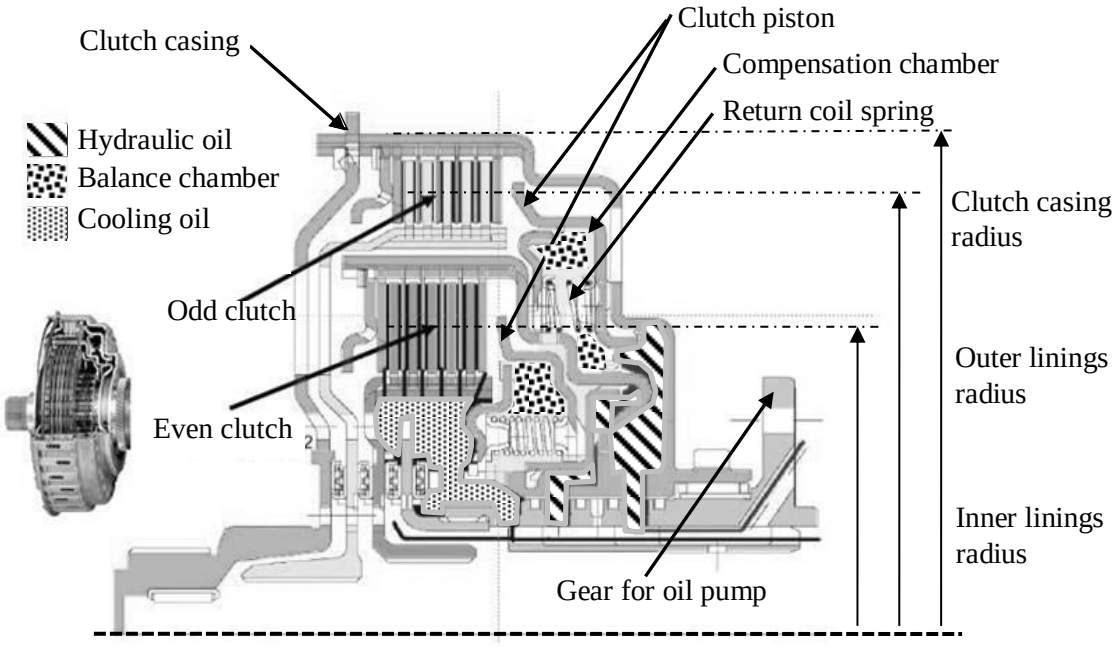

Figure 3.2: Cutaway drawing of the double clutch of the longitudinal seven-speed wet DCT [118].

To control the engagement of the double clutch individually, each clutch has its own clutch pressure control loop which is controlled by a pressure control solenoid valve. Moreover, the solenoid valve controls the clutch contact pressure through the clutch hydraulic piston oil as shown in Figure 3.2. The solenoid valve is driven by the electric current from the transmission control unit (TCU). The TCU determines the clutch hydraulic pressure that is required to transmit the requested engine torque based on the vehicle driving load and knowing the pressure in the clutch via a pressure sensor.

To engage the clutch, the pumped hydraulic oil pushes the clutch piston. In order to bring the clutch disc set into contact, the pumped hydraulic oil should overcome all of the counter forces that are coming from the return coil spring and thicker oil film in the gap between the clutch disc. Once the counter force is overcome, the disc clutch starts to slide. Furthermore, the TCU determines the transmitted torque based on a friction model which is stored in the TCU and it is influenced by some factors such as slide speed, temperature of the oil and the frictional properties of the frictional lining performance of the clutch disc. If the disc clutch is fully closed, the torque is then completely transmitted by a friction force on the disc clutch as a function of the disc clutch pressure force.

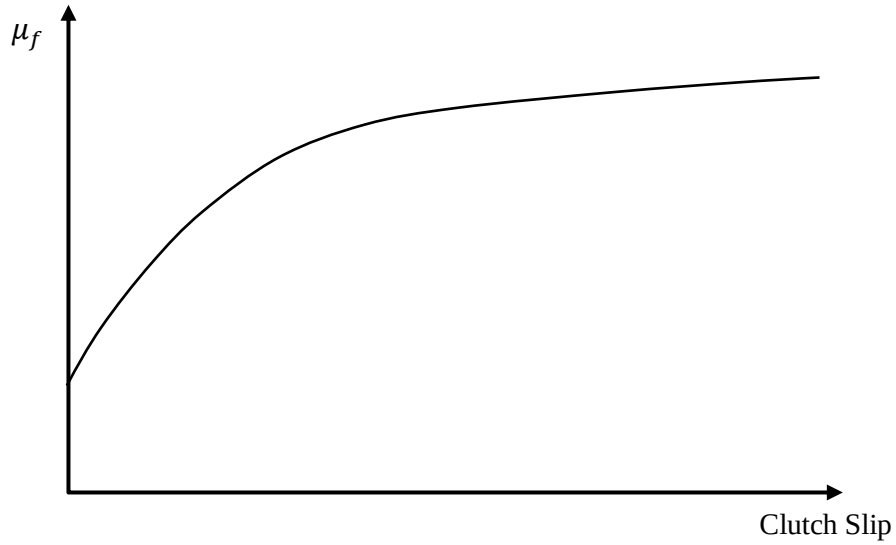

Figure 3.3: Various values of the clutch friction coefficient at different sliding speeds [72].

The amount of engine torque transmitted by the clutch depends on the friction that occurs between the pressed of outer and inner clutch disc. There are two friction phases that can be identified during the clutch engagement. The first phase is a slide phase where the outer and the inner clutch discs rotate at different speeds. In this phase, the engine torque is transmitted by the clutch through sliding friction. The second phase is a stick phase where the outer and the inner clutch discs rotate at the same speed with no slide. The transmission of the clutch torque can be calculated using the following formula:

$$T_C = z * r_m * F_R \tag{3.1}$$

where z is the number of pairings contact surfaces between the outer and inner clutch disc, r_m the friction lining mean radius, μ_f the friction coefficient of the friction lining and F_R the friction force between the clutch discs. Furthermore, the friction force (F_R) between the clutch discs is defined using Coulomb's friction law, which takes the static and kinetic friction into account:

$$F_R = \mu_f * F_N \tag{3.2}$$

In this case, F_N is the normal force provided by the clutch piston, which acts perpendicular to the friction surface. In the slide phase, the friction coefficient (μ_f) is varied depending on the relative speed between the friction clutch discs as shown in Figure 3.3. The friction coefficient also depends on the material properties of the clutch disc lining, the clutch temperature and the characteristics of the cooling fluid. In the stick phase, where there is no more speed difference between the friction clutch discs, the static friction coefficient is used. The static friction coefficient is generally greater than the sliding friction coefficient.

Although the clutch design is normally open, in the disengage or in the open clutch, the clutch cooling fluid makes the outer disc clutch stick with the inner disc clutch all the time due to the viscosity of the clutch cooling fluid which adversely affects the efficiency of the transmission. Moreover, the clutch outer disc rotates at different speeds or will slide with clutch inner disc causing the drag torque after the gear is preselected. The drag torque depends on several factors, such as the flow of the cooling oil, the oil temperature and the different speeds (sliding speed) of the clutch outer disc and clutch inner disc.

3.2 Double Clutch Actuator Piston

The double clutch performance is highly affected by three essential components of the hydraulic control system, which are the mechanical clutch actuator, the connection between the electro-hydraulic valve and the oil lines/channels. However, the influence of the lines/channels on the hydraulic control system is comparatively small, so it can be neglected [91]. The dynamic performance of the clutch piston as a mechanical actuator must be carefully considered since the hydraulic energy is transformed into a linear mechanical motion by this system. Furthermore, the dynamic performance of the piston corresponds to a damped spring-mass oscillator as explained in Chapter 3.1. For clarity, Figure 3.4 shows several forces acting on the odd clutch, however, similar conditions also occur in the even clutch.

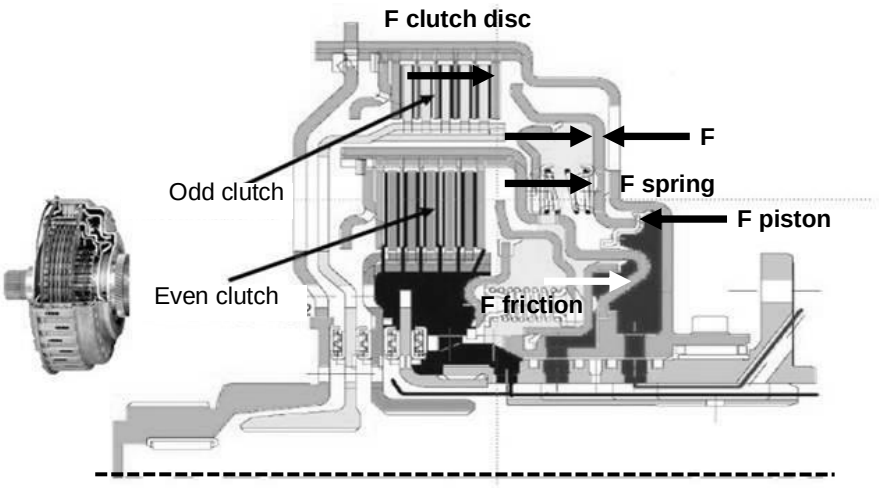

Figure 3.4: Several forces acting on the odd clutch [25].

In the rest or disengaged condition, the clutch is open and there is no force acting on the clutch disc. The clutch piston is resting in its initial position held by the return coil spring force and the clutch piston is also not being pushed by the hydraulic fluid. The clutch engagement process is started when the hydraulic fluid is supplied via rotary pump and

channels through the gear shafts in order to push the clutch piston. The hydraulic piston force must first break the thicker oil film in the clearance between the clutch discs before the clutch disc makes a surface contact. The optimum clearance between the clutch discs has been designed carefully and it has a large influence on the shift response time and the efficiency of the transmission. The small clearance result in responsive shifting but increases the drag torques directly. On the other hand, too large clearance would lengthen the distance between the clutch disc for making a direct contact and also making a larger volume of cooling oil thus making a longer operating time for clutch engagement. In addition, a large clearance would also cause clutch disc tumbling, which in turn would also increase the drag loss.

The hydraulic oil needed push the clutch piston in the piston chamber (coloured in red) will affected by a rotational movement, therefore producing a speed-dependent centrifugal force ($F_{Centrifugal}$). The centrifugal forces acting on both sides chambers of the clutch piston as shown in Figure 3.4 can be described as [9]:

$$F_{Centrifugal} = \pi * \rho_{oil} * \omega_e^2 * [r_{c1o}^4 - r_{c1i}^4] \tag{3.3}$$

where ω_e is the rotational speed of the engine, r_{c1o}, r_{c1i} the outer and inner radius of the first clutch and ρ_{oil} the oil density. The centrifugal force acts radially from the inside to the outside, but due to the confined space of the piston chamber, the centrifugal force will push the piston in the axial direction. Furthermore, the pressing force also depends on the temperature of the hydraulic oil, which in turn will change the viscosity (flowability) of the oil. For example, the pressing force is lower at high temperatures due to the centrifugal force as the hydraulic oil is thinner and lighter in this condition. To compensate this effect, the centrifugal force compensation chambers are provided on the side of the clutch disc and coil spring packages (coloured in yellow). In the compensation chamber, the cooling oil flows and is also subjected to a speed-dependent centrifugal force. In the best case, the two centrifugal forces which work in the chamber on both sides of the clutch piston will equal thus canceling to each other. Depending on the speed and the cooling fluid flow, there is a small difference between the forces on both sides.

The return spring force for the clutch piston has to be greater than the total centrifugal force acting on the clutch piston to ensure the clutch disc remain open until it is pressed by control solenoid valve through the pressure build up in the clutch piston chamber. Typically, a hydraulically balanced piston chamber is used to reduce the effect of centrifugal force, therefore lowering the required force of the return spring as explained above. There are two main types of return springs used in modern dual clutch transmissions, i.e. inner slotted disk and multiple round wire coil springs [117]. The multiple round wire coil springs are used in the longitudinal seven-speed wet DCT transmission due to their linear performance. The

return spring force depends on the spring stiffness (k_p) and the piston travel distance (x_P) and can be calculated using the Newtonian spring law as follows:

$$F_{Spring} = k_p * x_P \tag{3.4}$$

Furthermore, the clutch piston force will be generated after the piston is pressurized by the pressure regulating valve. This clutch piston force is equal to the piston pressure (P_P) and the effective piston area (A_P) and can therefore be calculated using the following equation:

$$F_{Piston} = P_P * A_P \tag{3.5}$$

Another force acting on the piston clutch is the frictional force ($F_{Friction}$) resulting from the seals of the piston. The clutch piston is made of metal, which is sealed by means of rubber sealing lips towards the clutch casing. The resulting frictional force through the sealing lips, counteracts the movement of the clutch piston. The friction force corresponds to the nonlinear Coulomb friction, which consists of the shares of static friction and sliding friction. The frictional force is a function of piston speed, temperature, and other factors. It is, however, negligible in comparison with the other forces.

Another force acting on the piston is the damping force. It is caused by the damping effect of the hydraulic oil in the compensation chamber and can be calculated using the following equation:

$$F_{Damping} = d_P * \dot{x}_P \tag{3.6}$$

with $\dot{x}_P$ as clutch piston speed and d_P as damping coefficient. Taking all those forces into account, the equation of the clutch piston motion can be expressed as follows:

$$m_P\ddot{x}_P + F_{Damping} + F_{Spring} = F_{Piston} - F_{Friction} + F_{Centrifugal-1} - F_{Centrifugal-2} - F_{Clutch\ Disc} \tag{3.7}$$

Furthermore, it can be written again after summaries of the centrifugal force in compensation chamber which compensate the centrifugal force in piston hydraulic chamber ($F_{Centrifugal-1} - F_{Centrifugal-2} = 0$) as follow:

$$m_P\ddot{x}_P + d_P\dot{x}_P + k_p x_P = P_P A_P - F_{Friction} - F_{Clutch\ Disc} \tag{3.8}$$

The drag force due to the clutch disc stiffness ($F_{Clutch\ Disc}$) occurs only when the clutch piston pushes the clutch disc set to overcome the clearance between the clutch discs. The clutch disc set afterward begins to touch each other and the engine torque is transmitted through the sliding friction (slide phase) between the clutch disc. At a certain point (kiss-point), the clutch discs start to stick, when the pressure force of the piston continues to increase and it comes to torque transmission by static friction in the stick phase as described in Chapter 3.1.

Furthermore, the force due to the clutch disc stiffness is called normal force. It is used in the stick phase to calculate the clutch torque transmitted by the multi-disc clutch. The normal force of the clutch disc is measured by the hydraulic pressure sensor in the mechatronics module used by the transmission control unit (TCU) for the actuation of the two multi-disc clutches based on the clutch control model. The normal force is very important to ensure that the friction force in the clutch disc is sufficient enough to transmit the requested engine torque.

3.3 Gear and Shaft Arrangement

The longitudinal seven-speed wet DCT is designed as a high speed gearbox using a special shaft and gear arrangement to fit the available space on the vehicle chassis with front engine, rear-wheel drive layout as shown in Figure 3.5.

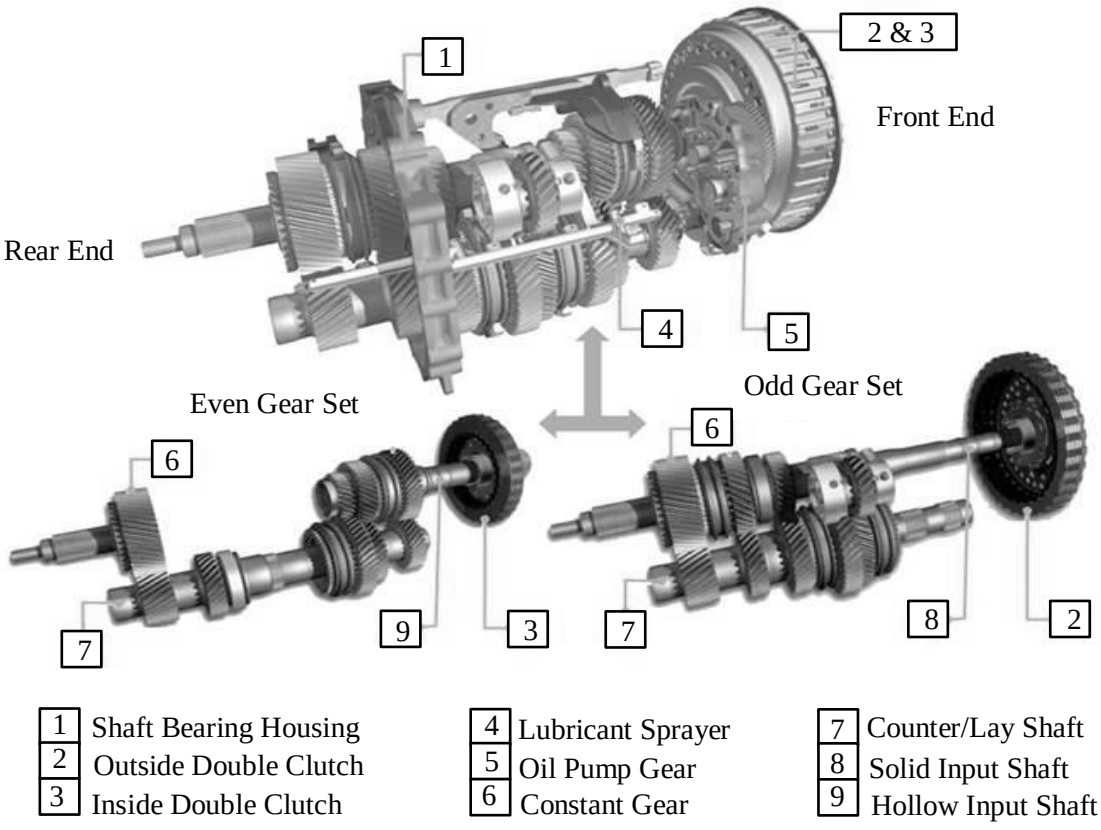

Figure 3.5: DCT shaft arrangement of the longitudinal seven-speed wet DCT [25].

In this arrangement, the torque of all gears is transmitted to the output shaft at a constant output level through a countershaft to ensure that the moments and masses to be synchronized are reduced although the internal transmission speeds are increased. This design, allows the

components to be smaller and therefore more compact. However, this arrangement also increases the complexity of the transmission.

This particular wet DCT has seven speeds to give a finer gradation of gear ratio to achieve high gear spread number. This high gear spread is required for the vehicle to drive with optimum fuel consumption at different loads. With higher gear spread, the vehicle can move at very low speeds due to the high gear ratio of the starting gear (1^{st} or reverse gear) while on the other hand, it can also move at higher speed with low rotational engine speed for fuel efficiency on the highway due to the small gear ratio of the overdrive 7^{th} gear.

3.4 Synchronizer System

In the DCT design, a synchronizer system is used to connect two separate rotating parts with positive interlocking made by meshing between the splines of several components as shown in Figure 3.6 (a). The hub has inner and outer splines that mesh with the shaft and sleeve splines. The sleeve can move in an axial direction from its neutral position towards the gear hub spline, as shown in Figure 3.6 (b). The strut with a notch is pushed by the helical spring to the outside in a radial direction to plug the sleeve detent groove and hold the sleeve in a neutral position while all sleeve spline lengths are in contact only with the hub spline. The ring has an inner cone friction surface which rubs the outer cone friction surface of the gear hub and acts as a synchronizer cone clutch. The ring has a narrow tab that fills the wider slot in the hub. Thus, the ring can rotate together with the hub and also spin relatively to it with a limited rotating degree depending on the cone clutch torque direction. This limited ring rotation at its maximum locking position will block the sliding path of the sleeve spline.

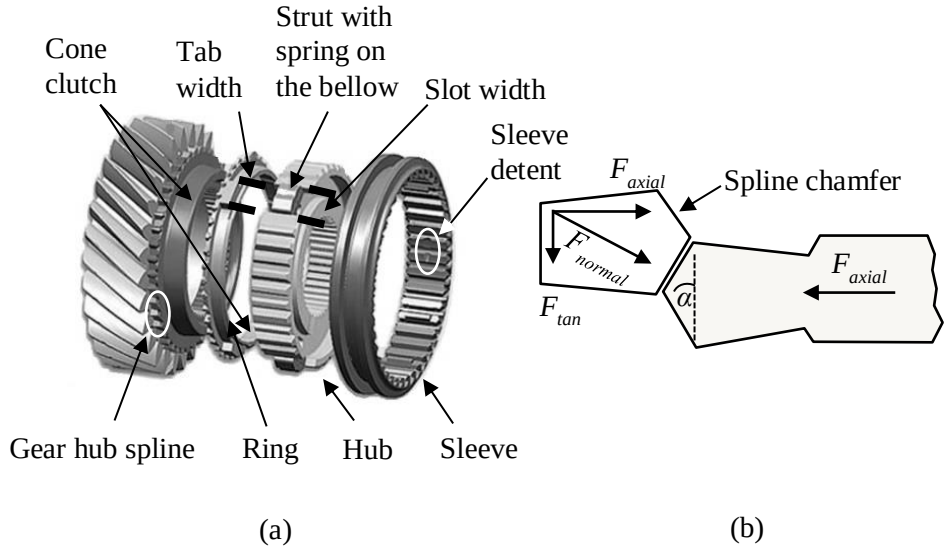

Figure 3.6: Three cone synchronizer system (a) and forces involved in its splines (b).

This particular longitudinal seven-speed wet DCT has four synchronizers with selector forks that engage in the grooves of the synchronizer sleeves to actuate the synchronizers back and forth for gear engagement as shown in Figure 3.7. All of the shift forks are operated hydraulically by the mechatronics unit and the displacement is sensed by magnetic displacement sensors that are located on the shift rods to inform the TCU about which gear is engaged by the synchronizer. The first synchronizer (see Figure 3.7) on the lay-shaft is for 1st and 3rd gear engagement while the second synchronizer is for 2nd and reverse gear engagement. Both these synchronizers are 3-cone types due to the very large masses to be synchronized by these gears. The third synchronizer is located on the hollow input shaft for 4th and 6th gear engagement and, the fourth synchronizer on the output shaft for 5th gear engagement and for locking the input solid shaft directly to the output shaft to create a 1:1 rotation ratio. The third and fourth synchronizers are single -cone synchronizers since less synchronization force is needed for 4th to 7th gear than for 1st to 3rd gear. This arrangement ensures, that the next higher or lower gear does not come from the same synchromesh. For reverse driving, the direction of rotation is reversed by an intermediate gear.

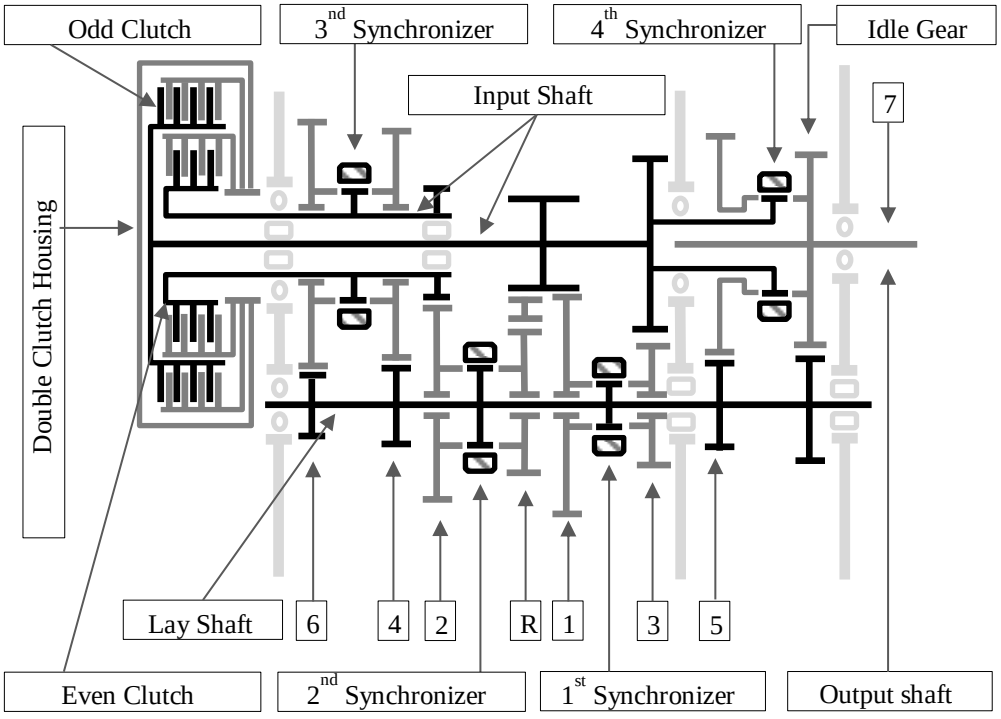

Figure 3.7: Longitudinal 7-speed wet DCT design with four synchronizers.

3.5 Mechatronics Module

The mechatronics module is the brain and nerve centre of the DCT transmission. In this module, all sensor signals are collected and monitored by the transmission control unit (TCU)

to control the gear shifting actions. It is mounted on the wall side of the transmission to ensure sufficient ground clearance for deep-seated and low ground clearance sports car as shown in Figure 3.8. Due to their location on the outside of the gearbox, the mechatronics unit and especially the TCU are possibly exposed to extreme and harsh ambient conditions includinghumidity, temperature, etc. To ensure correct operation of mechatronic module, it has to survive in all conditions including vibrations of up to 30g and temperatures ranging from -40 ° C to 150 ° C.

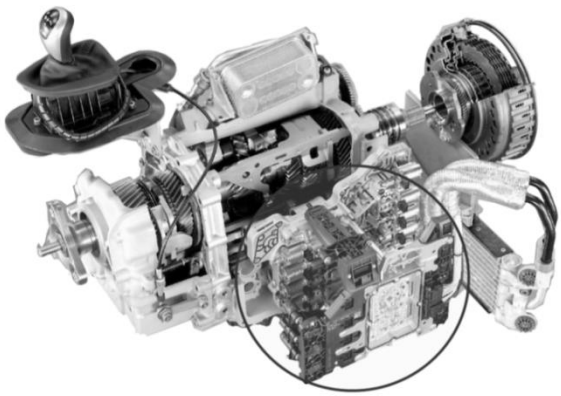

Figure 3.8: Position of the mechatronics module in the longitudinal 7-speed wet DCT [25].

The transmission uses an integrated hydraulic oil circuit with pressurized oil, which is supplied from the small gear pump. The hydraulic system of the mechatronics module uses this oil flow to control the multi -disc clutches for gear shifting. Furthermore, the hydraulic oil is also used for gear lubrication and cooling of the double clutch. The gearbox contains 7.8 litres of oil and filtered to guarantee purity in order to prevent abrasion in the oil channels and the electro-hydraulic valve due to contaminated hydraulic oil.

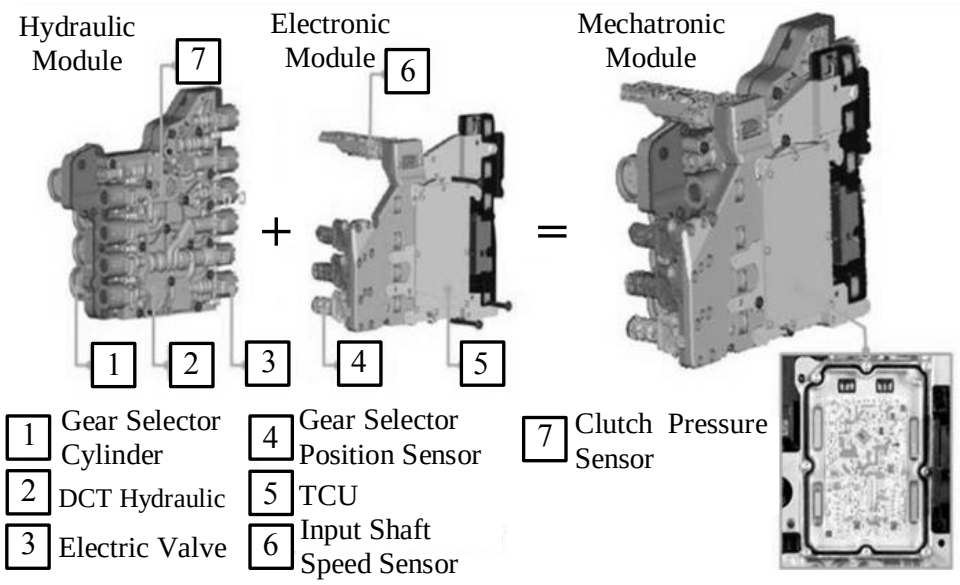

Figure 3.9: Design of the mechatronics module [118].

The mechatronics unit consists of a hydraulic module with the actuator and an electronic module with the transmission control unit (TCU) including its sensors as shown in Figure 3.9. The hydraulic module is composed of two hydraulic plates, which are separated by an intermediate panel made of aluminium. The hydraulic plates contain the oil channels, two pressure sensors to measure the clutch pressures, gate valves and seats for the solenoid valves. This particular DCT has 10 solenoid valves. Four of them are configured as pressure control valves and the remaining six are modulation valves supposed to work as a simple switching valve. In the shifting process, two pressure control valves control the pressure of the double clutches and eight shift cylinders to select the gear through four gears fork selectors as shown in Figure 3.10. The electro-hydraulic system will be further explained in Chapter 3.6.

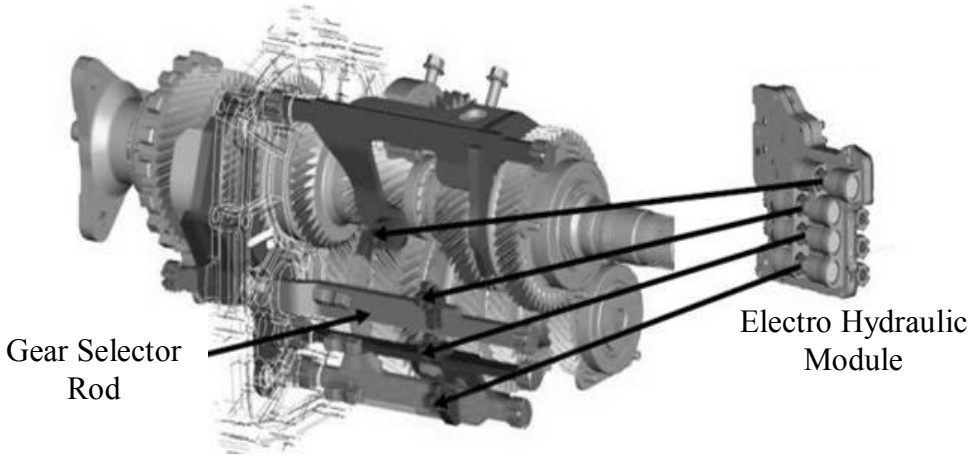

Figure 3.10: Hydraulic system to actuate the fork gear selector [118].

The electronics module includes the TCU, which is the brain of the transmission. It uses a 32-bit microcontrollers with embedded software containing the control algorithms of the double clutch transmission. The TCU software uses sensor data to determine the right strategy to control the double clutch during gear shifting through the solenoid valves.

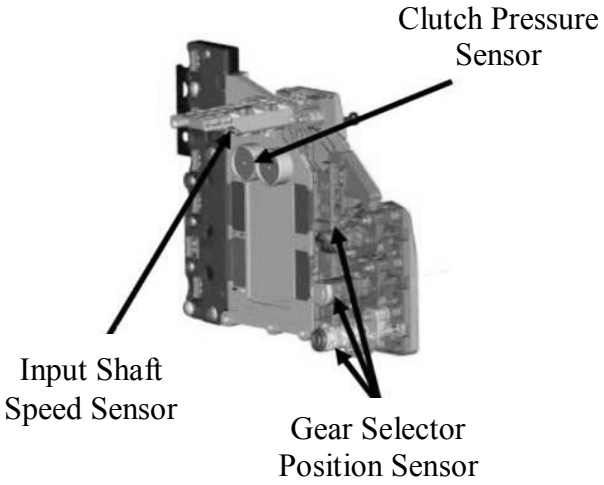

Figure 3.11: Sensors in the mechatronic module [118].

Furthermore, the position sensors detect the fork selector position and displacement via a permanent magnet on the shift rods. Thus, the TCU always knows which gear is engaged. The clutch pressure sensors use a piezoelectric system to measure the clutch disc normal force. Moreover, the shaft speed sensors are used to measure the input shaft speed of the odd and even clutch using the Hall principle as shown in Figure 3.11.

3.6 Electro-Hydraulic System

The electro-hydraulic system of the DCT comprises several mechanical components, which are the mechanical oil pump, the pressure regulator valve, the normally closed control valve, the clutch actuator piston and the synchronizer sleeve actuator piston. The electro-hydraulic unit of the transmission has the following main tasks:

- to control the double clutch piston pressure
- to actuate the synchronizer to engage/disengage the gear
- to keep the double clutch at working temperature using the cooling system
- to lubricate the gear mechanism

In order to accomplish all of the above tasks, the main hydraulic system requires a hydraulic pressure that is generated by the oil pump, which is driven directly by the engine. Figure 3.12 illustrates the main functions of the electro-hydraulics system.

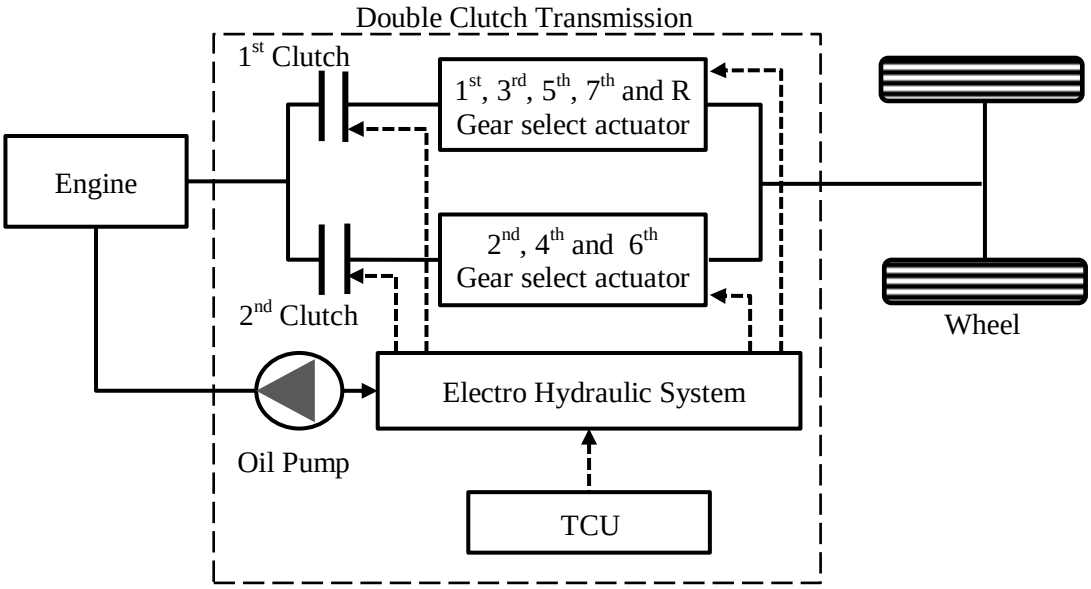

Figure 3.12: The main function of DCT hydraulic system.

Figure 3.13 shows how the double clutch is controlled by the electro-hydraulic system. The process starts with the collection of data (TCU). The TCU needs all the information on driving conditions and driver requests from shift lever, throttle, steering angle sensor and other sensors in the transmission to control the solenoid valve. Based on those data, the

transmission control unit calculates the target pressure in the clutch piston chamber. To control the solenoid valve, the TCU sends an electric current as a pulse width modulated signal to the pressure-regulating valve to regulate the flow of the pressurized hydraulic oil by movement of a spool. The solenoid valve through the clutch piston, builds up a pressure force on the clutch disc to transmit the required engine torque that is determined by the transmission controller.

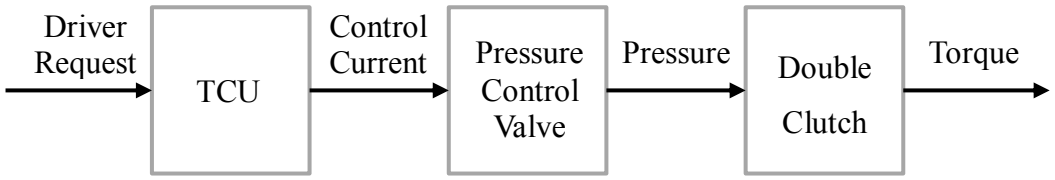

Figure 3.13: Principle of clutch control through the electro-hydraulic system [15].

Figure 3.14 shows the whole electro-hydraulic system of a DCT. Furthermore, the Figure 3.14 is zoomed in to Figure 3.15 and Figure 3.16 for a more detailed illustration of the double clutch piston and the synchronizer sleeve piston actuations.

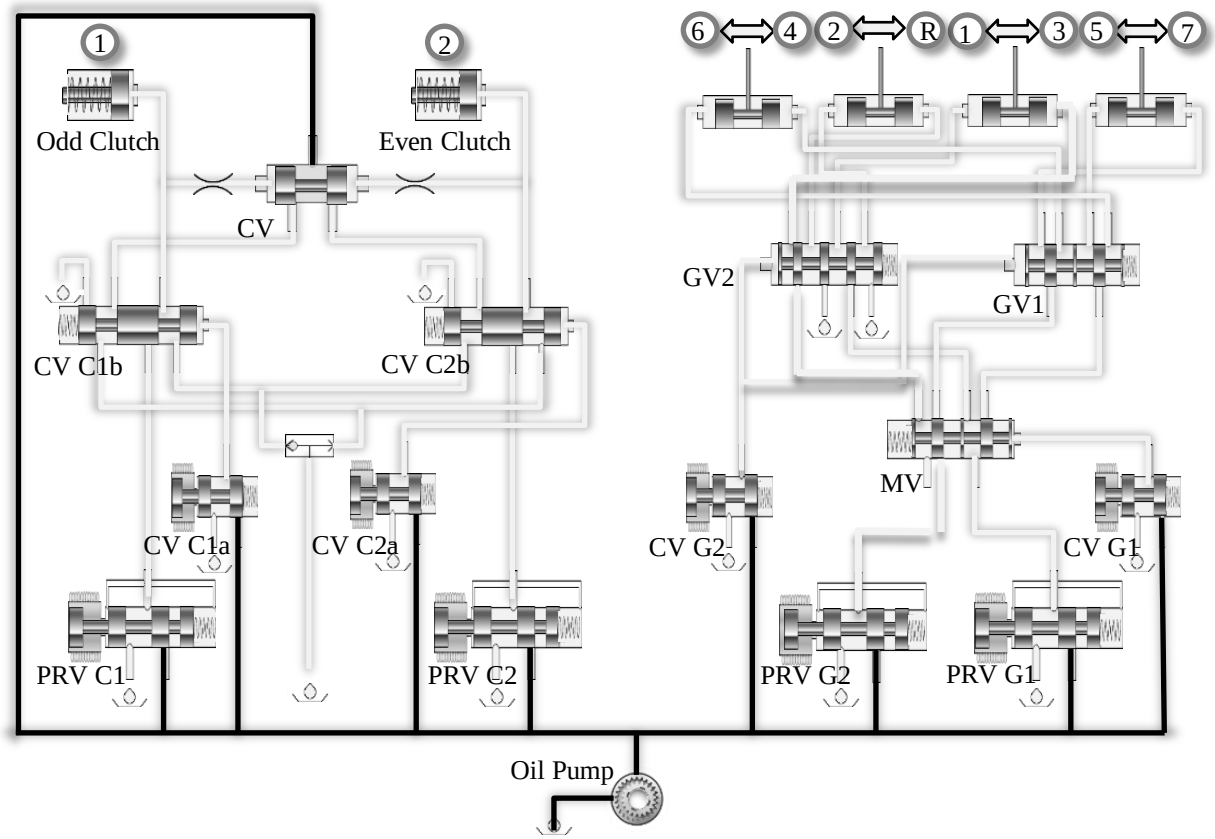

Figure 3.14: Diagram of the electro-hydraulic system for double clutch piston and synchronizer sleeve piston actuation of the longitudinal seven-speed wet DCT.

The electric current is needed in order to actuate the clutch piston as shown in Figure 3.15. The current will energize the spool in the control valve CV-C1a and open the valve. Once this valve has been opened, the hydraulic fluid as pilot-operated pressure, which is generated by the oil pump to control valve CV-C1b, will flow through it. The pilot-operated pressure then pushes the valve in CV-C1b to open the path for controlling the pressure yielded from the pressure regulator valve PRV-C1.

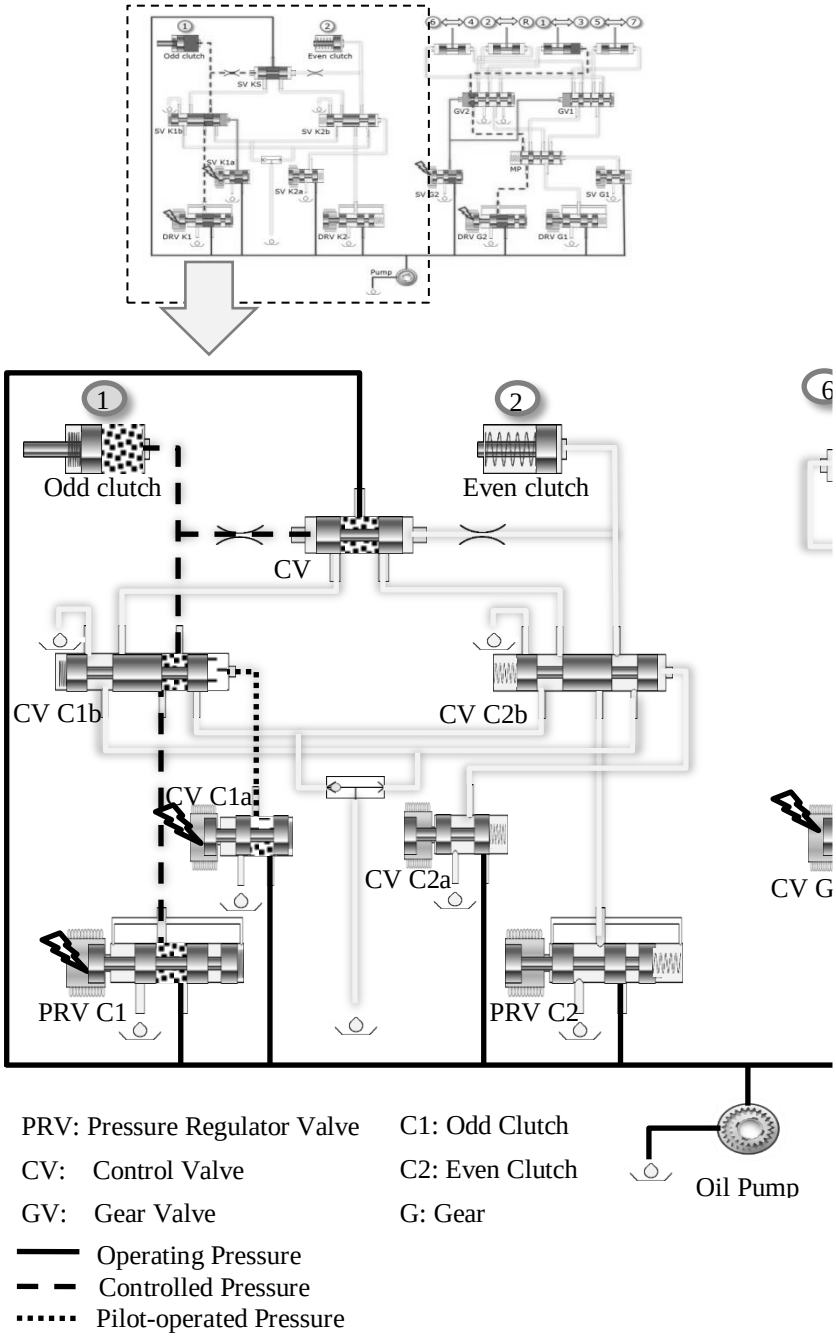

Figure 3.15: Diagram of the electro-hydraulic system for clutch piston actuation.

The pressure in the clutch piston chamber is controlled only by the pressure regulator valve while, the control valves CV-C1a and CV-C1bfunction as safety valves in this process. A

simplified diagram of a clutch piston pressure control is shown in Figure 3.15. The electric current has to be remained to control the pressure of the active clutch, which is a normally open type.

The synchronizer sleeve actuator arm can slide in two opposite directions from its neutral position for the engagement process as shown in Figure 3.16. There are four synchronizer

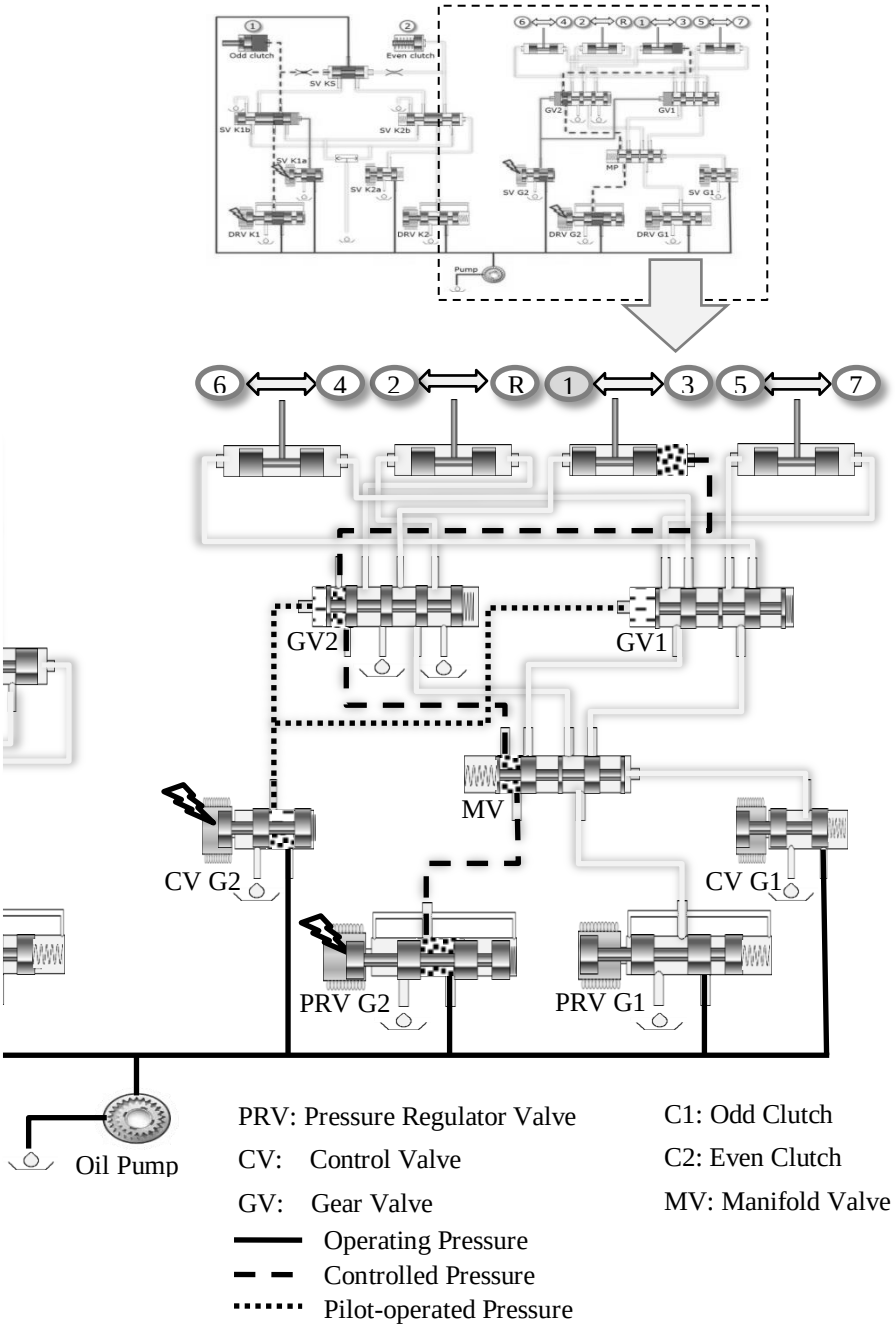

Figure 3.16: Diagram of the electro-hydraulic system for synchronizer sleeve piston actuation.

actuator cylinders used here, i.e. the first actuator cylinder for 6^{th} and 4^{th} gears, the second actuator cylinder for 2^{nd} and reverse gears, the third actuator cylinder for 1^{st} and 3^{rd} gears and

the fourth one for 5th and 7th gears. To engage the 1st gear, the sleeve actuator arm should move towards the 1st gear. In order to achive this, the electric current will be applied to the control valve CV-G2 to open the valve and let the hydraulic fluid flow from the oil pump to the gear valve GV2. Thus, the valve in gear valve GV2 is opened. For the 1st gear engagement, the supplied electric current will energize the spool in the pressure regulator valve PRV-G2 for opening the valve and controlling the pressure to the 1st-3rd gear actuator cylinders. After the first gear is engaged, the electric current will vanish from PRV-G2 and CV-G2. Therefore, it brings the entire valves in Figure 3.16 to their rest positions and blocks all operating pressures to the actuator cylinders.

It is shown in Figure 3.14 that the synchronizer engagement for the next gear, i.e. gear preselection, cannot be performed simultaneously with the synchronizer disengagement of the current gear, it has to be done afterwards. This is due to the fact that the one- valve system is intended for only one task at a time, not for two tasks at the same time as shown in Table 3.1. For example, the 2nd gear (gear preselection) cannot be engaged at the same time as the 1st gear is disengaged (please note that the disengagement of the 1st gear is equal to the engagement of the 3rd gear since both these gears are served by the same 1st synchronizer as shown in Figure 3.7) when shifting up from 1st to 2nd gear since the manifold valve (MV) and the 2nd gear valve (GV2) are both needed at the same time.

Table 3.1: The work sequence of the control valve system to engage the gear through the synchronizer of the longitudinal seven-speed wet DCT.

			To Engage																																			
			1st Gear					2 Gear				3rd Gear					4th Gear					5th Gear						6th Gear					7th Gear						R Gear			
Sequence			1	2	3	4	5	1	2	3	4	1	2	3	4	5	1	2	3	4	5	1	2	3	4	5	6	1	2	3	4	5	1	2	3	4	5	6	1	2	3	4
Control Valve	To control GV1 & GV2	CV-G1																																							
	To control MV	CV-G2																																							
To regulate pressure		PRV-G1																																							
		PRV-G2																																							
To divert oil		MV																																							
To divert oil		GV1																																							
		GV2																																							
Locked																																									

The pressure regulator valve (PRV) has one input and two output ports as shown in Figure 3.17. The valve has three main positions, i.e. the neutral position that blocks the flow as shown in Figure 3.17 (a), the maximum displacement position that regulates the oil flow from oil pump to clutch piston as shown in Figure 3.17 (b), and the rest position that regulates the oil flow from clutch piston to oil sump tank as shown in Figure 3.17 (c). The valve spool will move from its rest position ($x_{s\,min}$) to its maximum displacement position ($x_{s\,max}$) to regulate the oil flow and the pressure in the clutch piston chamber.

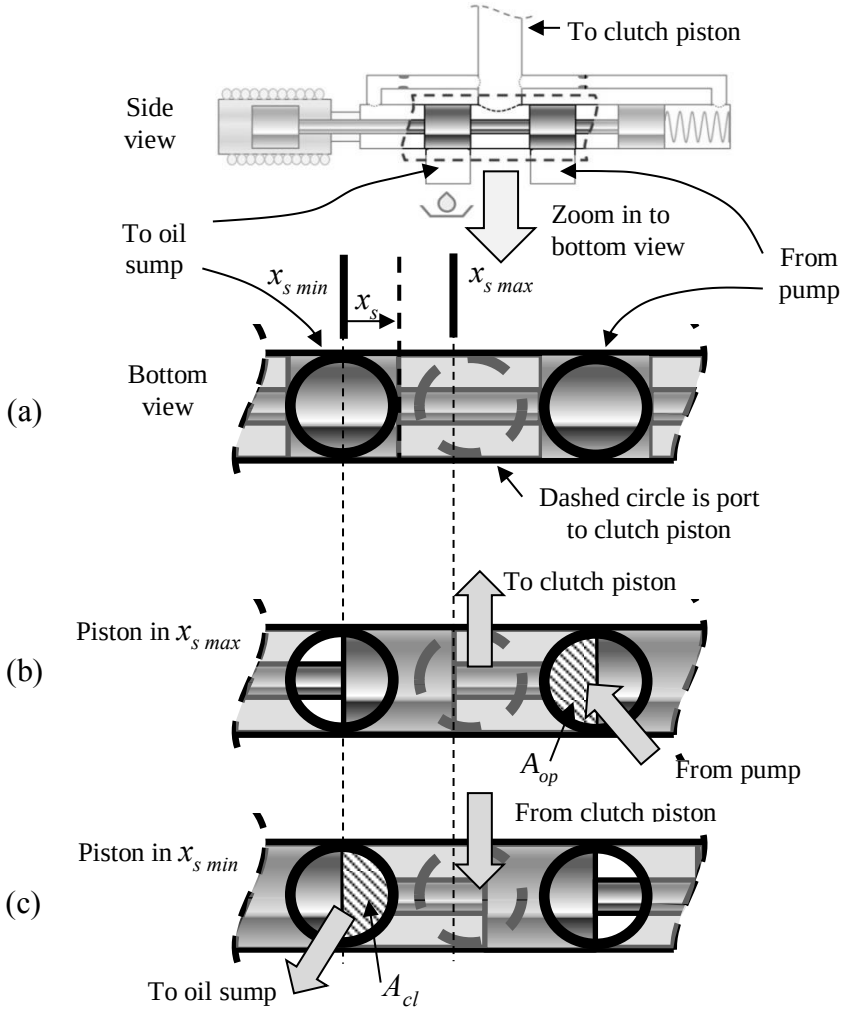

Figure 3.17: Pressure regulator valve (PRV in Figure 3.14) with spool in (a) neutral (b) maximum displacements and (c) minimum displacement position.

The areas of the port opening (A_{op}) and the port closing (A_{cl}) are a function of the valve spool displacement (x_s) and can be described as:

$$A_{op}(x_s) = \frac{n_o R^2}{2}\left[2cos^{-1}\left(\frac{R - x_s}{R}\right) - sin\left(2cos^{-1}\left(\frac{R - x_s}{R}\right)\right)\right], x_s > \frac{R}{2} \quad (3.9)$$

$$A_{cl}(x_s) = \frac{n_o R^2}{2}\left[2cos^{-1}\left(\frac{x_s + R/2}{R}\right) - sin\left(2cos^{-1}\left(\frac{x_s + R/2}{R}\right)\right)\right], x_s < \frac{R}{2} \quad (3.10)$$

where $A_{op}(x_s)$ is the port opening area as a function of the valve spool displacement (x_s), $A_{cl}(x_s)$ the port closing area as a function of the valve spool displacement (x_s), R the radius of the orifice as illustrated in Figure 3.18 (a) and n_o the number of orifices in each port. In this case, the opening area of the orifice is not linear as shown in Figure 3.18 (b).

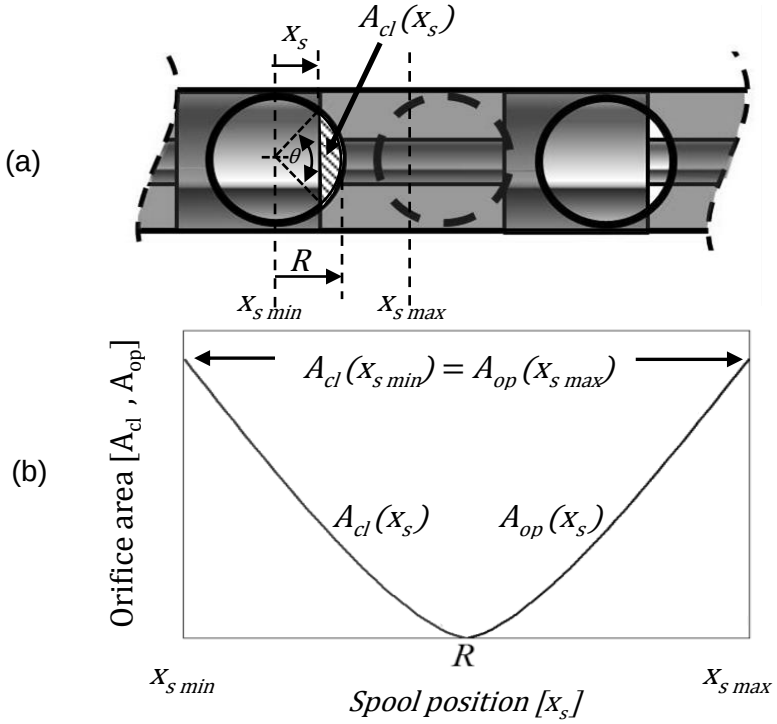

Figure 3.18: (a) Circular segments of charging and discharging orifice area and (b) its nonlinear relation to the spool position.

The magnetic force ($F_{magnetic}$) on the spool is expressed as:

$$F_{magnetic} = \frac{1}{2}.N.i_{magnetic}.\frac{d\varphi_{magnetic}}{dx_s} \quad (3.11)$$

where N is the number of coil turns, $i_{magnetic}$ the electric current and $d\varphi_{magnetic}/dx_s$ the change in the magnetic flux along the valve spool- stroke distance x_s with $\varphi_{magnetic}$ being equals to $L.i_{magnetic}$, where L is the electromagnetic inductance.

The hydraulic flow rate (Q_{net}) to the clutch piston is a nonlinear function of the orifice area and pressure drops which can be described as [90]

$$Q_{net} = A_{op}(x_s)c_v\sqrt{\frac{2(p_s-p_v)}{\rho_{oil}}} - A_{cl}(x_s)c_v\sqrt{\frac{(p_v-p_t)}{\rho_{oil}}} \tag{3.12}$$

where c_v is the discharge coefficient of the valve orifices, p_s the supply pressure directly provided by the oil pump depending on engine torque and speed, p_t the oil sump pressure, $p_v$the output pressure and ρ_{oil} the oil density.

Furthermore, the spool dynamics are described by Newton‘s force balance equation:

$$m_s\ddot{x}_s + d_s\dot{x}_s + k_s x_s = F_{magnetic} - F_{R1} + F_{R2} - F_{Initial} \tag{3.13}$$

where m_s is the valve spool mass, x_s the valve spool position, $F_{magnetic}$ the force caused by the solenoid current $i_{magnetic}$, d_s the damping coefficient resulting from viscous friction, k_s the spool spring stiffness constant and $F_{Initial}$ the initial mechanical spring force caused by the spool spring preload. The electromagnetic valve is beneficial due to its closed-loop control system. It leads to a loop process where the pressure feedback is determined by an internal chamber at each- side of the spool connected by the throttles (pressure restrictions) R_1 and R_2 of the pressure port which is then going to the piston chamber. Thus, the proportional feedback forces (F_{R1}, F_{R2}) to the clutch pressure acting on the valve spool side areas and the damping effects are provided to improve the dynamic performance of the spool as shown in Figure 3.19.

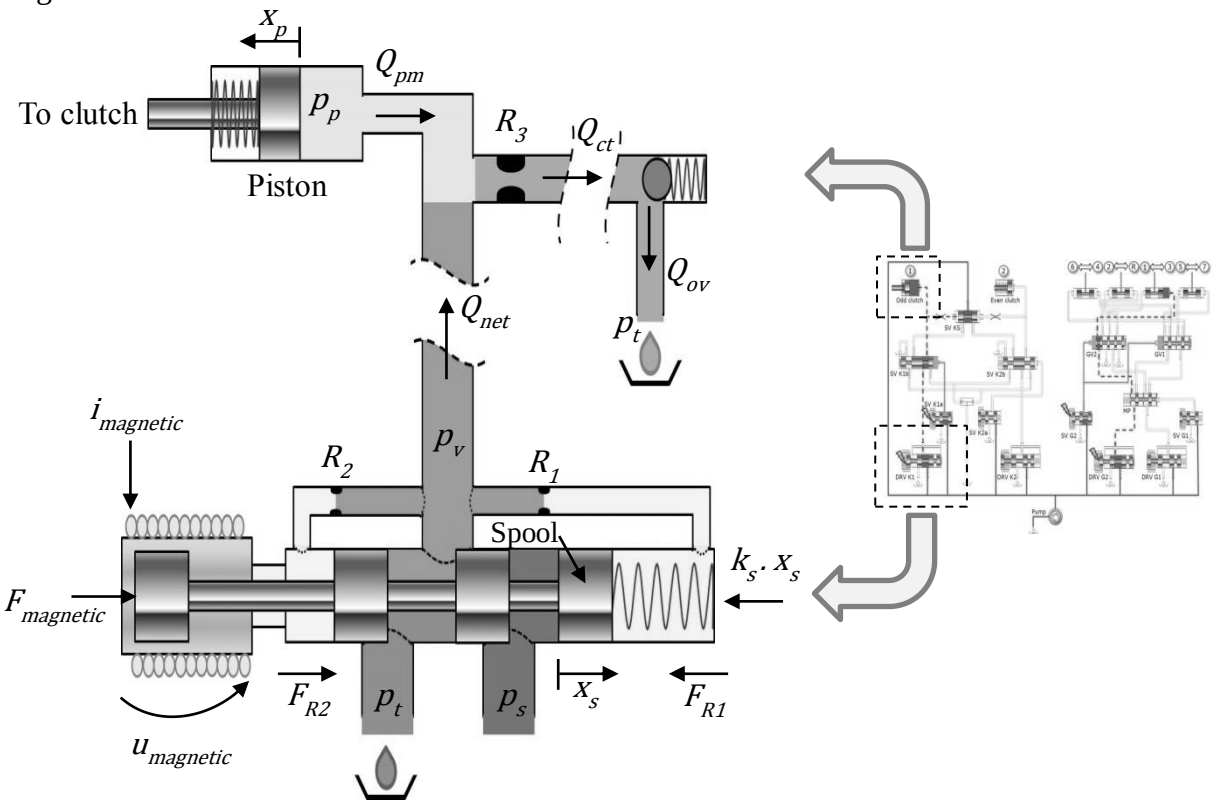

Figure 3.19: Schematic diagram of the electro-hydraulic wet clutch.

The double clutch dynamics highly depend on the hydraulic pressure that pushes the clutch piston with a spring as illustrated in Figure 3.19. The clutch pressure dynamics $\dot{p}_p$ are regulated by the pressure regulator valve and described as a continuity equation:

$$\dot{p}_p = \frac{E}{V}\left[Q_{net} - Q_{pm} - Q_{ov} - Q_{ct} - Q_{con}\right] \tag{3.14}$$

where E is the fluid bulk modulus, V the average piston chamber volume, Q_{net} the total volume flow rate, Q_{pm} the volume flow rate caused by the piston movement and equals to the change of the chamber volume $-\dot{x}_p A_p$, Q_{ov} the volume flow rate out of the system when reaching the maximum pressure (relief flow), Q_{ct} the volume flow rate out of the system through a small discharge orifice R_3 , and Q_{con} the volume flow rate losses through the seals and hydraulic lines. The small discharge orifice is necessary because the spool valve does not need to cross the dead zone $(x_s < R)$ to reduce the clutch pressure after the fast filling phase, hence oscillation and instability can be avoided.

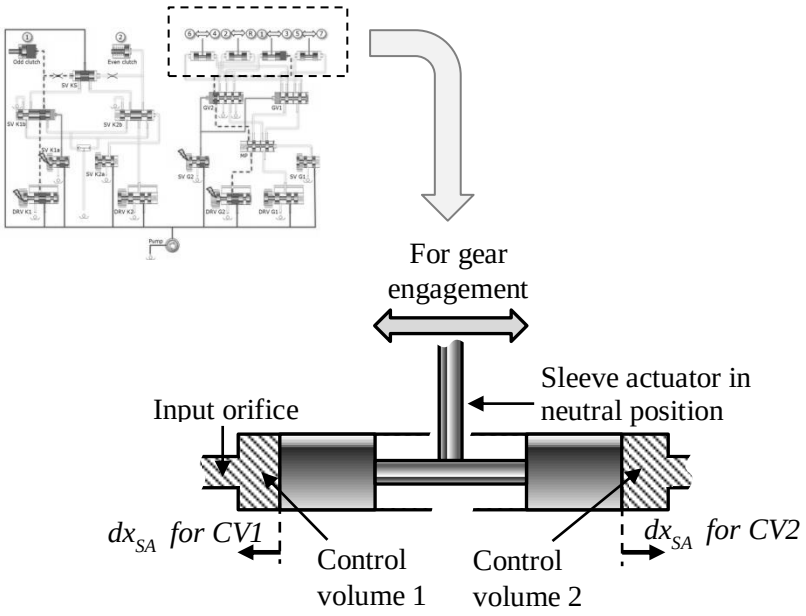

Figure 3.20: Piston cylinder to induce synchronizer sleeve sliding motion.

The synchronizer sleeve actuator is activated by double action hydraulic piston cylinders resulting in a sliding motion as shown in Figure 3.20. The hydraulic pressure in control volume (P_{CV}) will rise to push the piston for synchronizer sleeve actuation which can be described as [141]

$$P_{CV1} = \int \frac{\beta}{V_0 + dV}\left(C_D.\pi.\frac{D_{CV1}^2}{4}.\sqrt{P_S - P_{CV1}} - A_S.\frac{dx_{SA}}{dt} - C_D.\pi.D_S.c_{RS}.\sqrt{P_{CV1} - P_{EX}}\right)dt \tag{3.15}$$

$$P_{CV2} = \int \frac{\beta}{V_0+dV}\left(C_D.\pi.\frac{D_{CV2}^2}{4}.\sqrt{P_S - P_{CV2}} + A_S.\frac{dx_{SA}}{dt} - C_D.\pi.D_S.c_{RS}.\sqrt{P_{CV2} - P_{EX}}\right)dt \quad (3.16)$$

where β is the bulk modulus, V_0 the initial hydraulic volume with sleeve actuator at neutral position, C_D the discharge coefficient, D_{CV} the -orifice -diameter, P_S the -solenoid pressure, P_{CV2} the control volume pressure, A_S the cylinder area, dx_{SA} the sleeve actuator displacement, $D_S$the cylinder diameter, $c_{RS}$the radial clearance and P_{EX} the exhaust pressure.

3.7 Gear Shifting

The basic work of the DCT is explained here, using a 1st to 2nd gear upshift in the power flow diagram as shown in Figure 3.21 as an example. Once the odd clutch piston is pressurized, the inner odd friction clutch disc engages with the outer clutch disc on the clutch casing to ensure that the engine torque is fully transferred to the solid input shaft. In the 1st gear, the engine torque is transferred from the double clutch casing that is bolted to the double mass flywheel to the odd clutch disc pack and then to the 1st gear pair. One part of the 1st gear pair is an embedded part of a solid input shaft while the other part is a freely rotating gear located on the lay-shaft.

Furthermore, the first 3-cone synchronizer (on right side) on the lay-shaft engages the freely rotating gear to lock those gears with the lay-shaft. The locked synchronizer transfers the engine torque to the output shaft through the idle gear as shown in Figure 3.21 (b). The second 3-cone synchronizer (on the left side) now engages the 2nd gear and starts to lock the hollow input shaft together with the lay-shaft. This engagement process is known as gear preselection and prepares the next intended gear before the upshift as shown in Figure 3.21 (c). In addition, the off-going odd clutch pressure is now decreased while the on-going even clutch pressure is increase to allow an uninterrupted torque transfer from the odd to the even clutch. This phenomenon is known as power shift or clutch-to-clutch gear shifting. The off-going odd clutch is still rotated by the on-going even clutch through the first 3-cone synchronizer on the lay-shaft, until the synchronizer disengages the 1st gear as shown in Figure 3.21 (d). The engine torque is now transferred to the even clutch after the pressure of the even clutch is fully built up and the first 3-cone synchronizer is free as shown in Figure 3.21 (e).

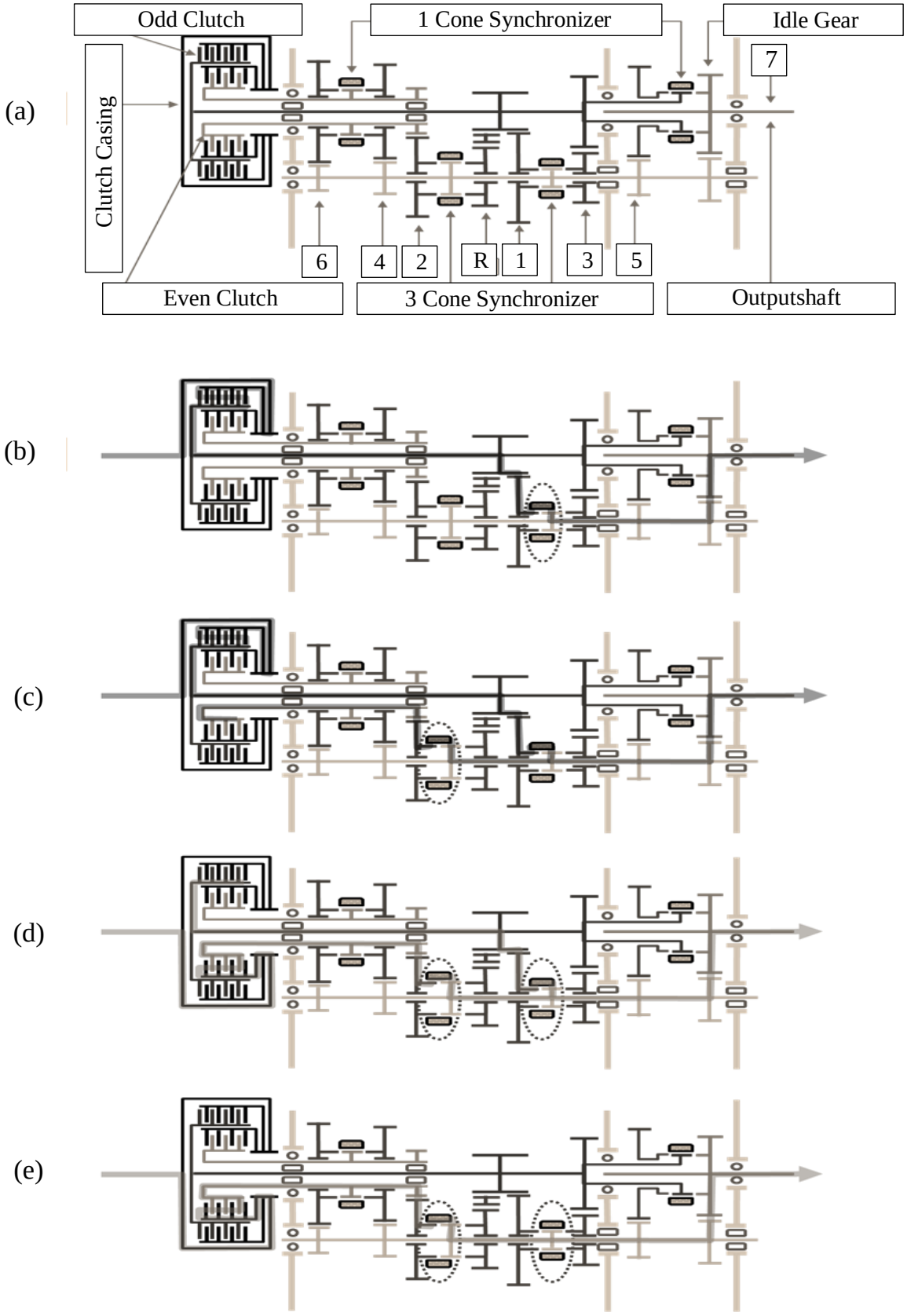

Figure 3.21: Diagram of the 7-speed wet DCT for a gear upshift from 1st to 2nd gear.

3.8 Gear Ratio Control

The transmission controller has an essential function in a double clutch transmission. Several functions of modern transmission control unit are to determine the timing to switch the gear ratio, to execute the shifting process according to the gear ratio switching point determination and for signal processing, monitoring and diagnostics of the vehicle drivetrain system. The DCT transmission control ensures that the shifting process, including gear preselection and gear disengagement, can be done. The transmission control unit, on the other hand, also has to be able to control the gear shifting as requested by the driver in the manual shift mode. The appropriate gear ratio is expected by a modern DCT that is exactly determined in all driving situations and thus avoids loss of comfort due to inappropriate gear shifting. The selection of an automatic gear shift point has therefore become a criterion for evaluating the shifting performance of a DCT.

Furthermore, all of the modern automatic transmissions, including double clutch transmissions, now employ the electro-hydraulic system which is controlled by the transmission control unit (TCU) to ensure precise and robust gear shifting. To accomplish that, the TCU software is developed by the transmission manufacturer and stored in the TCU. In the development process, the software for each new vehicle model is further developed and readjusted for better performance in terms of transmission, automotive and engine technology. Moreover, each DCT manufacturer adjusts the shifting strategy to the specific requirements of the vehicle manufacturers, with the main focus on sportiness, economy, comfort, or a mixture of those three required by the customer. Furthermore, the shifting strategy is documented as a control program in the TCU, known as a shift map.

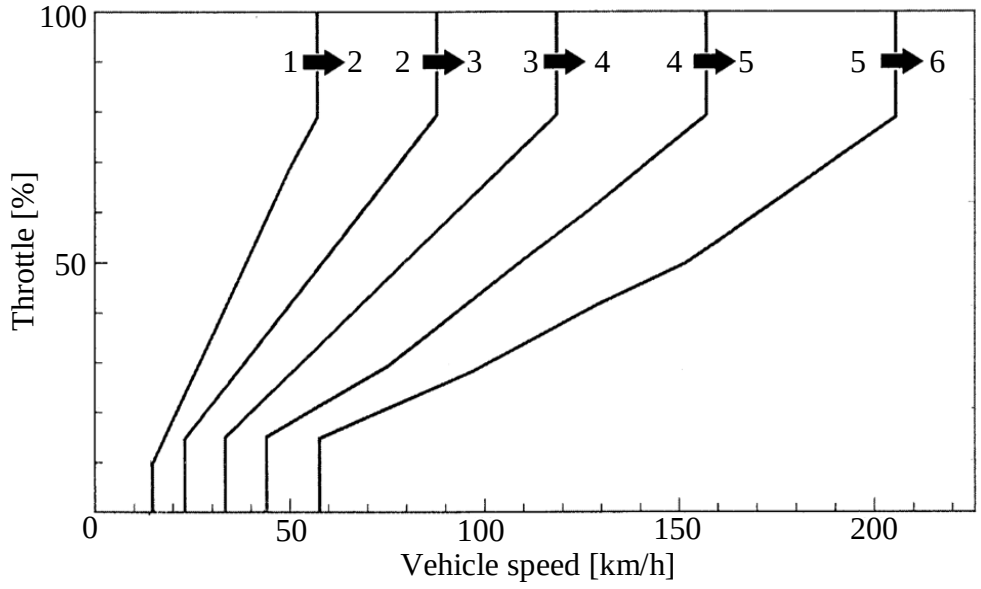

Figure 3.22: Example of 6-speed AT shift map for up-shifting [106].

Shift maps are a characteristic line diagram which considers the throttle pedal position and the vehicle speed to perform the upshift or downshift as shown in Figure 3.22 and Figure 3.23. This shift map is stored in the TCU to be used as a reference point or as a shifting strategy by the TCU to perform the upshift or downshift. The main purpose of that strategy is to continuously select the best and most appropriate gear ratio for the current driving situation from the current driver request. To this end, the transmission control unit receives all the sensor signal data through the CAN (Controller Area Network) interface of the vehicle information system, such as the accelerator pedal position and the vehicle speed.

Basically, a shift map must have the characteristic line at least in the amount of the total speed ratio available minus one. For example, the shift map of a six-speed transmission will have five (five is a result of six minus one) characteristic lines for upshifting as shown in Figure 3.22. The same condition also applies for the downshift map as shown in Figure 3.23. which shows five characteristic lines for a six-speed transmission. However, this simple example is no longer sufficient nowadays since the transmission control systems must be able to adapt to the different driving situations which possibly have different characteristics that apply to the specific case (i.e. for driving in the economic fuel consumption mode or in sports mode). Therefore, the different shift characteristics for the specific requirements, such as fuel efficient, sporty, normal or on a mountain road are stored in the control unit.

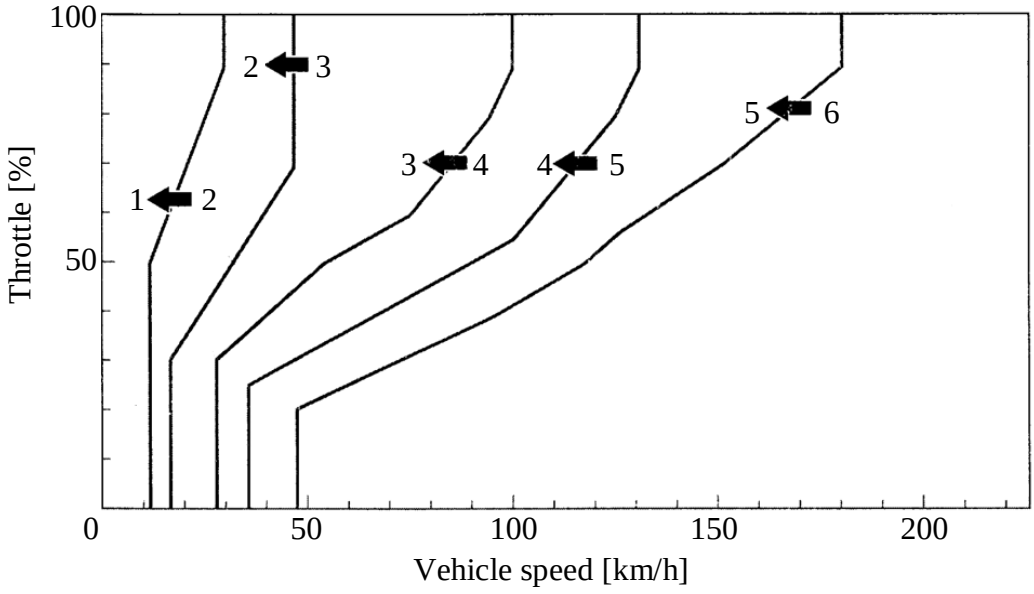

Figure 3.23: Example of a 6-speed AT shift map for down shifting [106].

Those different shift maps are virtually combined in the TCU and can be used together to ensure an ideal characteristic line is generated for every driving situation. The combination of different shift maps is also requested by modern vehicles for safety reasons, for example to avoid a wheel-spin that could happen during braking -and cornering, particularly with regard to winter driving maneuvers.

3.9 Shift Delay, Time and Response

The shift time refers to the time interval between gear changes in a transmission during which the engine torque delivery is interrupted. The shift time occurs during the gear ratio change phase and is easily felt/sensed by the driver since the change of vehicle acceleration mainly occurs in this phase, as shown in Figure 2.3. In comparison, the shift response refers to the time needed by the DCT to complete the gear shifting process. The process is started by fast filling after the driver pull/push the shift lever and ended by gear ratio change phase as shown in Figure 2.3. Therefore, the shift response is longer than the shift time. The time interval from the shift command signal to the beginning of the gear ratio change phase is known as shift delay.

In automatic shift mode, the driver cannot realize the shift delay or the shift response nevertheless can only realize the shift time due to he/she not knowing the exact time of gear shift command signals that is given by TCU based on the shift map. In manual shift mode on the other hand, the driver conscious the shift delay and the shift response due to he/she is the one who actively command the gear shift which then followed with the fast filling phase until the gear shifting process is completed. Thus, the driver always feels the time duration of gear shifting in manual shift mode (as a shift response) is longer than in an automatic shift mode (as a shift time) as shown in Figure 3.24.

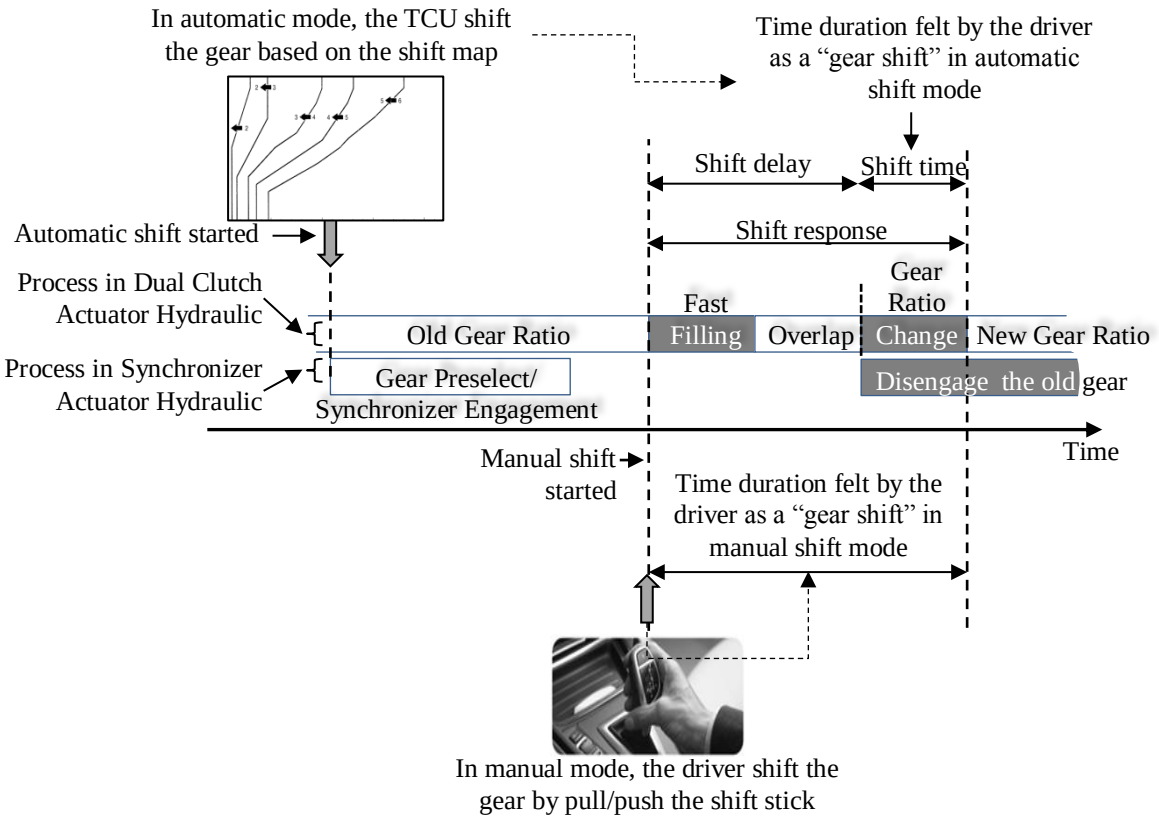

Figure 3.24: Shift delay, time and response in manual and automatic shift modes.

4 Drivetrain Model for Software-in-the-Loop Simulation

In this chapter, a double clutch transmission (DCT) is modelled and simulated in Matlab environment using Simulink and Simscape language program. Simscape is an object-oriented program used to model and simulate the drivetrain as a physical system instead of a math waveform as in a Simulink. As a special tool in Matlab, Simscape can work flawlessly with Simulink to simulate the drivetrain and its electromechanical system. The drivetrain modelled in this work does not only include the mechanical, hydraulic and electrical system, but also the control components for a high fidelity model. Furthermore, all of the constant parameters in the drivetrain model are adjusted using a parameter that was measured in the real vehicle. The aim of this model is to adapt the internal transmission dynamics of the real vehicle, particularly in terms of the shifting performance. Finally, the simulation results are analyzed and compared to the measured vehicle data for model validation.

4.1 Model of the Drivetrain System

The vehicle model is divided into four subsystems as shown in Figure 4.1. These subsystems are masked using a surface image for better presentation of their functions, e.g. engine, transmission, vehicle resistance and clutch control. In this chapter, each of the subsystems which consist of several important components of the drivetrain is described separately and explained in detail. For simplicity and efficiency in terms of simulation time, some of the drivetrain systems are modeled using a standard physical block that is available in the Simscape library while other unique components are modeled using Simulink. To guarantee that Simulink and Simscape work together in one Matlab environment, the interface connection is used to link the Simulink block using simple math waveforms to the Simscape block which use a physical signal.

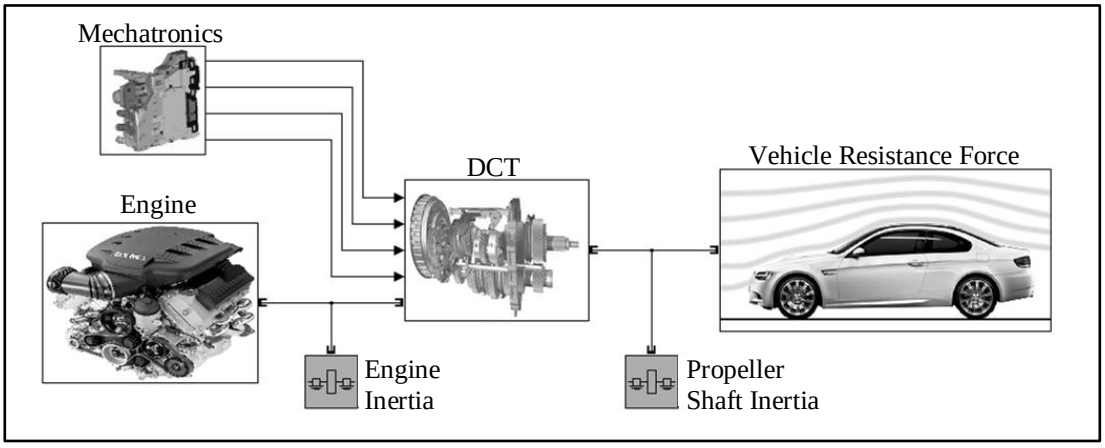

Figure 4.1: The vehicle model with four subsystems.

4.1.1 Engine

The engine is the first subsystem in the vehicle model to work as a torque generator. The engine torque is transmitted from the crankshaft to the wheel through the transmission system to move the vehicle. From the crankshaft, the engine torque is transferred to the dual mass flywheel that is directly bolted to the dual clutch casing. The torque is then transmitted to the odd or even transmission path depending on which clutch (odd or even clutch) of the double clutch is engaged by the clutch control. The transmission output torque is then transferred to the wheels through the propeller shaft and the rear axle. Furthermore, the engine torque at the driving wheel has to counter the driving force resistances.

To simulate the actual engine torque characteristics, a three-dimensional engine map as a function of engine temperature, engine speed and engine torque is developed from the measured vehicle data. The measured data is obtained from the engine control unit as numerical data values and stored as a data series in the Matlab workspace at a sampling rate of 0.001 seconds. To use this data series as the engine torque for the Simscape transmission, the torque actuator block from the Simscape library is used to convert the data series into a physical signal as a unitless input signal. Furthermore, the engine drag torque (i.e. internal engine friction caused by bearings and oil drag losses) is also taken into account before the engine torque is directed to the double clutch casing. To improve the simulation accuracy, the engine drag loss is subtracted from the measured engine torque before it is passed to the double clutch casing. At the end, the Simscape initial condition block is added after the torque actuator to give an initial engine angular velocity in rad/second. The initial engine angular velocity was measured from the engine speed at the beginning of the simulation to guarantee the fidelity of the model.

The drag torque in the outer double clutch disc set also occurs due to the viscous friction of the cooling fluid in the double clutch. Furthermore, that clutch drag torque is subtracted again from the measured engine torque to create a net engine torque, which is received by the inner double clutch disc set.

The drag torque is a quadratic equation which is determined experimentally. First, the rotational speed difference between the engine shaft and the transmission input shaft is calculated and then passed to the Simulink block with the fitted quadratic function as follows:

$$au^2 + bu - 0.15c \tag{4.1}$$

The coefficients of the equations were fitted to the engine drag torque curve to create a realistic net engine torque before it is transmitted to the double clutch.

4.1.2 Double Clutch

In this section, the double clutch system as a subsystem in the vehicle model is explained. For a better model presentation of the model, the subsystem is again divided into two second layer subsystems, i.e. the odd clutch and the even clutch assembly. In this second layer subsystem, the dynamic performance of the transmission branches is simulated with their multi disc clutches, synchronizer and gear ratio set system. Furthermore, the losses in the gearbox and the inertia of the gear shafts were also considered to increase the model fidelity. For clarity, the synchronizer system is explained in the next section.

The multi-plate clutches of the double clutch are modelled using a controllable friction clutch block from the Simscape library with an updated block parameter that is filled out by the parameter data obtained from the actual gearbox.

The controllable friction clutch block from the Simscape library offers an easy way to simulate the properties of a multi-disc clutch. That block links the clutch input shaft to the clutch output shaft by an adjustable sliding and static friction. All parameters of the real longitudinal seven-speed wet DCT can be set and adjusted in a graphical configuration interface to simulate the transmission dynamic performance as accurate as possible.

The first input parameter needed by the controllable friction clutch block is the rotational direction of the clutch halves that have to be chosen from two options: bidirectional (if the clutch halves rotate in opposite directions) or unidirectional (if the clutch halves rotate in the same direction), depending on the real clutch condition. In this case, the bidirectional option was chosen to simulate the real clutch condition that can rotate in opposite directions. The next parameter is the number of friction surfaces (z). Here, the number of friction surfaces between the clutch discs is entered. Furthermore, the average friction radius (r_m) is required (in meter), which represents the fictitious tangent point of the radial friction force of the clutch friction pair. This radius is calculated using the following formula:

$$r_m = \frac{2(r_o^3 - r_i^3)}{3(r_o^2 - r_i^2)} \tag{4.2}$$

with r_o as the outer radius of the clutch disc and r_i the inner radius of the clutch (both in meters). The fourth parameter is the peak or maximum normal force ($F_{N\,Peak}$) of the clutch when engine torque is transmitted. In addition, the coefficient of friction (μ) is entered via a lookup table since this coefficient is a speed-dependent coefficient, which depends on the different angular velocities between the clutches disc halves as shown in Figure 4.2. Another important configuration value is the static friction peak factor. That factor is a multiplication factor by which the sliding friction is multiplied at a differential speed of zero to determine the static friction torque.

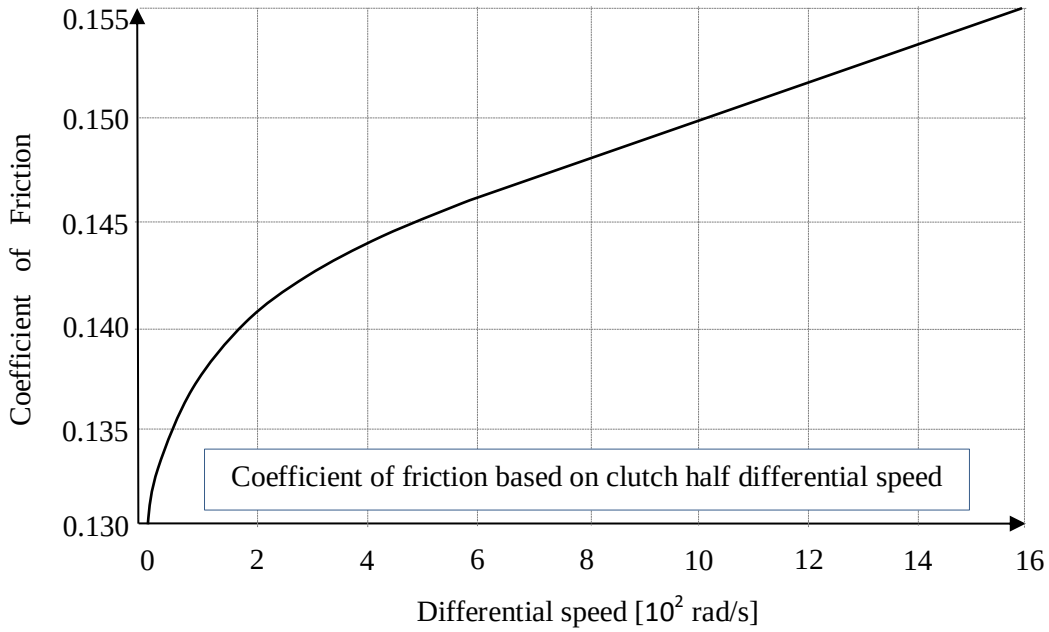

Figure 4.2: Coefficient of friction.

In the background of the controllable friction clutch block from Simscape uses a Matlab program to calculate the clutch torque in the sliding phase regarding to the input parameters with the following equation:

$$T_{Sliding\ Clutch} = z \,.\, r_m \,.\, \mu \,.\, F_{N\ Peak} \,.\, Normal\ force\ signal \tag{4.3}$$

Furthermore, if the clutch is locked or engage (differential angular velocity = 0), the torque transmitted is calculated using the following formula:

$$T_{Locked\ Clutch} = (static\ friction\ peak\ factor) * T_{Sliding\ Clutch} \tag{4.4}$$

To model the dual clutch system as realistic as possible, the transmission efficiency (the ratio of the output power compared to the input power from the engine) is also taken into account in the simulation. The transmission efficiency is around 95% due to friction losses, oil drag losses, oil churning losses and other losses. The loss of efficiency or torque loss due to the drag torque is modeled with a Simulink gain block. A SimDriveline torque sensor block is built into the transmission input shaft to measure the torque on the clutch disk. Furthermore, the torque without losses is multiplied by a gain block with a value of -0.05 as a drag torque then withdrawn through a torque actuator block to the transmission shaft.

To improve the modelling accuracy of the system, the rotational inertia of the individual gear shafts (intermediate shafts) was added. An inertia block for a drive shaft is connected to the transmission shafts with an updated rotational inertia value of the wet DCT drive shafts. At the end of the sub-transmission, a SimDriveline torque sensor block was installed in order to

determine the torques of the two partial transmissions before it was transmitted to the rear axle through the propeller shaft.

4.1.3 Synchronizer

The synchronizer model is modelled using a Simulink block which is derived from the five phases of the engagement process as a function of sleeve axial displacement from its neutral position towards the gear hub as depicted in Figure 4.3. The five phases are sleeve neutral position breaking, speed synchronization, ring unblocking, hub indexing and spline locking.

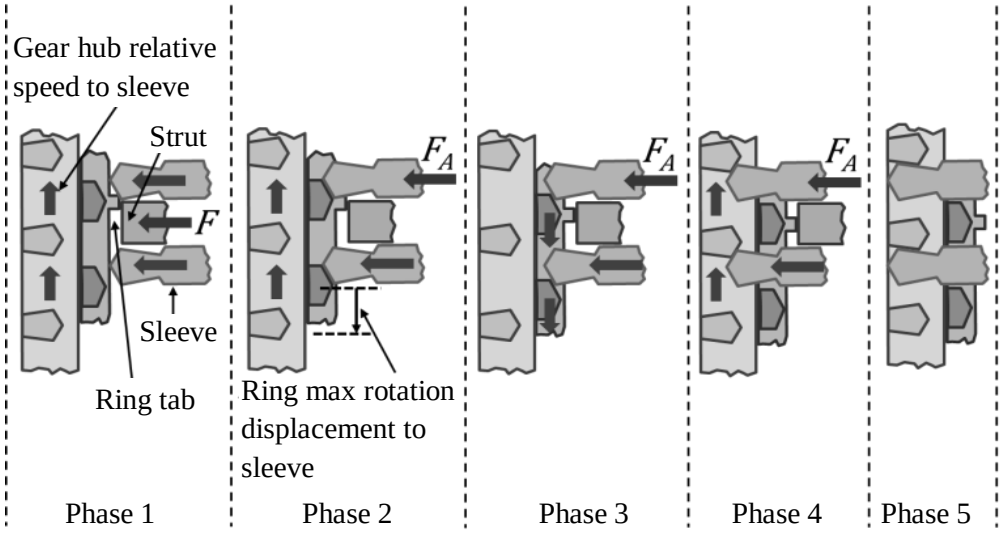

Figure 4.3: Five phase of synchronizer engagement process.

In the first phase, the sleeve is pushed by a hydraulic gear lever actuator with an axial force F_A toward the gear hub. This initial force rises until the break through the load (BTL) value is exceeded in order to overcome the resistance of the strut spring force that holds the sleeve on its neutral position. The BTL can be described as [116]:

$$BTL = 3.F_R.\left(\frac{\mu_{str}+\tan\theta}{1-\mu_{str}\tan\theta}\right) \tag{4.5}$$

where F_R is the reaction force of the strut spring, μ_{str} the friction coefficient between strut and sleeve detent groove- and θ the sleeve detent ramp angle. Before the axial force F_A value reaches the BTL, the sleeve brings the strut to push the ring tab and start squeezing the oil film in cone clutch friction surface [141] and creating a cone torque T_C that can be described as:

$$T_C = 4.\pi.R_C^3.b.\left(\frac{\omega_S}{h}\right) \qquad for \;\; x_S < X_0 \tag{4.6}$$

where R_C is the cone mean radius, b the width of the cone contact surface, ω_S the cone slip speed, h the film thickness, x_S the sleeve displacement and X_0 the minimum sleeve displacement for cone contact.

In the second phase, the sleeve is sliding towards the gear hub after the axial force F_A has exceeded the BTL. The movement will be stopped when the sleeve sliding movement is blocked by ring spline chamfer. The tangential force F_{tan} in the ring spline, which is a reaction of the axial force F_A (see Figure 3.6 (b)), creates a chamfer torque T_B that can be derived as

$$T_B = F_A . R_I . \left(\frac{1-\mu_I \tan\beta}{\mu_I + \tan\beta}\right) \tag{4.7}$$

where R_I the chamfer pitch radius, μ_I the friction coefficient of the chamfer and β the chamfer angle. At the same time, the axial force F_A will also create a cone torque T_C synchronizing the targeted gear speed that can be calculated as:

$$T_C = \frac{\mu_C . F_A . R_C}{\sin\alpha} \qquad for\ x_S \geq X_o\ and\ \omega_s \neq 0 \tag{4.8}$$

where μ_C and α are the cone friction coefficient and angle, respectively.

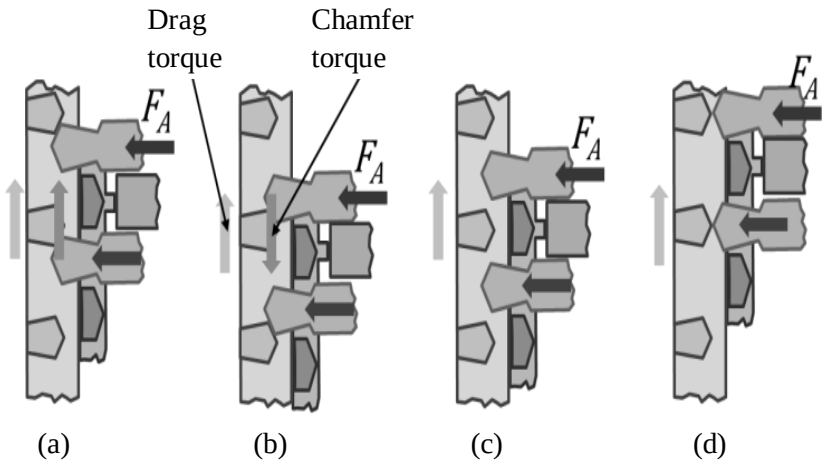

Figure 4.4: Four possibilities of the gear hub spline indexing.

In the third phase, the ring unblocking is started when the chamfer torque T_B exceeds the cone torque T_C. The axial force F_A through the sleeve spline chamfer rotates and pushes the ring as a cone clutch for finishing the speed synchronization process during ring unblocking. The cone torque T_C at the end of the speed synchronization is:

$$T_C = T_D + I_{FW} . \alpha_{FW} \qquad for\ x_S \geq X_0\ and\ \omega_s = 0 \tag{4.9}$$

where T_D is the drag torque, I_{FW} the freewheeling inertia and α_{FW} the angular acceleration of the freewheeling component. The drag torque T_D is a total resistance torque comprising all resistances from the bearings, seals, gears and friction which can be written as:

$$T_D = -sign(\omega_G).(T_W + T_F + T_B).-sign(\Delta\omega_{CL}).(T_{SH} + T_B \ + T_{CL}) \tag{4.10}$$

where ω_G is the gear speed, T_W the gear windage torque, T_F the gear tooth friction torque, T_{SF} the shaft drag torque, T_{CL} the clutch drag torque and $\Delta\omega_{CL}$ the clutch slip speed.

In the fourth phase, the sleeve continues to slide towards the gear hub until it is blocked again by the gear hub spline chamfer. The gear hub splines are randomly aligned to the sleeve splines as shown in Figure 4.4. Therefore, there are four possible schemes that can be obtained in this step. The first one is when drag torque and chamfer torque have the same direction, as shown in Figure 4.4 (a). In this case, the need of the axial force to finish the spline engagement will significantly be reduced. Meanwhile, the second possibility occurs when the drag torque suffers the axial force to unblocking and finishes the spline engagement as shown in Figure 4.4 (b). The phenomenon of this axial force suddenly rising is known as a second bump. The third possibility, however, shows the best alignment without any chamfer torques as shown in Figure 4.4 (c). The worst possibility, on the other hand, is achieved with tip-on-tip spline alignment. In this case, the synchronizer will block out or fail to lock the gear hub splines as shown in Figure 4.4 (d). The spline tip is designed as sharp as possible to avoid a surface contact when tip-on-tip spline alignment occurs. Thus, the sleeve can still continue to slide and unblock the sliding way. There are four indexing torque T_I equations regarding to the gear hub spline alignments which can be described in Equation 4.11. The sleeve is then fully locked with the gear hub spline in the fifth phase after passing the gear hub splines blocking.

$$T_I = \begin{cases} F_A.R_I.\left(\frac{1-\mu_I \tan\beta}{\mu_I+\tan\beta}\right) & for\ +T_D\ ,+T_I\ \ direction \\ F_A.R_I.\left(\frac{1+\mu_I \tan\beta}{\mu_I-\tan\beta}\right) & for\ +T_D\ ,-T_I\ \ direction \\ -F_A.R_I.\left(\frac{1+\mu_I \tan\beta}{\mu_I-\tan\beta}\right) & for\ -T_D\ ,+T_I\ \ direction \\ -F_A.R_I.\left(\frac{1-\mu_I \tan\beta}{\mu_I+\tan\beta}\right) & for\ -T_D\ ,-T_I\ \ direction \end{cases} \tag{4.11}$$

The spline chamfer angle (α) is designed to create enough friction force on the cone friction surface to stop the slip between the ring and the gear hub before the sleeve continues to slide again towards the gear hub. Increasing the spline chamfer angle will decrease the friction force on the cone friction surface and reduce the effectiveness of speed synchronization. On the other hand, lowering the spline chamfer angle will increase the axial force needed to

unblock the synchronizer ring blocking. In order to increase the speed synchronization effectiveness, more friction surface areas can be created by using more than one cone as used in this particular longitudinal seven-speed wet DCT. In that system, a triple cone synchronizer system is used for the lower gears (i.e. the 1st, 2nd, 3rd and reverse gear) which have a relatively high drag torque compared to the higher gears (4th,5th, 6th and 7th gear).

4.1.4 Vehicle Resistance

To be able to move, a vehicle engine must overcome the vehicle resistances which are coming from ambient air, road gradient, rolling components and vehicle acceleration as shown in Equation 4.12.

$$F_{Resistance} = F_{Road\ Gradient} + F_{Air\ Drag} + F_{Rolling} + F_{Acceleration} \tag{4.12}$$

In reality, the engine power required- to overcome the resistances mentioned above is only transmitted to the driving wheel through the transmission system. Based on this condition, all of the vehicle resistance is now modelled in the driving wheel which directly encounter by the engine power. In terms of gear shift quality assessment, only the longitudinal movement of the vehicle is considered in the model while other movements such as cornering or horizontal maneuvers, are neglected to decrease the model complexity and to increase the time efficiency.

The road gradient resistance ($F_{Road\ Gradient}$) is calculated from the road gradient angle (α) and the vehicle mass ($m_{Vehicle}$), as presented in the following Equation:

$$F_{Road\ Gradient} = \sin\alpha \,.\, m_{Vehicle} \,.\, g \tag{4.13}$$

Furthermore, the air resistance ($F_{Air\ Drag}$) is calculated according to the following Equation:

$$F_{Air\ Drag} = c_D \,.\, \frac{\rho_{air}}{2} \,.\, A_{Vehicle} \,.\, (V_{Air\ Relative})^2 \tag{4.14}$$

This air resistance force is for a vehicle with a certain frontal area ($A_{Vehicle}$) which moving with a certain speed in the surrounding air movement ($V_{Air\ Relative}$) in m/s and have an aerodynamic drag coefficient (c_D). The aerodynamic drag coefficient (c_D) depends on the vehicle shape and range from a small value of around 0.25 for a sporty car to around 1.1 for a truck. This air resistance force increases with the square of the relative air flow velocity around the vehicle ($V_{Air\ Relative}$). In no wind condition, this relative air flow velocity is equal to the vehicle speed.

The next resistance is the rolling resistance, which caused by the deformation of the tire and the road surface due to the vehicle mass. It is calculated using the speed dependent rolling

resistance coefficient (f_R). The rolling resistance coefficient is a dimensionless parameter that depends on the tire characteristics and road conditions. At high speeds, the rolling resistance increases significantly and is calculated using the following Equation:

$$F_{Rolling} = f_R . m_{Vehicle} . g \tag{4.15}$$

The acceleration resistance force ($F_{Acceleration}$) caused by the mass and inertia of the vehicle and the rotating parts of the drive train is not given here because it was already considered in the Simscape model by a special inertia block.

The subsystem that is made of a combination of Simscape and Simulink models of propeller shaft, differential gear, wheels and vehicle resistance. The input for this subsystem model is the double clutch transmission output torque, which rotates the rear wheel through propeller shaft and differential gears. The Simulink driving resistance subsystem gives an output as vehicle speed and acceleration that is calculated from the rotational speed of the rear wheels. Furthermore, a gain block to negate the driving resistance torque is applied after the Simulink driving resistance block before it goes back to the rear axle via a torque actuator block to subtract the drive torque in a feedback loop.

The propeller shaft is modelled using a standard torsional spring damper block of Simscape. This block represents the torsional elasticity of a long shaft in the drive train during acceleration against the driving resistance. The stiffness and damping value as torsional parameters of the block are aligned, adjusted and evaluated with regard to the corresponding properties of the vehicle. Furthermore, the differential gear is modelled using a standard simple gear block from Simscape after the propeller shaft. The tested vehicle differential final gear ratio is 3.15 and added to the simple gear block parameter. To account for the inertia of the vehicle, an inertia block was connected to the rear axle shafts. In addition, the vehicle inertia is calculated from the vehicle's weight and tire radius using the following Equation:

$$I_{Vehicle} = m_{Vehicle} . r_{Tire}^2 \tag{4.16}$$

The mass of the vehicle, including the driver, is 1735 kg and the tire radius is 0.307 meters, giving a vehicle's inertia value of around 163 kg.m. Furthermore, the speed sensor block of Simscape is added to the rear axle before it goes to the speed dependence of vehicle resistance block that is modelled in the Simulink form through the Simulink gain block. The Simulink gain block converts the Simscape speed sensor output in rad/sec to km/h by multiplying it with the tire radius and conversion factor.

There are only two (out of four in total) driving resistances that are considered in this model: aerodynamic drag and rolling resistance. The road gradient resistance is neglected due to the

fact that the vehicle drives in the zero road gradient. The acceleration resistance is also neglected because the vehicle inertia system already includes the model as a Simscape inertia block as explained before. Furthermore, the vehicle speed signal is divided into the yellow block to calculate the air resistance and the cyan block to calculate the rolling resistance.

The air resistance is calculated using Equation 4.14. The speed signal in km/h is converted to m/s through a gain block and then squared by a math block. To fulfill Equation 4.14, the squared vehicle speed is multiplied with the vehicle coefficient drag, vehicle frontal area and the half of air density with the value of 0.28, 2.15 and 0.601, respectively.

The rolling resistance force (F_{Roll}) is calculated using Equation 4.15. The vehicle- mass ($m_{Vehicle}$) is filled with the driver's weight (85 kg) and the vehicle's curb weight (1650 kg). In addition, the speed-dependent rolling resistance -coefficient (f_R) is determined in the subsystem named rolling resistance coefficient, using this following Equation [73]:

$$f_R = 0.01 + 0.002 \frac{v}{100} + 0.0004 \left(\frac{v}{100}\right)^4 \tag{4.17}$$

A fixed coefficient of 0.01 is always used to calculate the rolling resistance coefficient in the summing point. Additionally, there is a second coefficient of 0.002 which is multiplied by the velocity then divided by 100. A third coefficient of 0.0004 is multiplied by the fourth power of vehicle velocity in the calculation.

4.2 Model of Electro-Hydraulic System and Shift Element

The electro-hydraulic system of a double clutch transmission is modeled and discussed in detail in this chapter, particularly with regard to the dual clutch and synchronizer actuation systems. It plays an important role of the gear shift quality as well as the odd/even gear set engagement to its double clutch through the synchronizer system. The chapter also describes the hydraulic circuit, which consists of the pressure and the drain line. The pressure line connects the hydraulic pump that generates the hydraulic pressure to the chamber of the clutch and the synchronizer actuator system. The drain line, on the other hand, connects the actuator chamber to the oil tank to reduce the actuator chamber pressure.

4.2.1 Spool Dynamics in the Solenoid Valve

The electro-hydraulic valves of the clutch pressure control are an important factor which directly affects the gear shifting process of the dual clutch transmission. The entire electro-hydraulic subsystem model does not only consist of the solenoid valve, but also includes the

oil pump, the oil channel circuit and the clutch actuator piston. In Chapter 3.6, the physical principles for the structure and dynamics of an electro-hydraulic valve, particularly the valve spool, were developed. Those valve spool physical principles are now implemented in a Simulink model.

The input variable for the valve spool dynamics model is the electric current from the transmission control unit to generate the magnetic force ($F_{Magnetic}$) in the solenoid. Furthermore, the generated electromagnetic force slides the valve spool to open or close the valve inlet or outlet orifice. The magnetic force also has to overcome the resistance forces, which are the initial spring preload resistance force ($F_{Initial}$), the damping resistance force ($F_{Damping}$) and the spring resistance force (F_{Spring}). Furthermore, the valve -spool dynamic are described using the following acceleration equation:

$$\ddot{x}_s = \frac{1}{m_s} * \left[F_{Magnetic} - F_{Initial} - F_{Damping} - F_{Spring}\right] \tag{4.18}$$

where m_s is the spool mass in kilograms and x_s, $\dot{x}_s$, $\ddot{x}_s$ the spool position, spool velocity and spool acceleration.

The correlation of the electric current flows to the valve solenoid to generate the magnetic force is linear, thus, the magnetic force arises depend on the applied current (I in milliamps) that flowing to the valve solenoid and can be calculated using this equation:

$$F_{Magnetic} = k_c * I \tag{4.19}$$

with k_c as a constant factor that converts the current value (I) into the force (in Newton). Furthermore, the magnetic force has to overcome the first resistance force acting on the valve spool which is the spring force ($F_{Initial}$). That force exists due to a preload of the spring that is installed in the system. That parameter was also modified or adjusted in the simulation setup to produce an accurate simulation.

The next resistance force that has to be overcome by the magnetic force is the spring force (F_{Spring}) of the valve spool spring. That force depends on the spool movement that will push the spring and can be described using the following equation:

$$F_{Spring} = k_s * x_s \tag{4.20}$$

The experiment showed, that the spring stiffness (k_s) is about 444.4 N/m. That parameter was later adjusted in the simulation and shows that the dynamics of the real spool sliding movement correspond sufficiently.

The oscillation of a spring mass which represents the valve spool movement normally will cause a damped vibration. This damped vibration must be considered to ensure the disturbing

performance of the system is captured in the model. Thus, the next resistance force that has to be overcome by the magnetic force is the damping force ($F_{Damping}$) of the valve spool. That damping force includes all frictional forces acting on the valve spool including the viscous friction. The damping force attenuation is proportional to the spool speed ($\dot{x}_s$) thus can be written as:

$$F_{Damping} = d_s * \dot{x}_s \tag{4.21}$$

with d_s as the damping coefficient. Furthermore, the equation for the damping coefficient of longitudinal vibrations can be expressed as [138]:

$$d_s = 2 * m_s * \delta \tag{4.22}$$

while the decay constant (δ) is calculated using the following equation:

$$\delta = D * \omega_0 \tag{4.23}$$

According to [138], the damping value (D) of 0.7 is a good compromise for a lightly damped oscillation. Furthermore, the natural angular frequency (ω_0) of an undamped oscillation is derived from the root of the ratio of the spring stiffness of the valve spring (k_s) and the valve spool mass (m_s) as follows:

$$\omega_0 = \sqrt{\frac{k_s}{m_s}} \tag{4.24}$$

The damping coefficient (d_s) in Equation 4.22 can be rewritten by inserting all the other parameters of Equation 4.23 and 4.24 as follows:

$$d_s = 2 * D * \sqrt{m_s * k_s} \tag{4.25}$$

The result for the damping coefficient (d_s) from the optimum damping value D of 0.7, the valve spool mass (m_s) of 0.0016 kilograms and the spring stiffness (k_s) of 444.4 N/m is 1.18 Ns/m.

Furthermore, Equation 4.18 can be rewritten by inserting Equations 4.19, 4.20 and 4.21 as follows:

$$\ddot{x}_s = \frac{1}{m_s} * [k_c * I - F_{Initial} - d_s * \dot{x}_s - k_s * x_s] \tag{4.26}$$

That model of the valve spool dynamics has an input of an electric current (I), to give an output of a valve spool sliding distance (x_s). The constant parameter (i.e. spool mass, dimension of component) of the wet DCT is obtained from the DCT component measurement at the workshop. All forces as described in Equation 4.26 are summed up in the

Simulink add block with the magnetic force as a positive value (as described in Equation 4.19). The other acting forces are connected to the minus port of the Simulink add block to subtract the magnetic force as a resistance force. The damping force ($F_{Damping}$) is the first-resistance force that is connected to the minus port of the Simulink add block while the spring force (F_{Spring}) is the last resistance force connected to it after a constant value of the initial spring preload resistance force ($F_{Initial}$). The gain block that follows is placed after the add block to multiply the combined forces with the reciprocal of the valve spool mass. The wave signal value after the gain block is the acceleration of the valve spool ($\ddot{x}_s$) and becoming as a valve spool velocity ($\dot{x}_s$) after integration by the integrator block. Therefore, after the first integrator, the spool velocity was tapped and multiplied by the damping coefficient (d_s) to generate the damping force ($F_{Damping}$) before it goes back to the summing point. The spool travel (x_s) is obtained after further integration of the valve spool velocity ($\dot{x}_s$). Furthermore, the spring force (F_{Spring}) is taken into account by returning the signal wave line of the spool travel (x_s) and multiplying it with the spring stiffness (k_s).

Depending on the type of solver and the simulation steps entered in the Simulink simulation settings, the loops are calculated and processed in fixed or variable increments several thousand times per second. This simulation sets a solver with a fixed step and a step size of 0.001. This increment means that the feedback loop through 1000 times per second are calculated. After varying the step size several times, it was found that it had a significant impact on the simulation result. In fact, an accurate simulation result was only obtained at a sampling rate of 1000 per second. From the measurement, it is known that the maximum valve spool travel in the valve casing is 2.1 millimeters. To implement that maximum travel into the model simulation, the Simulink saturation block is used to limit the calculation of the spool travel to the maximum value of 2.1 millimeters.

4.2.2 Solenoid Valve Discharge

The oil flow discharge from the solenoid control valve is controlled by the electric current in the valve solenoid. Furthermore, the generated magnetic force in the valve solenoid will slide the valve spool to control the oil flow against the variable hydraulic resistance through the valve orifice. The hydraulic resistance is comparable to the resistance of a simple sharp edged orifice [90]. The orifice opening cross section area is variable and depends on the valve spool position. Thus, the second layer model subsystem of solenoid valve discharge is modeled on the relationship between the valve spool position (x_s), the valve orifice opening area ($A_{op}(x_s)$) and the valve orifice closing area ($A_{cl}(x_s)$). The valve spool is distributed radially over its circumference, which covers the valve orifice hole with a diameter of 3.4 millimeters.

Through this orifice hole, the hydraulic oil can flow either to the oil tank or to the clutch piston chamber. As already described in Chapter 3.6, the characteristic of the orifice opening area ($A_{op}(x_s)$) is a response of the valve spool position (x_s) as a curve as shown in Figure 3.18. All of those valve dimensions are obtained from the measurements of the removed valve spool.

It is shown in Figure 3.18 that the oil channel from the clutch piston chamber will be connected to the channel of the oil tank if the axial distance between the two outer edges of the orifice hole of 0.85 mm is traveled by the valve spool from the neutral rest position to the left side. Thus, the clutch piston chamber will be drained until this distance. On the other side, the connection between the hydraulic system pressure channel of the oil pump to the clutch piston chamber is opened, once the valve spool is pushed by the magnetic force to a distance of more than 0.85 mm from its neutral rest position to the right side. The solenoid valve will therefore discharge the hydraulic oil to the piston clutch chamber. The maximum orifice opening area ($A_{op}(x_{s\,max})$) is obtained at a maximum valve spool displacement of 2.1 mm from the neutral rest position to the left side as well as to the right side. Furthermore, the orifice opening characteristic as a function of the valve spool displacement is modeled in the Simulink and Simscape model.

The input signal for the Simscape solenoid valve discharge is coming from the output signal of the Simulink spool dynamics model. The output signal of the spool dynamic model is a unit-less Simulink signal that should be converted into the Simscape physical signal through a "Simulink-PS Converter" block before it goes to the Simscape solenoid valve discharge model. Furthermore, the Simscape input signal line splits into two separate paths. The first path is for the filling of the clutch piston chamber while the second path is for the draining. The latter is started when the valve spool move between 0 and 0.85 mm from the neutral rest position to the left side, while the filling is started when the valve spool displacement is larger than 0.85 mm from the neutral rest position to the right side. Furthermore, the first path of the Simscape physical signal of valve spool displacement (x_s) goes to the one dimensional lookup table to be converted as a value of the orifice opening area ($A_{op}(x_s)$) for filling of the clutch piston chamber. The displacement distance of the valve spool is ranging from 0 to 2.1 mm as an input for the Simscape lookup table block. The displacement distance is divided with an interval of 0.05 mm in the lookup table to present the characteristic of the orifice opening area ($A_{op}(x_s)$) from each vector value input of the valve spool displacement. The same procedure is applied to the second path of the Simscape signal for the draining of the clutch piston chamber.

After the surface of the orifice opening or closing area was generated by the one dimensional lookup table for clutch filling and emptying, they are passed as a physical input to the standard Simscape "variable orifice" block available in the Simscape sub-library named SimHydraulics. The SimHydraulics library contains various hydraulic components for the simulation of hydraulic systems, such as pipes, hydraulic cylinders, valves, pumps, various covers and other typical hydraulic elements. The calculation formulas for the components are hidden behind the blocks. Furthermore, the typical characteristics of the components can be adjusted via a graphical configuration interface. The variable orifice block is very well suited to simulate a volume flow as the changing of the orifice opening areas. For this purpose, the Simscape block has three port terminals: the “AR” port for a physical signal link which consist a value of the orifice opening/closing area and the other two ports “A” and “B”, which are the hydraulic channel connection. Furthermore, an oil flow is generated due to a pressure difference that exists between the two hydraulic connections.

Port A of the upper variable orifice block is connected to the oil sump through the oil pump which generates the oil pressure to actuate the clutch piston. Port B on the other side of the block- connects the solenoid valve to the piston clutch chamber. Thus, the oil flows from the oil pump to the piston clutch chamber. The variable orifice block calculates the oil flow rate based on the flow coefficient α of the pump and the oil density (ρ_{oil}), resulting in the following flow rate formula:

$$Q_{Discharge} = \alpha * A(x_s) * \sqrt{\frac{2*\Delta p}{\rho_{oil}}} \tag{4.27}$$

On the other hand, the lower second variable orifice block works in the reverse direction to drain the clutch piston chamber. The higher pressure is in the valve port A from the piston chamber while the valve port B is connected to the oil tank, which has an atmospheric pressure of 1 bar. Thus, the oil discharge is from the piston clutch chamber of the oil sump.

For measuring the pressure in the clutch piston chamber, a hydraulic pressure sensor is installed behind the two variable orifices blocks. The pressure sensor is also a standard SimHydraulics block from the Simscape sub-library. The pressure sensor measures the pressure difference between the two hydraulic connections of the clutch piston chamber and the hydraulic oil tank with a reference of the atmospheric pressure, then gives a physical pressure signal. Furthermore, the pressure build-up measured in the clutch piston chamber is implemented in the clutch piston subsystem as a mechanical movement of the clutch piston.

4.2.3 Oil Pump

This chapter describes the oil pump of the mechatronic hydraulic circuit which consists of the pressure and the drain line. The pressure line connects the hydraulic pump that produces the hydraulic pressure to the chamber of the clutch and the synchronizer actuator system. On the other hand, the drain line connects the actuator chamber to the oil tank to reduce the actuator chamber pressure. The output of the oil pump subsystem is the hydraulic pressure and the input a supply pressure value. This oil pump subsystem forms an oil pump circuit with a connection to the oil tank. To establish the hydraulic oil flow, a SimHydraulic block is needed to simulate the properties of the oil. The SimHydraulic block is called “custom hydraulic fluid“ where the typical characteristics of the hydraulic oil, such as density, viscosity, compressibility and enclosed air volume, can be adjusted through a graphical configuration interface. Furthermore, an oil tank is connected to the circuit to receive the hydraulic oil from the actuator chamber during the decrease of the actuator chamber pressure. The atmospheric pressure in the oil tank is 1 bar and its volume is infinitely larger compare to the oil channel lines and the piston chamber.

In addition, a Simscape block named "ideal hydraulic source" is used as an oil pump to generate the main hydraulic pressure in the oil circuit. That oil pump generates a hydraulic flow of the main pressure in the system based on an input pressure signal. Here, the block relates to the volume of oil from the oil tank and amplifies the oil by the atmospheric pressure to the required supply pressure. It is also possible to feed the pressure signal to the Simscape oil pump block as the measured variable of the transmission power which drives the oil gear pump. This significantly improves the accuracy of a pressure generation in the clutch piston chamber when simulated in variable engine RPM. The hydraulic pressure in the transmission depends on many factors, such as the transmission temperature, the drive torque and the input speed. However, a constant supply pressure of 8 bars was found to be realistic enough for the short duration of the simulation of gear shifting. Furthermore, the solver configuration block is included in this physical system to set the simulation.

4.2.4 Clutch Piston Dynamics in the Double Clutch System

The clutch piston dynamics subsystem is modeled after the model of the solenoid valve and the oil circuit. The subsystem connects the hydraulic power that is generated and controlled by the solenoid valves to the mechanical clutch torque that is generated due to the pressure built up in the clutch piston chamber. The input variable for the clutch piston dynamic subsystem is the solenoid valve discharge to the clutch piston chamber as explained in Chapter 4.2.2 and the output variable the normal force on the clutch disc.

The solenoid valve discharges the hydraulic oil to the clutch piston chamber to build up the chamber pressure. Furthermore, the pressure built up in the clutch piston chamber presses the clutch disc with a certain clutch piston force (F_{Piston}) through the clutch piston system including its return spring and piston seal. The normal force (F_{Normal}) on the clutch disc is obtained from the equation of the clutch piston movement by considering all the forces acting on the clutch piston as shown in Figure 3.5 and as described in Chapter 3.2 as follow:

$$F_{Normal} = F_{Friction} = F_{Piston} - F_{Clutch\ Disc} - m_P\ddot{x}_P - d_P\dot{x}_P - k_p x_P \qquad (4.28)$$

where m_P is the clutch piston mass in kilograms and $x_P, \dot{x}_P, \ddot{x}_P$ the clutch piston position, clutch piston velocity and clutch piston acceleration respectively. Furthermore, by expressing the clutch piston force (F_{Piston}) with the Equation 3.5, the above-mentioned Equation 4.28 can be rewritten as follows:

$$F_{Normal} = F_{Friction} = P_P A_P - F_{Clutch\ Disc} - m_P\ddot{x}_P - d_P\dot{x}_P - k_p x_P \qquad (4.29)$$

The normal force on the clutch (F_{Normal}) is converted into the clutch torque (T_C) that is a transmitted engine torque by the clutch disc as described in Equation 2.1 & 3.1.

The generation of the clutch piston force is in the Simulink model. Initially, the clutch piston chamber pressure unit is converted from bar to Pascal before it goes to the Simulink multiplier block. For the purpose of converting the pressure unit, the Simulink gain block is added after the clutch piston chamber pressure block. Furthermore, the clutch piston chamber pressure is multiplied with the piston surface area in the Simulink multiplier block to create the clutch piston force (F_{Piston}) as described in Equation 3.5. Furthermore, the clutch piston force in Simulink wave form is transferred to the Simscape physical signal through a Simulink-PS converter block before it goes to the piston model system. This is necessary because the piston system (coloured in yellow) is largely composed of physical Simscape components.

The piston mass is added to the clutch piston model using a Simscape mass block. The mass of the piston of clutch 1 is known from measurements, 750 grams. Furthermore, a force is generated on the piston mass through a Simscape block named "Ideal Force Source". That block generates a force proportional to the input signal. The input signal is calculated at a summing point and consists of the pressure force acting on the piston subtracted with the force that through the clutch disc stiffness together.

The embedded MATLAB function block calculates the drag of the clutch disc stiffness ($F_{Clutch\ Disc}$) existing in the clutch disc. The generated drag corresponds with the position of the clutch piston that is measured by a Simscape motion sensor. Furthermore, the Simulink output signal from the embedded Matlab function block return to the Simscape sum block through a Simulink-PS converter block. The drag of the clutch disc stiffness ($F_{Clutch\ Disc}$)

from the embedded MATLAB function block arises only when the clearance between the clutch discs is overcome. Moreover, the drag ($F_{Clutch\ Disc}$) arises following the exponential graph as shown in Figure 4.5.

The "Translational Spring" and "Translational Damper" Simscape block is used to simulate the coil spring and the damping force of the clutch piston system. Both blocks are connected to the piston mass by Simscape lines. The "Translational Spring" block represents a mechanical coil spring with the adjusted value of the spring stiffness and the initial spring strain. The spring stiffness is known from measurements (1.6e5 N/m). The "Translational Damper" block is used to represent the damping force of the piston.

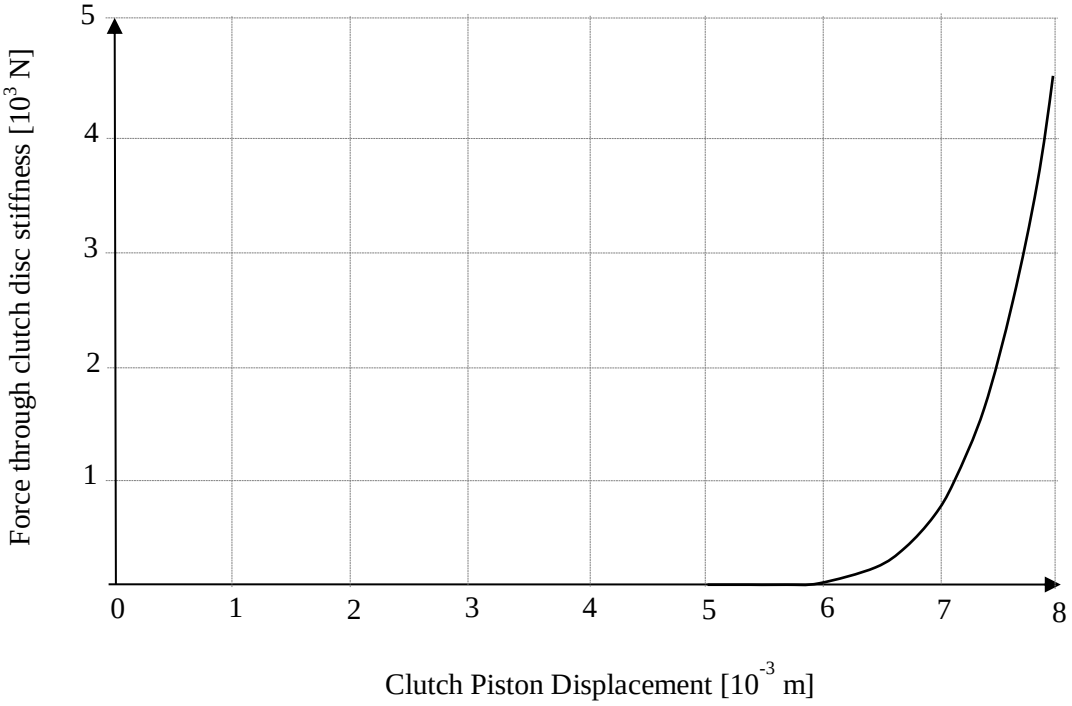

Figure 4.5: The characteristic of the clutch disc stiffness drag force which correspond to the clutch piston displacement [10].

To guarantee the Simscape simulation can be run successfully, the Simscape "Solver Configuration" block is included in the physical system model. The green part of the subsystem is used to determine the normal force which then generates the friction force between the clutch discs. The normal force corresponds to the drag of the clutch disc stiffness ($F_{Clutch\ Disc}$) that was generated by the embedded MATLAB function and- to the clutch piston force (F_{Piston}) minus spring force ($k_p x_P$) and damping force ($d_P \dot{x}_P$). The spring force ($k_p x_P$) and the damping force ($d_P \dot{x}_P$) in the mechanical system model are measured by the Simscape force sensors block before being transffered to the physical signal PS-add block. The PS-add block summarizes the two forces (spring and damping force) before it goes to the next PS-add block to subtract the clutch piston force (F_{Piston}). The output signal from the

clutch piston dynamics subsystem is the normal force on the clutch disc which is then fed into the model of the transmission.

4.3 Gear Shifting Control

The gear shifting process in a double clutch transmission (DCT) is controlled by the transmission control unit (TCU) that is located in the mechatronics module as shown in Figure 4.6. The gear shift command is triggered automatically based on the shift map program in the TCU or manually by the driver through the shift paddle, which activates the transmission control unit in order to control the dynamics of the shifting process through the electro-hydraulic solenoid valves. The solenoid valves then generate an oil pressure in the actuator pistons of the gear selector and in the dual clutch actuator piston chamber. The oil pressure generated in the gear actuator pistons chamber moves the gear selector fork, which then moves the synchronizer rings to engage the on-going gears (preselection). On the other side, the oil pressure generated in the dual clutch actuator piston chamber will move the clutch piston to control the power shift as described in Chapter 3.2.

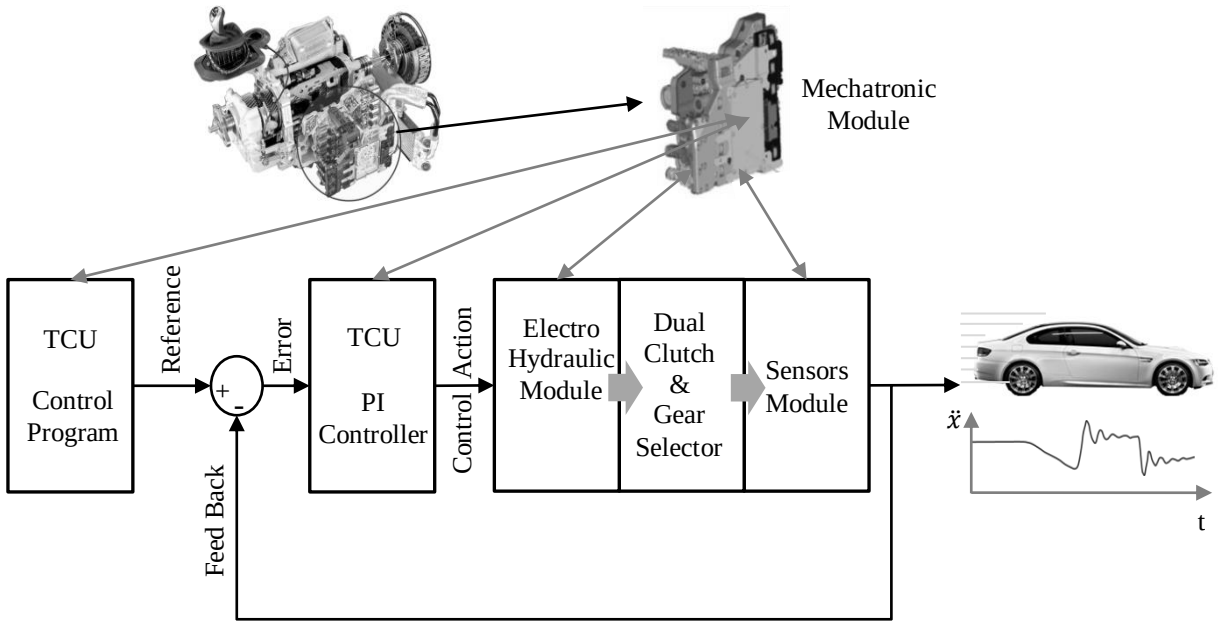

Figure 4.6: The closed-loop control strategy in the mechatronics module.

The TCU controls the dynamics of the dual clutch and the engaged gear using the closed-loop control strategy. To accomplish that strategy, the TCU measures the dynamics of the dual clutch and the engaged gear through several sensors in the mechatronics module as shown in Figure 3.11. The odd and even clutch speeds are measured by the input shaft speed sensors

while the pressure in their clutch piston chambers are measured by the clutch pressure sensors. Furthermore, the readiness of the preselected gear is known by the TCU through the gear selector rod position sensor. The TCU also obtains the engine speed data to calculate the slip that occurs in the clutch when the clutch speed is different from the engine speed.

The closed-loop control strategy minimizes the error between the measured values of the dual clutch pressure and the reference value that is presented as a reference line of pressure in the clutch piston chamber as shown in Figure 4.7. For this purpose, the proportional integral (PI) controllers are initialized to the last set value of the controller [10]. For a PI controller, the proportional term is defined by the proportional factor of the deviation or error, while the integral component arises from the difference between the last set point and the proportional action of the controller.

The detail of the reference control line is explained in this chapter, using the example of the upshift from 1^{st} to 2^{nd} gear. The reference control line to be followed by the pressure in the on-going and off-going clutch piston chambers are present after the existing of the up shift commands, which denoted by the rise of the gear activation status at t_1 in Figure 4.7 (g). At the same time (t_1), the gear selector engages the next or on-going gear (2^{nd} gear) through the synchronizer system. The gear preselection is finished when the next gear is fully engaged, denoted by the lock position of the gear selector in "T_On-going_Gear_Engagement" time. At t_1, the reference control line for the on-going clutch is raised for hydraulic oil fast filling into the clutch piston chamber with a "P_FF" pressure value during "T_FF" elapsed time. Furthermore, the "P_F" filling pressure is set to prepare the engagement of the on-going clutch. On the off-going clutch side, the clutch pressure decreases after a "T_off_s1" delay time to the level of "P_off_s" pressure for "T_off_s2" duration time with the intention of a slip in the off-going clutch. When the slip does not occur, the off-going clutch pressure is further lowered with the negative gradient "P_off_ramp" ramp.

The "P_engine_speed_regulator" control line starts after the "T_off_s3" time is elapsed the in overlap phase. This control line present simultaneously during the rising of pressure with positive gradient ramp "P_on_grad_1" on the on-going clutch side to control the initial slip in the off-going clutch. The decreasing pressure in the off-going clutch element and the increasing pressure in the on-going clutch are further done to the point at which the function of the off-going clutch slip control no longer works. To this end, the TCU the off-going clutch slip ensures that the off-going clutch pressure is reduced. The engine torque is simultaneously reduced during the overlap phase in the up shift process as described in Chapter 2.1.1. This engine torque intervention is done after the delay time "T_ETI_off_ramp" with a negative gradient ramp which is defined by the parameters "T_ETI" and "ETI_main". At the same time, the PI controller controls the engine speed profile to follow the target ramp.

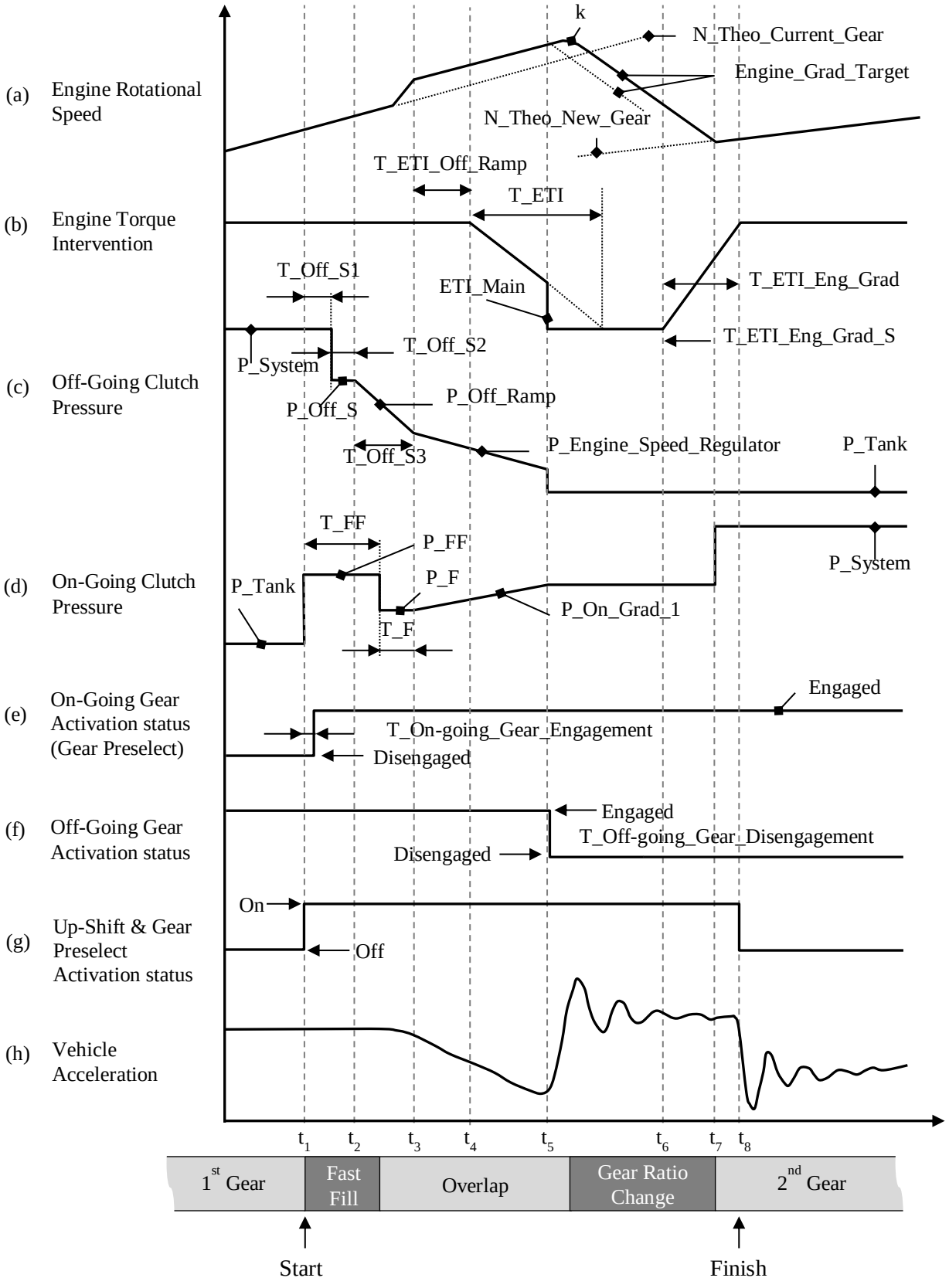

Figure 4.7: Reference control parameters in the TCU for up shift [10].

After the overlap phase, the gear ratio change phase of the engine torque transfer starts. The load is now taken entirely by the engaged on-going clutch and the off-going clutch pressure is further decrease to the pressure level of the oil tank. The beginning of the gear ratio change phase directly affects the peak-to-peak value of the longitudinal acceleration as shown in Figure 4.7. (h), which has an essential significance for the shifting comfort. The on-going clutch pressure must be further increased in t_7 so the speed adapts to the new path of the new gear ratio "N_Theo_New_Gear".

The initial controller parameters are not necessarily ideal for the entire up-shift process. Therefore, a change of those parameters as well as the target size is provided. If the gradient of the engine speed decreases below the target gradient, the controller will modify the parameters and the target gradient will be reinitialized at the same time. During the gear shifting, a calculation of the time and the expected remaining time is carried out continuously until the synchronization point is reached. The remaining time is required to calculate the start time "T_ETI_eng_grad_s" of the positive gradient reference ramp. Furthermore, the duration of that reference ramp is defined by the "T_ETI_eng_grad" parameters.

Table 4.1: Ten control parameters for up shift in the TCU program [10].

No.	Control Parameter	Description	Shift Phase
1.	P_On_Grad_1	Pressure gradient of on going clutch	Overlap
2.	Engine_Grad_Target	Gradient target of engine rotational speed	Gear ratio change
3.	k	Proportion of engine speed regulator	Gear ratio change
4.	T_Off_S1	Delay time of off going clutch pressure	Fast filling
5.	P_Off_S	Off going clutch pressure	Fast filling
6.	T_ETI	Start of engine torque intervention	Overlap
7.	T_ETI_Off_Ramp	Duration of off going clutch pradient pressure	Overlap
8.	ETI_Main	Engine torque intervention	Gear ratio change
9.	T_ETI_Eng_Grad_S	Start to rule the engine speed gradient	Gear ratio change
10.	T_ETI_Eng_Grad	Duration to rule the engine speed gradient	Gear ratio change

The initial controller parameters are not necessarily ideal for the entire up shift process. Therefore, a change of these parameters as well as the target size is provided. If the decrease of the gradient of the engine speed is below the target gradient, the controller will modify the

parameters and simultaneously the target gradient is reinitialized. During the gear shift, a calculation of the time and the expected remaining time is carried out continuously until reaching the synchronization point. This remaining time is required to calculate the beginning time “T_ETI_eng_grad_s” of the positive gradient reference ramp. Furthermore, the duration of this reference ramp is defined by the “T_ETI_eng_grad” parameters.

Overall, the reference control line has approximately 25 to 30 parameters that have an influence on the shifting comfort and spontaneity. That number of influencing variables is clearly too high for the planned DCT shifting optimization process, therefore, only ten of them are used with regard to the work done in [10]. Those ten control parameters are listed in Table 4.1.

4.4 Data Collection for Model Verification

After offsetting up the drivetrain model, the next step is to verify the model system performance to ensure the fidelity of the model. For this purpose, the model output is compared to the performance of the real vehicle. The performance is obtained from the measurement of vehicle performance parameters, such as vehicle speed, vehicle acceleration, engine speed, current gear, etc.

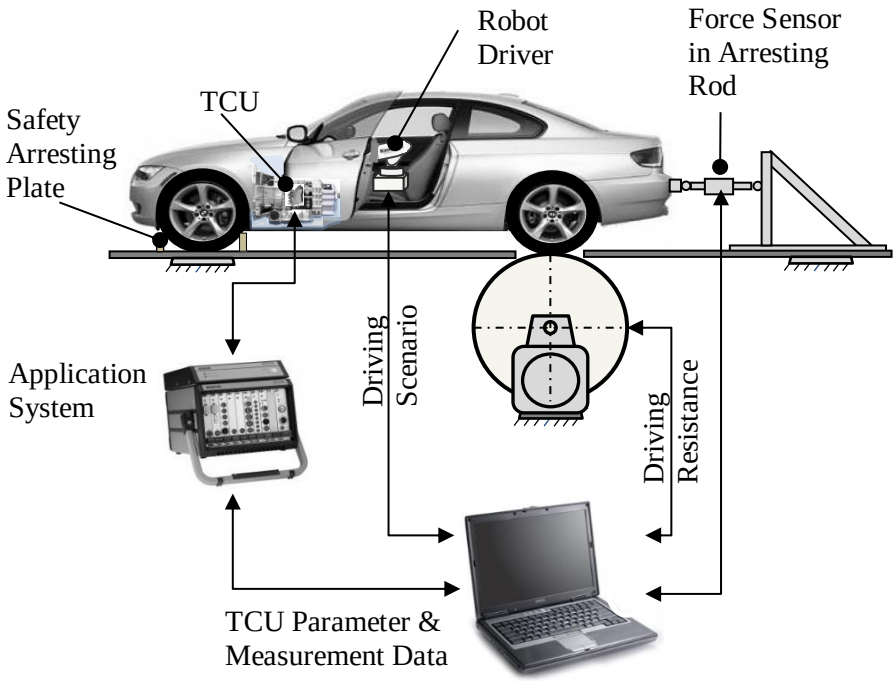

Figure 4.8: Experimental setup of the automated transmission tuning on the chassis dynamometer [10].

To guarantee an unbiased comparison between the model and the real vehicle, the same input is given to both systems (i.e. upshift command input). The data of the real vehicle performance (i.e. vehicle with 7-speed DCT transmission) is collected on the chassis dynamometer as shown in Figure 4.8.

The vehicle is held in the rest position by the rigid arresting rod that is bolted to the rear bumper bracket. The additional safety arresting plate is located in the front and rear of the front tire to catch the vehicle in case the arresting rod fails or gets broken. The load cell force sensor is attached integrally to the arresting rod to measure the vehicle's tractionsing force. The tractionsing force is interpreted as longitudinal vehicle acceleration in a certain operating point (i.e. engine speed, vehicle speed, gear position, etc.). Furthermore, the driving task (i.e. the operation of throttle pedals, etc.) is performed by a driving robot that simulates the vehicle to the certain operating points according to the specifications of the experimental design.

The adjustment of the TCU control parameters is carried out via an application system. Depending on the application, the measurement and adjustment of the TCU parameters are carried out via the CAN bus or via an ETK33. Furthermore, the detailed descriptions of the test environment and the experimental procedure for the various automated application methods can be found in [19] and [43].

5 Objective Evaluation of the Shift Quality

This chapter discusses the objective evaluation of the shift quality, including shift comfort and shift spontaneity based on the objectification process. This objective assessment is an essential requirement for the development of new DCT shifting strategies to guarantee a proper shift quality.

The shift quality, however, mainly depends on the subjective feeling of the test driver. Due to that subjective feeling, the test driver might feel a different sensation although the vehicle behaves in the same way in the manual and in the automatic gearshift. This happens because the manual shift is wanted by the driver and results in the preparation of the driver`s body and mind for the change in vehicle performance (i.e. the vehicle acceleration) during shifting. In the other case, the test driver does not know when the gear shifting will be performed by the transmission control unit (TCU) through the shift map program, so the driver is not prepared for the changes in vehicle performance. This last case, possibly also occurs to the vehicle occupant who did not know when and how the gear shift is done [45]. The different subjective score also possibly occurs in the same shifting performance, but present in the different situation. The same significant change in vehicle acceleration normally gets a good score if it happens in manual or kick down mode, but it gets a bad score if it happens when cruising. The objectification correlates the measurement of the vehicle performance (i.e. vehicle acceleration and jerk) to the driver’s subjective feeling, resulting in a quantitative quality score.

Basically, there are four criteria used to evaluate automatic gear shifting [10]:

1. the shock of gear shift that relates to the shift comfort,
2. shift spontaneity,
3. the noise inside the vehicle and
4. the frequency of gear shifting.

[37] and [74] have dealt with the evaluation of the shift quality in detail, which is mainly affected by the resulting longitudinal vehicle acceleration and its derivative (jerk) during shifting. The subjective score in general is also reduced if the shifting can be heard inside the vehicle and if it takes place often. The gear shifting frequency is strongly affected by the choice of the engine operating points and is therefore in conflict with the objective criteria of fuel economy, performance and emission characteristics while the interior noise is influenced by several aspects such as test environment, engine and transmission placement, vehicle insulation and exhaust system.

5.1 Objectification of the Shift Comfort

The objectification of the shift comfort is followed by four steps as shown in Figure 5.1. The first step is known as “definition of gear shift events” and defines specific operating points, such as up or down-shift, throttle percentage, transmission input speed and torque as well as gear ratio. The second step, “characteristic parameter calculation” is followed by “subjective evaluation” as the third step. The process is completed by “objective score calculation“ using a multiple linear regression equation through statistical methods. A complete explanation of the objectification process can be found in [10]. Furthermore, the four steps of shift quality objectification are also explained briefly in the following chapter.

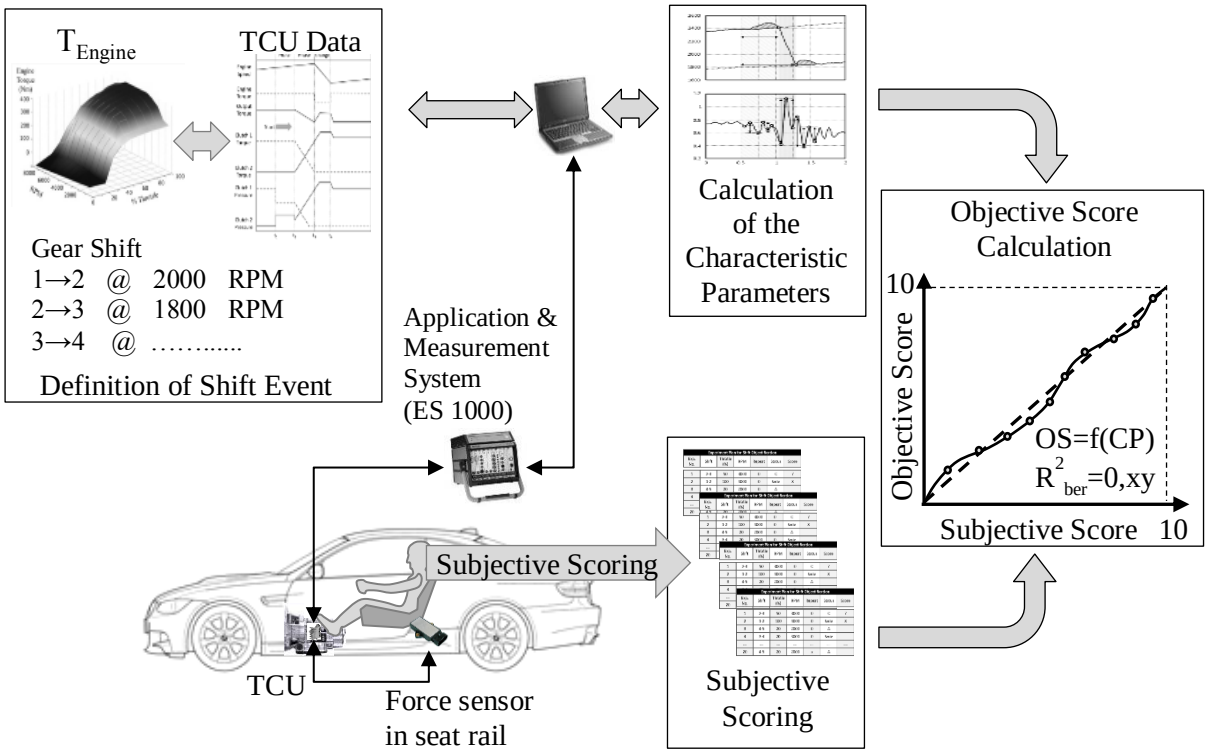

Figure 5.1: Shift comfort objectification process [10].

5.1.1 Definition of Shifting Events

The first step of shift comfort objectification is known as “definition of gear shift events”. In this step, the specific operating points, such as up or down-shift, throttle percentage, transmission input speed and torque as well as gear ratio, are defined. Those specific operating points are prepared according to the “Design of Experiment” (DoE). The DoE is proposed to obtain the large sample number of gear shift points to be investigated in order to improve the quality of the objective score calculation by using a statistical methods. The list of planned gear shift points is used to determine the expected acceleration level and to

calculate the characteristic parameters from longitudinal acceleration and transmission input speed as shown in Table 5.1.

Table 5.1: Gear shift points for the experiment [10].

Experiment Plan for Shift Objectification						
Exp. No.	**Shift**	**Throttle (%)**	**RPM**	**Repeat**	**Status**	**Score**
1.	2 – 3	50	3000	0	C	7
2.	1 – 2	100	4000	0	Series	8
3.	4 – 5	20	2000	0	A	
4.	3 – 4	20	3000	0	Series	
…..	…..	…..	…..	…..	…..	…..
20.	4 – 5	20	2000	x	A	

To be able to average the subjective score without large differences, it is important that all of the proposed operating points have similar characteristic parameters. Thus, to ensure that all tests are carried out at defined accelerator pedal position and therefore also defined transmission input torque, the vehicle is equipped with stop sleeves for the accelerator pedal. The complete procedure is available in [21] and [72].

5.1.2 Recognition and Identification of Characteristic Parameters

The recognition and identification of a characteristic gear shift parameter is a fundamental step for the shift comfort objectification process. The characteristic parameter is obtained from change in vehicle acceleration during shifting through the accelerometer installed in the driver seat rail as shown in Figure 5.1. The acceleration change frequency that can be sensed by the human is ranging from 2-9 Hz [10]. Therefore, a low pass filter is used to obtain the characteristic parameter of gear shifting in that frequency range. Furthermore, the calculation routine from [43] is used for the reliable and advanced algorithm to recognize the characteristic up-shift parameter.

Figure 5.2 (a) shows the engine speed during up-shifting for a vehicle with an automatic transmission. At 0.5 seconds, the up-shift starts as well as the characteristic parameter calculation program. t_d shows the delay time which is characterized by the drastic change in the engine speed gradient in the gear ratio change phase, while t_s shows the shift time which

is characterized by the ended of the engine speed negative gradient in the synchronization point. Furthermore, the important characteristic parameters from the engine speed diagram are the shift gradient SG and the integral area of the clutch slip speed before and after the negative shift gradient.

Figure 5.2 (b) shows the vehicle acceleration which is directly correlated with the engine speed during up-shifting. In the overlap phase, the load is taken over by the engaging clutch which reduces the acceleration significantly causing a reduction of comfort (i.e. $\Delta\ddot{x}_3$). That acceleration drop also occurs in the overlap phase denoted by the negative gradient $Grad_A$ due to the reduction in transmission output torque. The negative gradient acceleration in the overlap phase is felt by the driver (i.e. the back support from the seat to the driver's body is slightly reduced) before the acceleration gradient turns into positive in the gear ratio change phase.

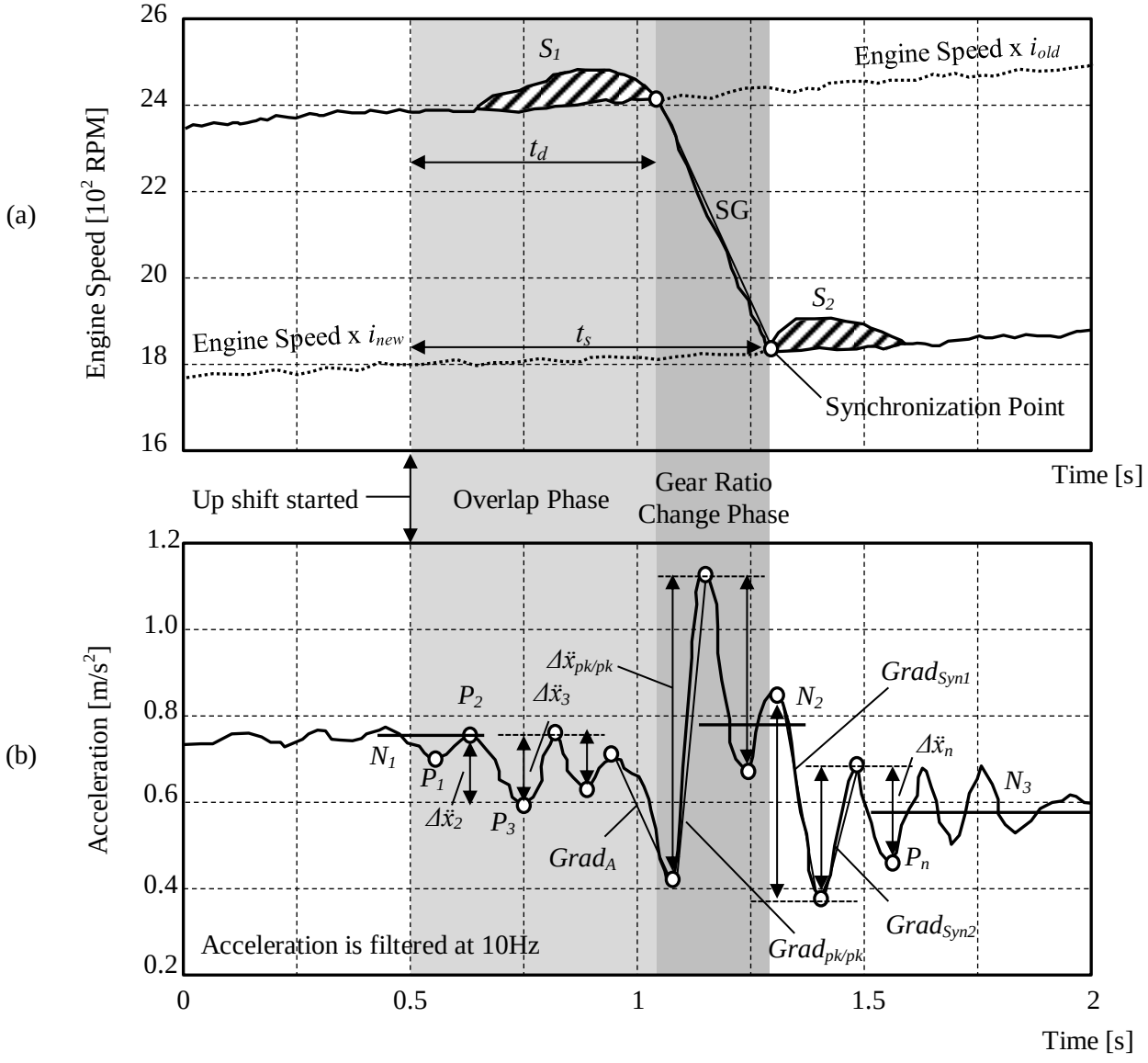

Figure 5.2: Engine speed (Fig. a) and vehicle acceleration (Fig. b) during up-shifting [10].

The highest acceleration change with positive gradient in the gear ratio change phase is denoted by the peak-to-peak value $\Delta\ddot{x}_{pk/pk}$ and these two peaks point is related -with the positive gradient line $Grad_{pk/pk}$ which is also felt by the driver by the increasing of the back support force from the seat. The acceleration fluctuation further occurs after the synchronization point and is denoted by the synchronization gradients $Grad_{Syn.1}$ and $Grad_{Syn.2}$. The acceleration levels N_1 to N_3 are used as important characteristic parameters of the acceleration diagram. Furthermore, the gear shift acceleration in the relevant frequency range of 2-9 Hz is described using the RMS value [109] with the following Equation 5.1:

$$a_w T = \sqrt{\frac{1}{T}\int_0^T a_w^2(t)dt} \tag{5.1}$$

where $a_w(t)$ is a weighted and filtered of the longitudinal vehicle acceleration and T the oscillation period.

Furthermore, to rate the vibration effect on the human body, the industry uses the vibration dose value (VDV) that is also relevant for this work. The VDV with a power of 4 is used as an approach according to [108] that reacts sensitively to the acceleration peaks. The VDV is calculated as shown in Equation 5.2:

$$VDV = \left\{\int_0^T [a_w(t)]^4\, dt\right\}^{\frac{1}{4}} \tag{5.2}$$

where $a_w(t)$ is a weighted and filtered of the longitudinal vehicle acceleration and T the measurement duration. In studies, it has been found that the standard deviation of the acceleration signal is a good parameter which correlates to the description of the gear shift comfort. There are several standard deviations recorded by varying the filtering as characteristic parameters in the analysis. The equation for the standard deviation σ of the low pass filtered acceleration signals $a(t)$ during the gear shifting is described as follows:

$$\sigma = \sqrt{\frac{1}{n}\sum_{i=0}^{n}\left(a_i(t) - \bar{a}(t)\right)^2} \tag{5.3}$$

5.1.3 Subjective Evaluation

The subjective evaluation of gear shifting is done in a short travel on the well road and environment. The road surface quality should be high to reduce the disturbance from the road to a minimum level by using good quality asphalt. To allow the test driver to fully concentrate on driving the vehicle, an additional test engineer inside the vehicle is involved in the test process to control the process, e.g. tuning the gearbox program and other important tasks.

The shifting speeds are defined by the gear stored program so that the test driver only has to press the accelerator pedal down to the stop sleeve for starting the circuit. Furthermore, the verbal descriptions for the subjective evaluation of gear shifting are related to the ATZ -rating scale according to [7] as shown in Table 5.2. ATZ is an abbreviated of "Automobiltechnische Zeitschrift" or 'automotive technical magazine' in English. ATZ is a German specialist journal for technology-oriented management in the automotive industry and provides the latest information from research and development.

Table 5.2: The ATZ scoring system for subjective evaluation [7].

ATZ Score System									
Not Acceptable				**B***	**Acceptable**				
1	2	3	4	5	6	7	8	9	10
Desscription of Gearshifting									
Permanently Slip	Strongly Slip	Distorted	Hard	Disturbing	Clearly Noticeable	Noticeable	Slightly Noticeable	Soft/Smooth	Not Noticeable
Noticed By									
All Customers	Average Customer			Serious Customer			Experienced Assessor		Experts

*: Border

5.1.4 Calculation of the Objective Score

The objective score of shift comfort is calculated using a multiple linear regression equation. The generated equation is then checked by comparing the correlation coefficients for plausibility and is, in contrast to models of higher order, most likely for an extrapolation characteristic parameters which lie outside the domain. Table 5.3 shows the six best subjective scores correlated to the characteristic parameters. As first noted in [43], the peak-

to-peak value $\Delta\ddot{x}_{pk/pk}$ and the effective longitudinal acceleration $\ddot{x}_{eff}$ value in the frequency range of 2-9 Hz of the characteristic parameters are best correlate with the subjective comfort rating. The next characteristic parameter of the correlation with a similar level (r_{xy}= 0.91) is the effective longitudinal acceleration $\ddot{x}_{eff}$ value in the frequency range of 2-12 Hz. The standard deviation of longitudinal acceleration $\ddot{x}_{\sigma}$ in the frequency range of 1-10 Hz indicates the alteration strength of the acceleration in the middle of the up-shift. The longitudinal acceleration of the VDV $\ddot{x}_{VDV}$ is generated without a weighting and has almost the same correlation. The highest acceleration difference $\Delta\ddot{x}_{max}$ correlated significantly worse than the peak-to-peak longitudinal acceleration value $\Delta\ddot{x}_{pk/pk}$ which indicate that the $\Delta\ddot{x}_{pk/pk}$ value is the most strong acceleration alteration during the up-shift.

Table 5.3: The correlation coefficient and the adjusted coefficient of determination for up-shift comfort scoring described using a simplified linear model [10].

Characteristic Parameter	**Correlation Coefficient (r_{xy})**	**Adjusted Coefficient of Determination (R^2_{adj})**
$\Delta\ddot{x}_{pk/pk}$, 12 Hz, Low pass	-0.92	0.84
$\ddot{x}_{eff}$, 2-9 Hz	-0.91	0.83
$\ddot{x}_{eff}$, 2-12 Hz	-0.91	0.83
$\ddot{x}_{VDV}$, 1-10 Hz	-0.86	0.73
$\ddot{x}_{\sigma}$, 1-10 Hz	-0.85	0.71
$\Delta\ddot{x}_{max}$, 12 Hz, Low pass	-0.83	0.67

The model for the objectification of the tractions up-shift (TUS) is as described by Equation 5.4 as follows:

$$OS_{TUS} = 10 - b_1.\ddot{x}_{eff,2-9Hz} - b_2.\ddot{x}_{\sigma,1-10Hz} - b_3.\ddot{x}_{VDV,1-10Hz} - b_4.\Delta\ddot{x}_{max,12Hz,Low\ pass} \quad (5.4)$$

where the adjusted coefficient of determination of the regression model is set to R^2_{adj}= 0.87. A further increase in the model order will provides a better explanation for the given subjective score. In addition, the complete calculation of the objective score can be found in [10].

5.2 Calculation of the Shift Spontaneity

The score for the shift spontaneity depends on the delay time (t_d), the shift duration time (t_s) and the shift gradient (SG) of the shifting process [110] as shown in the characteristic curve in Figure 5.2. Furthermore, the shift spontaneity score is determined using the evaluation functions curve as shown in Figure 5.3 with delay time (t_d) and shift duration time (t_s) as input parameters. Those curves are generated using a customized Sig-mode-function [110].

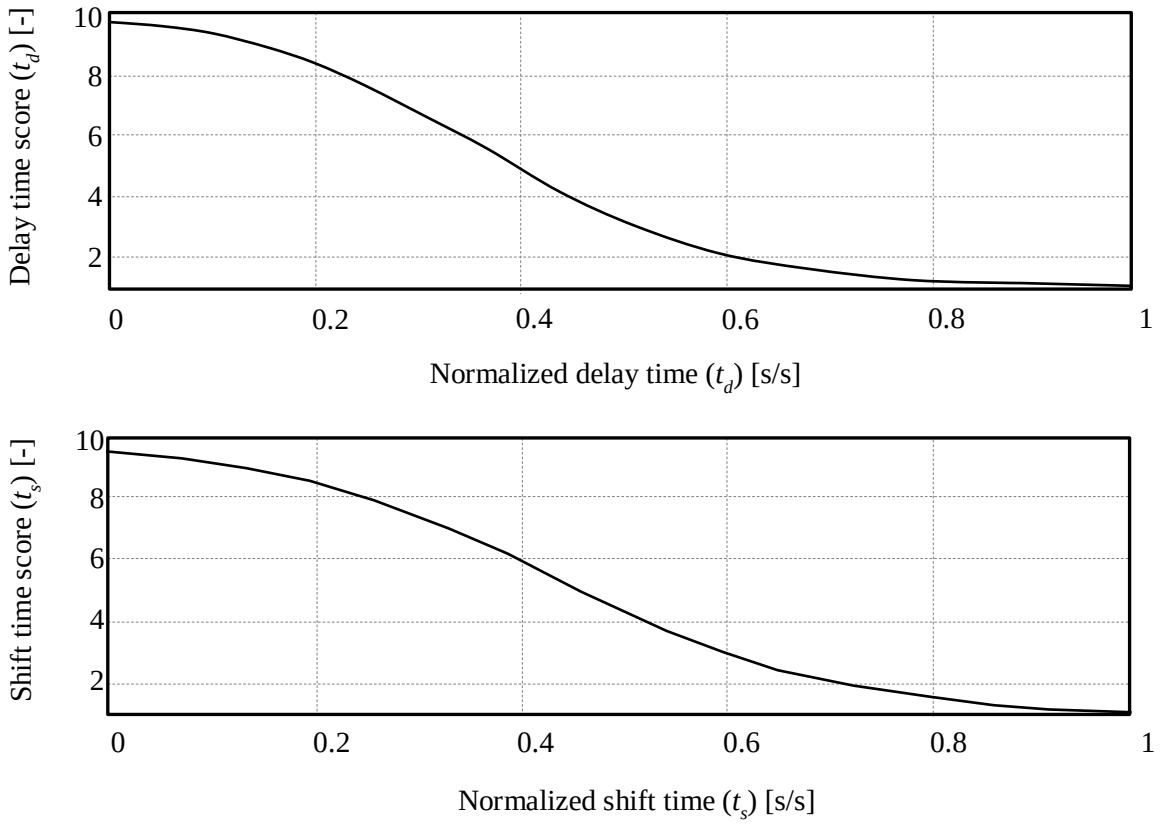

Figure 5.3: The weight function to rate the delay time (t_d) and the shift time (t_s) [10].

The score for shift spontaneity is determined by a mean value of the delay time (t_d) and the shift duration time (t_s) as shown in Figure 5.4 using the following Equation 5.5:

$$OS_{SP} = \frac{OS_{t_d} + OS_{t_s}}{2} \tag{5.5}$$

Figure 5.4 shows that a good objective score (above 5) for shift spontaneity (OS_{SP}) is achieved for $t_d > 0.5 * t_{d,normalized}$ second and $t_s > 0.6 * t_{s,normalized}$ second.

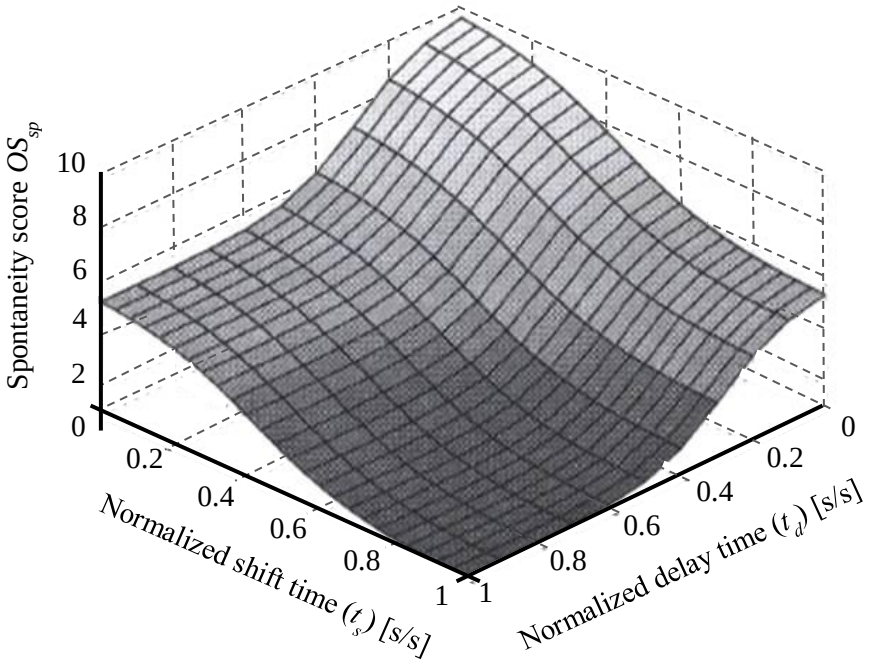

Figure 5.4: Function to rate the shift spontaneity with regard to delay time (t_d) and shift time (t_s) [10].

5.3 Weighting Function to Define the Shift Quality

To satisfy the different customers, modern vehicles with automatic transmission as well as the tested vehicle offer several types of shift programs that vary in terms of shift comfort and shift spontaneity. The studied vehicle in fact has five different shift programs, from the most convenient program (D1) to the most sporty one (D5). Those five different driving programs have different shift maps as well as shift characteristics. D1 offers a smooth shift at a relatively low engine speed to optimize the fuel consumption while, on the other hand, D5 is the sportiest program, characterized by high shift spontaneity occurring at higher engine speeds to achieve high acceleration. The shift quality in D1 could have the same score as D5 although they both have completely different shift characteristics. This is due to the fact that the objective score of shift quality is as a function of the objective scores of shift comfort and shift spontaneity. The objective score of shift quality as a function of those two objective scores is described in the following Equation 5.4 [10].

$$OS_{SQ} = f\left(OS_{Comf}, OS_{Sp}\right) \tag{5.4}$$

Furthermore, the weight function is used to define the objective score for shift quality as described in Equation 5.5 [10].

$$OS_{SQ} = \frac{w_1.OS_{Comf} + w_2.OS_{Sp}}{w_1 + w_2} \tag{5.5}$$

The weight functions ($w_1$and w_2) in Equation 5.5 have different values for several driving programs (i.e. comfort, economy, launch mode, winter, sport and manual shift) as shown in Figure 5.5.

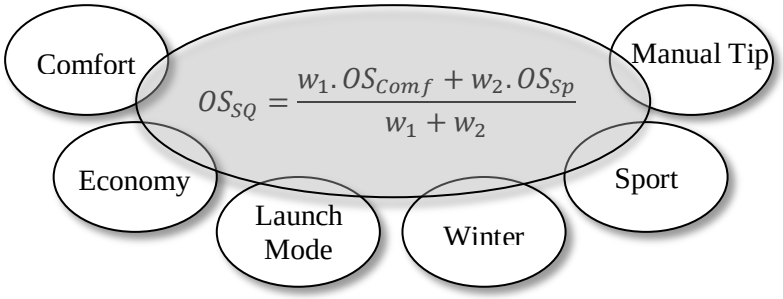

Figure 5.5: Driving programs for different purposes and shift modes [10].

The objective scores of gear shift comfort and spontaneity in Equation 5.4 use the ATZ scale as shown in Table 5.2. Furthermore, to present the shift quality score from Equation 5.5 in a more simple form, that score is now expressed by the normalized objective score as described in Equation 5.6 based on the work in [10]:

$$OS_{SQ} = \left(\frac{w_1.OS_{comf,norm}^{x} + w_2.OS_{sp,norm}^{x}}{w_1 + w_2}\right)^{1/x}, x \in R\backslash\{0\} \quad (5.6)$$

Equation 5.6 represents the objective shift quality score from Equation 5.5 in the form of an S-diagram to shows the effect of the two different weight functions ($w_1$and w_2) [10] as shown in Figure 5.6. Equation 5.6 is valid for real numbers for all value of exponent number (x) except zero. Furthermore, the difference value of the two weight functions is shown if the exponent is smaller than one (x < 1).

Figure 5.6 shows of an S-diagram of the objective score of shift quality for a constant weight ratio w_1/w_2= 0.2 and the exponent x = -2. The blue line is the optimization algorithm for the objective score (OS_{SQ}) with the red arrows indicating the optimization direction. For example, point A indicates the condition of the shift comfort score equal to nine and the shift spontaneity score equal to five. The red arrows around point A indicate to move point A to upper side to optimize the shift quality. Point B is another example of the shift comfort score equal to four and the shift spontaneity equal to six. The red arrows around point B indicate the direction for shift quality optimization. It is clear from the S-diagram that in order to reach the blue line with a value of 0.5, point B has to be moved either to the right side (optimization to achieve a better shift comfort score) or to the upper side (optimization for a better shift spontaneity score) to optimize the objective score of shift quality. However, the case is

different for point A. Here, the optimization in order to achieve better shift spontaneity score is the only possible way to improve the shift quality score.

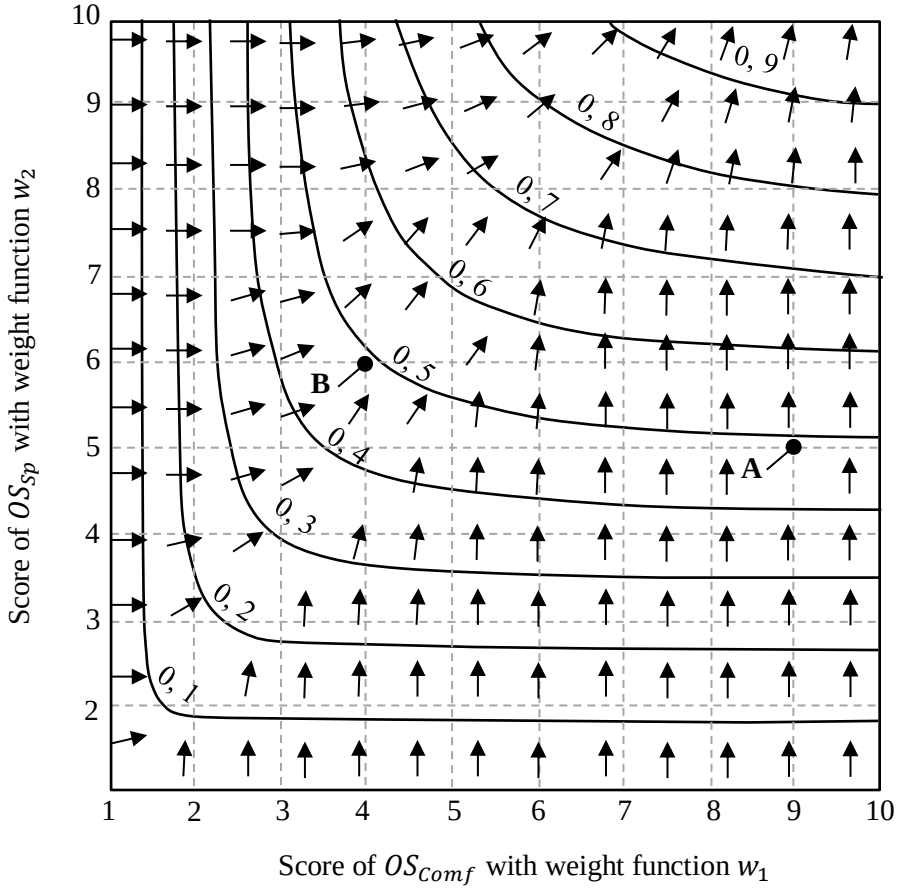

Figure 5.6: S-diagram for constant weight ratio w_1/w_2= 0.2 and exponent x = -2 [10].

6 Optimization of Wet DCT Gear Shifting through SiL Simulation

The optimization method is used to find the optimum shift quality of the longitudinal seven-speed wet DCT which employed alternative gear preselect schedule by considering the hydraulic process in the dual clutch mechatronics module and the DCT hardware design for preselecting seamless gear changes. In general, the optimization process for control parameters is completed using the genetic algorithm and the shift quality scorer program as shown in Figure 6.1. The genetic algorithm will continue to optimize the control parameter value as listed in Table 4.1 until the objective target score is met.

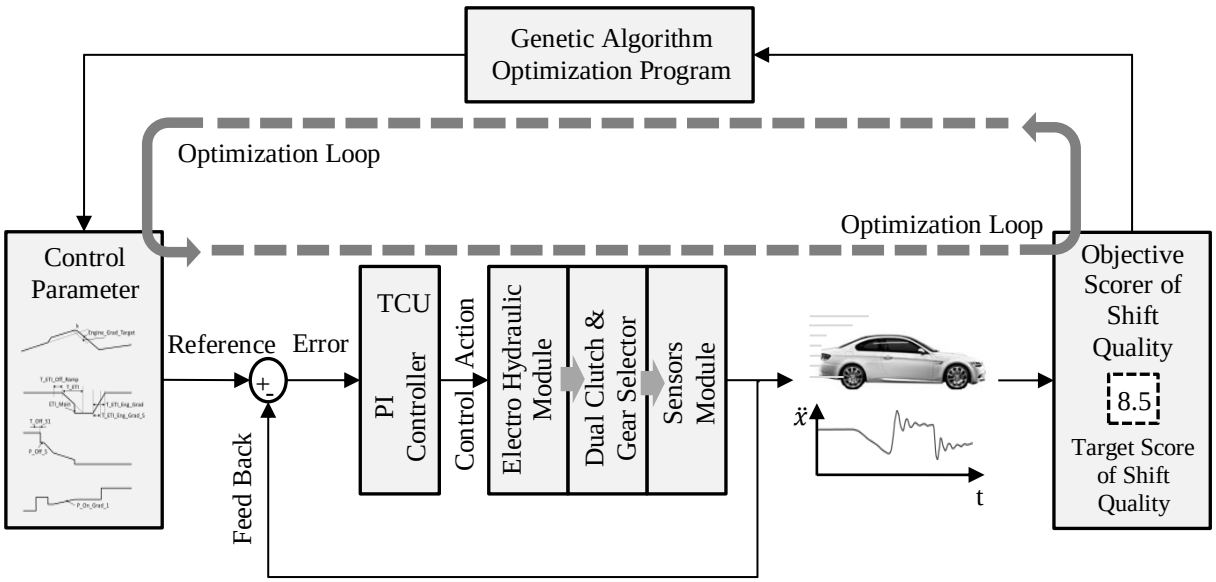

Figure 6.1: Optimization process for control parameters using genetic algorithm and shift quality scorer program.

The optimization was basically aimed to maximize or minimize the objective function to find a setting that provides the best result. On both cases usually only depends from the formulation of the problem instead of the direction of objective function. It is crucial to consider the problems definition of the optimization objectives and constraints. Therefore, the problems existing for this particular wet DCT were presented before the new gear preselection strategy was developed in order to find a solution. The optimization process in this work is based on the objective score of gear shifting and adds some constraints derived from the development of the new gear preselection strategy.

6.1 Problem Definition

With the longitudinal seven-speed wet DCT, gears can be changed either in automatic or manual mode. In the automatic mode, the shifting is done automatically by a TCU command

based on the throttle percentage and the vehicle speed as mapped in the shift map. In the manual mode, the driver shifts the gears manually by shifting the gear lever to the front to up-shift or to the rear to down-shift. Manual gear shifting also be done by pulling the shift paddles located behind the steering wheel instead of using the gear lever. With the shift paddles, the paddle on the right is used to shift up and the one on the left to shift down.

The longitudinal 7-speed wet DCT was designed to be used in sport cars[4]. In fact, a lot of sport cars currently available in the market also use the DCT for their transmissions, i.e. Audi R8, Porsche 911, Mercedes GT AMG, Bugatti Veyron, Lamborghini Huracan, Mc Laren MP4-12C, Nissan GTR and Mitsubishi Evolution [5]. Those cars are designed to meet the extreme driving condition by a sporty driver in several road settings which has a similar condition as in the car race. Based on the 3D -parameter space[5], the extreme driving condition which is used as a basis for designing a sport car is plotted as a red circle in Figure 6.2. In those nine driving conditions, the manual mode is desirable for the sporty driver due to its advantages. Only with manual gear shifting, the sporty driver has full control at any time to manage the transmitted engine torque to the wheel through the selection of available gear ratios. Thus, the reliability of shifting in manual mode is important for sports cars in the toughest driving conditions and is therefore in the focus of this work.

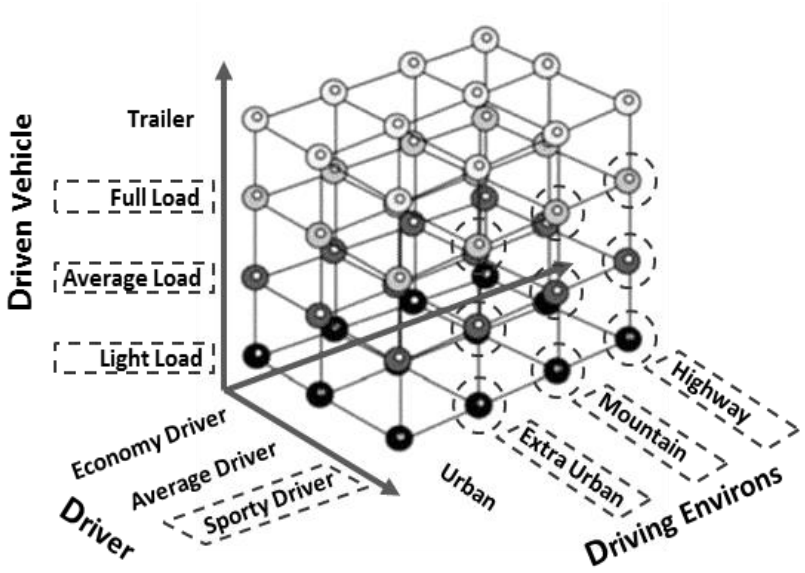

Figure 6.2: Nine extreme driving conditions for sports cars in the 3D (Driver, Driving environs and Driven vehicle) parameter space.

[4] The longitudinal 7-speed wet DCT is used in high performance cars e.g. BMW M–Series, Mercedes SLS, Ferrari California and Ferrari 458.

[5] The 3D-Parameter Space was developed at the Institute of Automotive Engineering TU-Braunschweig and is used to identify the customers requirements in order to meet their demands [75].

For most DCTs including the wet DCT used in this study, the gears are preselected automatically for both manual and automatic mode. It is done prior to shifting to guarantee that the on-going clutch is engaged with the wheel through the transmission output shaft for uninterrupted torque transfer during gear shifting. However, the problem could arise in manual shift mode when the preselected gear (preselected automatically by the TCU) does not match with the intent of the driver. If this happens, the DCT will change the preselected gear to the next one as desired by the driver, which results in delayed shift response as shown in Figure 6.3.

The other problem faced by wet DCT as explained in Chapter 3.1 is relating to the inefficiency due to the use of clutch fluid as a coolant for heat dissipation to lengthen the clutch pad life time. This clutch fluid is tending to stick the clutch pad pairs and build the drag torque when this fluid is sheared by the clutch pad pair which rotating with different speed after gear preselects action as shown in a shaded area in Figure 6.3.

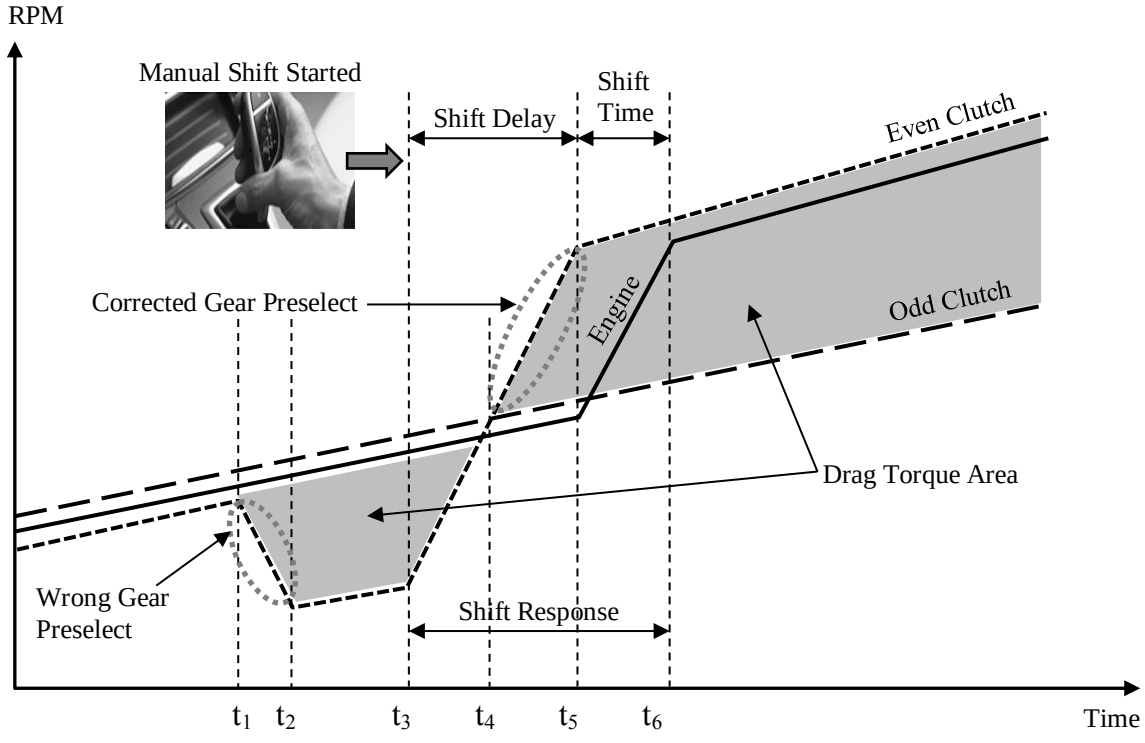

Figure 6.3: Gear preselection with no match in manual down-shift mode. In this example, the TCU prepared the next gear for up-shifting in t_1, but the driver commands a down-shift in t_3, so the TCU change the preselected gear to the next gear as desired by the driver for down-shifting. The down-shift is done in t_5 after the next gear is fully prepared.

Therefore, the problems defined for that particular longitudinal 7-speed wet DCT are:

1. The reduction of shift reliability in manual shift mode if the next preselected gear is wrong.
2. The mechanical inefficiency due to the drag torque which occurs after the gear preselection.

6.2 Objective Function

To prevent wrong gear preselection in manual shift mode, one DCT manufacturer[6] offers a manual and independent gear preselection directly done by the driver. That manual gear preselection strategy guarantees that the preselected gear matches the gear the driver desired. Rather than providing a manual gear preselection mode that provides an additional task to the driver, a new gear preselection strategy is developed in this work where the gear preselection is delayed until after the driver decided to go with gear shifting. This process will definitely lengthen the gear shift response compared to the conventional gear preselection strategy, but the new strategy will completely eliminate the frustrating situation where the preselected gear does not match the next gear desired by the driver.

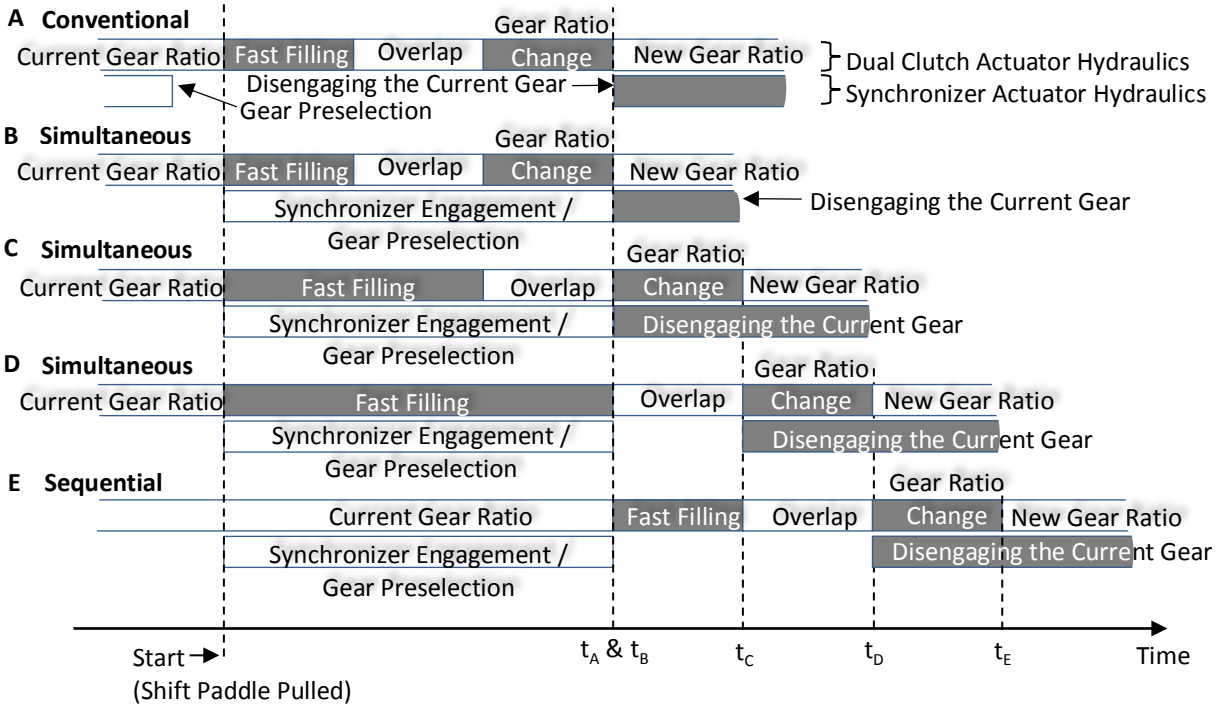

Figure 6.4: Four possibilities (B to E) for a new gear preselection strategy.

[6] The manual gear preselection is offered by Graziano, the DCT manufacturer for McLaren MP4-12 [95].

The new gear preselection strategy will also eliminate the unnecessary drag torque in an open clutch pack that occurs after the gears are preselected and the need to prepare the next gear with regard to the driving condition that makes the transmission busy (e.g. due to the vehicle acceleration, the next upper gear is prepared, but the preparation action will suddenly change the prepared gear to the lower gear if the vehicle doing deceleration and this situation always repeated while preparing the next gear).

A careful analysis of the DCT hardware design and its ability was done inline with the initiative to develop a new gear preselection strategy by changing the software control without modifying to the DCT hardware. The mechatronics module has a pressure sensor (as shown in Figure 3.11) to measure the hydraulic pressure in the dual clutch that activates the actuator piston. It also has three gear selector position sensors with a Hall Effect sensor (as shown in Figure 3.10) to confirm the synchronizer sleeve movement is in the fully locked position or fully engaged.

The parallel or simultaneous action needs an entirely separated hydraulic circuit actuator to actuate the dual clutch and the synchronizer sleeve, while the serial or sequential action still compensates the single hydraulic circuit actuator. Based on the hydraulic circuit, parallel or serial action is possible for the wet DCT.

With regard to the hydraulic circuit in the mechatronics modules as explained in Chapter 3.6, there are at least four possible strategies to activate the gear preselection as shown in Figure 6.4. All of the possibilities are started by gear preselection to guarantee that the next gear is ready. The first three possibilities (Figure 6.4, B-D) include gear preselection simultaneous or parallel to the power shift phase while in the last possibility, (Figure 6.4, E) it is done serially or sequentially.

Scenario A describes a current or conventional gear preselection where the the gears are preselected prior to the shift command and the next gear change is estimated by an algorithm in the TCU. Scenario B is achieved by preselecting the gears simultaneously after the shift command during the first three phases of clutch-to-clutch shifting (fast filling phase, overlap phase and gear ratio change phase), which results in shortest gear shift period among the new gear preselection strategies. However, scenario B has more risks and is difficult to accomplish while the synchronizer engagement process has uncertainty situation concerning to the contact condition between the tip of hub sleeve and synchronizer ring sleeve during synchronizer engagement as explained in Chapter 3.4, resulted in unexpected gear preselect time period. That uncertainty is difficult to estimate and requires full closed loop control in dual clutch power shift which is quite impossible to achieve in a short time period.

Scenario C is less difficult to compare to the previous one, but it still has a similar control complexity compared to scenario B. Scenario D has the least difficult process amongst other simultaneous strategy while basically the clutch-to-clutch power shift needing a full control process is not yet occurred in the fast filling phase. This means the fast filling phase represents a waiting phase of the dual clutch actuator for the completion of the gear preselection before the next phase. Scenario E is the most convenient and the safest strategy as this scenario is basically similar to the conventional strategy, apart from the fact that the gear is preselected after the driver pulled the shift paddle. However, strategy E results in the longest gear shift period, which is not beneficial for sporty use.

By adapting strategy D in Figure 6.4, the synchronizer is engaged immediately after the shift command is given by the driver by pulling the shift paddle. At the same time, the hydraulic actuator starts to fast fill the hydraulic piston chamber in order to push the on-going clutch. However, the hydraulic does not push the clutch until the synchronizer sleeve sensor confirms that the synchronizer is fully engaged. The waiting time will vary depending on how fast the synchronizer is engaged as explained in the synchronizer model in Chapter 4.1.3. Furthermore, the next clutch-to-clutch power shifting phase will follow after the fast fill phase finished in completing the clutch-to-clutch shifting process.

After the gear preselection, the next phase is to disengage the current gear to reset the transmission. That process only can be done after the new on-going clutch is fully engaged to prevent torque interruption during gear shifting. The process of disengaging the current gear is much simpler than gear engagement and can be performed independently in any phase of dual clutch actuator hydraulic (e.g. overlap phase and gear ratio change phase) without any uncertainties (gear engagement through synchronizer engagement). The disengagement of the current gear is faster than the gear engagement, while this disengagement process is only to slide out the engaged synchronizer hub sleeve splines from engaged splines of shaft and synchronizer ring without any frontal contact of sleeve and synchronizer splines tip.

Considering all the parameters described previously, the objective function for the optimization of DCT gear shifting with a new gear preselection strategy to create a seamless preselection aiming at minimizing a function value is defined as follows [10]:

$$min \stackrel{!}{=} 1 - OS_{SQ} = 1 - \left(\frac{w_1 . OS_{comf,norm}^{x} + w_2 . OS_{sp,norm}^{x}}{w_1 + w_2}\right)^{1/x} \tag{6.1}$$

The following constraints therefore apply:

1. Acceleration ≥ 0
2. Overlap phase is performed after the gear preselection.
3. Current gear is disengaged soon after the gear preselection.

The optimization process is performed using genetic algorithms to find the most suitable input for an optimal result in terms of shift quality. The control input parameters are described in the next section.

6.3 Optimization of Gear Shifting

The optimization of wet DCT gear shifting with the objective function as stated in Equation 6.1 is performed virtually through model simulation using several input parameters as shown in Table 4.1. The input parameters are explained in Chapter 4.3, consisting of a pressure reference line, followed by dual clutch hydraulic system pressure and engine torque reference as well as engine torque. The T_off_s_1 period value depends on how fast the synchronizer is engaged as this is a fast filling phase that has to wait for the synchronizer engagement process to be completed. The current gear is then disengaged after the gear preselection is completed. Furthermore, the model of simulation result particularly the characteristic of vehicle acceleration is calculated in simulation environment through shift quality scoring block using the objectification method as illustrated in Figure 6.1.

The method of calculating the shift quality score used in the simulation (as explained in Chapter 5.3) can be adjusted for several driving modes e.g. for sport mode (where good shifting is characterized by spontaneity rather than by comfort) or for comfort mode (where comfort is more important than spontaneity). Taking also into account the work and power losses in the dual clutch pack that are transferred into heat, the virtual optimization can furthermore be stored in the TCU database as lookup table and reference to control the DCT gear change based on the input parameters collected from vehicle sensors (e.g. vehicle speed, throttle percentage, vehicle brake, wheel slip, etc.).

The advantages of this new gear preselection strategy are prevalent in manual shift mode because it eliminates the risk that a wrong gear is preselected and the next gear preparation action. Another advantage is its suitability to be adapted in fully automatic mode without sacrificing the gear shift time duration. This is due to the gear shifting response in automatic mode is only felt by the driver and occupant on the gear ratio change phase as illustrated in Figure 6.5.

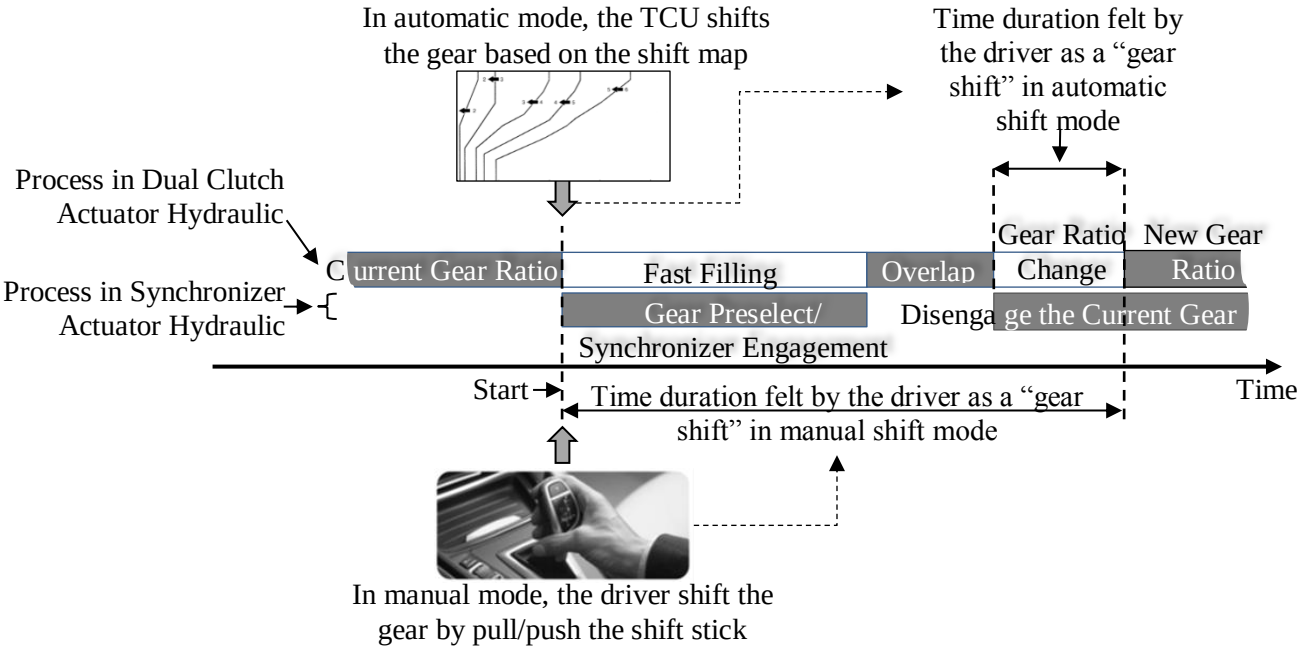

Figure 6.5: Gear change felt by the driver with the new seamless gear preselection strategy.

6.4 Result of Gear Shifting Optimization

One result of gear shifting optimization is shown in Figure 6.6. It shows the active-tractions up-shift from 1th to 2nd gear with the new gear preselection strategy (strategy D in Figure 6.4 with simultaneous gear preselection during clutch-to-clutch power shifting). The optimization process is shown in Figure 6.1, with the shift quality target score adjusted to 8.5. The target score depicts the shift comfort score and the shift spontaneity score with a weighting ratio (shift comfort to shift spontaneity) of 0.2 as shown in Figure 5.6. The weighting ratio was chosen due to the fact that the shift spontaneity is considered more important than the shift comfort in order to comply with the nine driving conditions in the 3-D parameter space as shown in Figure 6.2.

Although the simulation results of rotational speed (Figure 6.6 (b)) show that the gears are preselected sequentially (during t_2-t_3) with clutch-to-clutch power shifting (represented as a gear ratio change phase during t_5-t_6 in Figure 6.6 (b)), they are in fact preselected simultaneously during t_1-t_4 of the fast filling phase. The gear preselection starts immediately after the driver/TCU command the up-shift in t_1. At the same time in t_1, the hydraulic oil of the on-going clutch fills the clutch actuator piston chamber (fast filling process) to prepare the clutch-to-clutch power shifting.

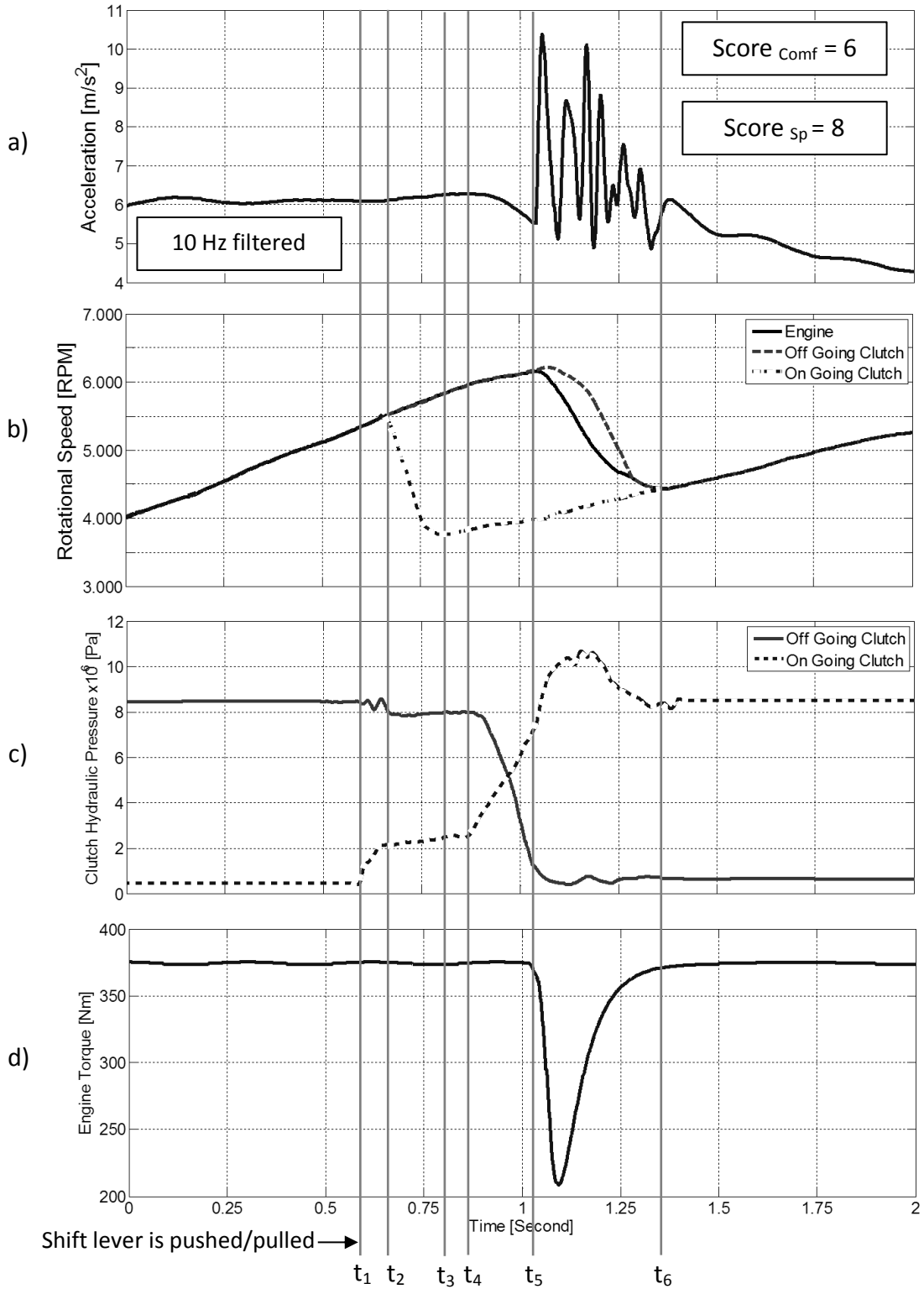

Figure 6.6: Example of a seamless gear preselection during an up-shift from 1th to 2nd gear in D5 (the sportiest) mode. a) Acceleration of the vehicle. b) The rotational speed of engine, on-going clutch and off-going clutch. c) Clutch hydraulic pressure of on-going clutch and off-going clutch and d) Engine torque. The clutch-to-clutch power shifting is done in t_4 immediately after the completion of the gear preselection.

The gear preselection is started at t_1 and the engagement in t_2. The t_1-$t_2$duration is the synchronizer engagement delay time required by the actuator to prepare the 1st phase of the engagement process as shown in Figure 4.3. The current gear is disengaged after the overlap phase in t_5 to achieve uninterrupted torque during gear shifting. Furthermore, the clutch-to-clutch power shifting follows in t_4 after the gear preselection is completed which is confirmed by the synchronizer engagement sensor in t_3.

The shift delay ($t_1 – t_5$) is around 450 milliseconds, followed by the shift time (t_5 - t_6) with around 300 milliseconds, so the shift response (t_1 - t_6) is around 750 milliseconds. The simulation confirms that the new gear preselection strategy can be used as proposed in Chapter 6.2 and to accomplish the objective of this research work as stated in the end of Chapter 1.1.

7 Summary

The DCT is the latest vehicle transmission technology introduced to the global vehicle market after MT, AT, CVT and AMT. Its current share on the vehicle transmission market is around 30% and it is predicted to increase by around 40% in 2020. Although the concept was not new, it was not until 2004 that the DCT was introduced to the global market by VW. There are two types of DCTs regard to the clutch type, the dry DCT, which uses a dry friction clutch, and the wet DCT, which uses a friction clutch that is immersed in oil. Since this type of transmission is quite new, there are still many areas for improvement.

The DCT gained popularity due to the following advantages:

1. It has a robust design and construction that is adopted from the manual transmission.
2. It allows a wide gear ratio spread for good drive ability and efficient fuel consumption.
3. It has free combinations of gear ratios due to its spur gear design.
4. It has an uninterrupted torque flow during gear shifting due to clutch-to-clutch power shifting.
5. It has a positive engine-gearbox engagement without slip due to the use of a friction clutch.
6. It offers high comfort or high spontaneity gear shifting due to the adjustable friction clutch.
7. It can be operated either manually to provide full driver control or automatically for driver comfort.
8. It can be combined with other driver assistance systems such as adaptive cruise control and electronic stability control.
9. It can be combined with a hybrid engine.

This work focused on the longitudinal seven-speed wet DCT that is used in some high performance sports cars due to its capability to handle high rev and high torque output engine. The capability is due to the use of a wet friction clutch, which is able to dissipate more heat generated by high torque engine in slipping clutch during the engagement process.

Although a wet DCT has many advantages, it still has to be improved to increase efficiency and use-ability. One of the inefficiencies arises from the use of clutch fluid as a coolant to lengthen the lifetime of the clutch pad. The clutch fluid tends to stick the clutch pairs, causing the drag torque when the fluid sheared by the clutch pair that rotates with different speed after the gear preselection.

The other disadvantage is in the manual shift mode, when the gear that is automatically preselected by the TCU before the gear shifting does not match the next gear as desired by the driver. This problem was solved by one of the DCT manufacturers by letting the driver pre select the next gear manually. However, that strategy adds a task for the driver although the manual shift mode is preferred in motor sports or by enthusiast drivers of sports car who want full control of their vehicles at any time. The aim of this thesis was to find a solution for the problem mentioned above by improving only the control algorithm and not the DCT hardware for reason of cost efficiency using the SiL method. The seamless gear preselection strategy was therefore developed to minimize the duration of gear preselection.

The thesis starts by introducing the DCT. The introduction chapter is followed by a chapter on the state of the art which focuses on DCT design, an empirical system model and on objectification and optimization methods using a simulation environment to prepare the virtual optimization of gear shifting. In chapter three, the concept of the wet DCT is explained including the double clutch and the mechatronics system. A complete vehicle drivetrain model is developed using Matlab -Simulink and –Simscape in chapter four. The model includes engine, dual clutch, synchronizer, vehicle resistance and transmission mechatronics modules. Ten control parameters were given as an input to model to control the power shift in dual clutch. Moreover, the complete simulation including shift quality is compared to measured data from the real vehicle for validation and to guarantee model fidelity.

After the model is confirmed, the optimization of wet DCT gear shifting using the genetic algorithm method is explained in chapter five. The vehicle acceleration during gear shifting as a simulation result was assessed to derive the shift spontaneity and shift comfort scores using the objectification method. In addition to the previous ten input control parameters to control the dual clutch gear shifting, the simulation model for optimization has one more input to activate the engagement of the dog clutch synchronizer as a gear preselection.

The new gear preselection strategy is particularly recommended for manual shift modes where the gears are preselected just after the driver pushes/pulls the shift lever or shift paddle. It is done simultaneously during the hydraulic fast fill phase to the dual clutch piston actuator before the TCU continue to push the oncoming engaging clutch after the synchronizer lock status available. The proposed strategy was chosen in regards to the capability of the longitudinal seven-speed wet DCT, particularly the configuration of the hydraulic valve and the gear shift actuator, and the optimization was done based on the software only, without any further modifications of the hardware. The new gear preselection strategy was calculated using the genetic algorithm method in order to meet the optimization objectives including shift quality, uninterrupted torque during gear shifting and limited heat losses. The simulation result confirms that the new strategy can be adapted to the longitudinal seven-speed wet DCT

as proposed in Chapter 6.2 and accomplish the objective of this research work as stated in the end of Chapter 1.1.

Although the new gear preselection strategy is particularly useful in manual shift mode to avoid that the gear preselected automatically by the TCU, does not match the one desired by the driver, it can also be adapted to the shifting control algorithm in automatic shift mode. This preselection strategy results in a simpler gear control algorithm since there is no independent gear preselection for both dry and wet DCTs. Thus, it increases the mechanical efficiency- particularly in wet DCTs- by eliminating of unnecessary drag torque which occurs after gear preselection.

References

[1] ABDEL-HALIM, N. A., D. C. BARTON, D. A. CROLLA, A. M. SELIM: *Performance of Multicone Synchronizers for Manual Transmissions*. Proceedings of the Institution of Mechanical Engineers, Part D: Journal of Automobile Engineering 214: 55, 2000.

[2] ADACHI, K., Y. OCHI, S. SEGAWA, A. HIGASHIMATA: *Slip Control for a Lock-up Clutch with a Robust Control Method*. SICE Annual Conference in Sapporo, August 4th, 2004, Hokkaido Institute of Technology, Japan, pp. 744-749, 2004.

[3] ADHITYA, M., R. MUSTAFA, A. PLÖTNER, F. KÜÇÜKAY: *A New Control Strategy of Wet Dual Clutch Transmission (DCT) Clutch and Synchronizer for Seamless Gear Preselect*. SAE World Congress April 16-18, 2013, Cobo Center Detroit, Michigan, USA, 2013.

[4] ADHITYA, M., R. MUSTAFA, A. PLÖTNER, F. KÜÇÜKAY: *Seamless Gear Preselect for Dual Clutch Transmission (DCT) Manual Gear Shift Mode*. JSAE Annual Congress (Spring) on May 23rd, 2013, Yokohama, Japan, 2013.

[5] AHLAWAT, R., H.K. FATHYA, B. LEE, J.L. STEIN, D. JUNG: *Modeling and Simulation of a Dual Clutch Transmission Vehicle to Analyze the Effect of Pump Selection on Fuel Economy*. Vehicle System Dynamics, 1–18, 2009.

[6] AHLAWAT, R., H. K. FATHY, C. GUO, B. LEE, J. L. STEIN, D. JUNG: *Effect of Pump Selection on Fuel Economy in a Dual Clutch Transmission Vehicle*. American Control Conference Hyatt Regency Riverfront, St. Louis, MO, USA June 10-12, 2009.

[7] AIGNER, J.: *Zuverlässige Beurteilung von Fahrzeugen*. ATZ 9/84, pp. 447-450, 1982.

[8] ALVERMANN, G.: *Entwicklung einer Schaltpunktregelung für einen Fahrroboter*. Diplomarbeit, Institut für Fahrzeugtechnik der TU Braunschweig, 2002.

[9] ALVERMANN, G., F. KÜÇÜKAY, J. SCHULZ: *Simulation und Verifikation von Überschneidungsschaltungen*. VDI-Schwingungen, Dynamik und Regelung von Automatischen Getrieben, VDI-Berichte 1917, 125-149, 2005.

[10] ALVERMANN, G.: *Virtuelle Getriebeabstimmung*. Dissertation, Institut für Fahrzeugtechnik der TU Braunschweig, 2009.

[11] ASAHARA, N., H. OTSUBO, H. KIMURA: *Development of Robust Servo System for Synchronous Shifting of a New Compact Five-Speed Automatic Transmission*. 0-7803-0582-5/92©IEEE, 1992.

[12] BARASZU, R. C., S. R. CIKANEK: *Torque Fill-In for an Automated Shift Manual Transmission in a Parallel Hybrid Electric Vehicle*. Proceedings of the American Control Conference Anchorage, AK May 8-1 0, 2002.

[13] BASTIAN, A., S. TANO, T. OYAMA, T. ARNOULD: *System Overview and Special Features of FATE: Fuzzy Logic Automatic Transmission Expert System*. 0-7803-2461-7/95/©IEEE, pp. 1063-1070, 1995.

[14] BASTIAN, A.: *Fuzzy Logic in Automatic Transmission Control*. Vehicle System Dynamics, 24 (1995), pp. 389-400 0042-3 1 14/94/2304-389S6© Swets & Zeitlinger, 1995.

[15] BAUER, H., D. FORNOFF: *Elektronische Getriebesteuerung*. Robert Bosch GmbH, Plochingen, 2004.

[16] BENCKER, N. M., B. SCHLECHT: *Gearshift-Comfort Oriented Transmission and Drive Train Simulation at BMW*. Simpack News, Vol. 9, July 2005.

[17] BARTSCH, K.:*Objektivierung der Schaltqualität für Fahrzeuge mit Automatikgetrieben*. Diplomarbeit, Institut für Fahrzeugtechnik der TU Braunschweig, 2003.

[18] BITTER. T.: *Objektivierung des dynamischen Sitzkomforts*. Dissertation, Institut für Fahrzeugtechnik der TU Braunschweig, 2006.

[19] BÖHL, J.: *Effiziente Abstimmung von Automatikgetrieben*. Dissertation, Institut für Fahrzeugtechnik der TU Braunschweig, 2007.

[20] BÖHL, J., F. KÜÇÜKAY: *Objektivierung des Schaltkomforts für ein Fahrzeug mit Doppelkupplungsgetriebe*. IfF-Bericht Nr. 69, Institut für Fahrzeugtechnik der TU Braunschweig, 2006.

[21] BÖHL, J., G. ALVERMANN et al.: *Objektivierung der Schaltqualität bei Fahrzeugen mit automatisiertem Schaltgetriebe*. IfF-Bericht Nr. 48, Institut für Fahrzeugtechnik der TU Braunschweig, 2004.

[22] BÖHL, J., G. ALVERMANN et al.: *Schaltkomfortobjektivierung bei automatisch schaltenden Getrieben*. Fachkonferenz Getriebeelektronik der IIR Deutschland GmbH, 2004.

[23] BÓKA, G., L. LOVAS, J. MÁRIALIGETI, B. TRENCSÉNI: *Engagement Capability of Face-Dog Clutches on Heavy Duty Automated Mechanical Transmissions with Transmission Brake*. Proceedings of the Institution of Mechanical Engineers, Part D: Journal of Automobile Engineering 224:1125, 2010.

[24] BRECHTER, D.: MeMo: *Eine offene Integrationsplattform zur modellbasierten Entwicklung von Fahrzeugsystemen*. Dissertation, Fakultät für Elektrotechnik, Informationstechnik und Physik der TU Braunschweig, 2008.

[25] BREITFELD, C., S. RINDERKNECHT: *The New BMW Dual Clutch Transmission*. ATZ, No. 8, pp. 38-46, 2008.

[26] CAMPBELL, R., D. BRUMM, T. TAYLOR, B. BOCK: *Modulated Scatterer Microwave Telemetry Inside Automobile Engines and Transmissions*. 0-7803-2009-3/94©IEEE, pp. 1914-1917, 1994.

[27] CHOI, S. B., J.K. HEDRICK: *Experimental Implementation of Sliding Controls on Automotive Engines*. IEEE, ACC/WPI3, 1992.

[28] DAI, Z., Y. LIU, X. XU, W. SHUHAN: *The Application of Multi-domain Physical System Simulation Method in the Study of Automatic Transmissions*. 978-0-7695-3570-8/09©IEEE, DOI 10.1109/WCSE, pp. 504-508, 2009.

[29] DECARLO, R. A., M. S. BRANICKY, S. PETTERSSON, B. LENNARTSON: *Perspectives and Results on the Stability and Stabilize Ability of Hybrid Systems*. Proceedings of the IEEE, Vol. 88, No. 7, pp. 1069-1082, July 2000.

[30] FAUST, H.: *Powertrain Systems of the Future: Engine, Transmission and Damper Systems for Down Speeding, Downsizing, and Cylinder Deactivation*. 10th Schaeffler Symposium April 3-4, 2014.

[31] FOURNIER, L.: *Learning Capabilities for Improving Automatic Transmission Control*. Intelligent Vehicles Symposium, 24-26 October 1994, 0-7803-2135-9©IEEE pp. 455-460, 1994.

[32] FURUKAWA, H., K. HAGIWARA, M. FUJITA, K. UCHIDA: *Robust Control of an Automatic Transmission System for Passenger Vehicles*. 0-7803-1 872-2/94©IEEE, pp. 397-402, 1994.

[33] GALVAGNO, E., M. VELARDOCCHIA, A. VIGLIANI: *Dynamic and Kinematic Model of a Dual Clutch Transmission*. J. Mechanism and Machine Theory 46 (2011) pp. 794-805, 2011.

[34] GAO, B., H. CHEN, H. ZHAO, K. SANADA: *A Reduced-Order Nonlinear Clutch Pressure Observer for Automatic Transmission*. 1063-6536©IEEE, 2009.

[35] GAO, B., H. CHEN, H. ZHAO, K. SANADA: *A Reduced-Order Nonlinear Clutch Pressure Observer for Automatic Transmission Using ISS*. Proceedings of the 47th IEEE Conference on Decision and Control. Cancun, Mexico, Dec. 9-11, 2008.

[36] GAO, B., H. CHEN, K. SANADA: *Clutch Slip Control of Automatic Transmission Using Back Stepping Technique*. ICROS-SICE International Joint Conference 2009. August 18-21, Fukuoka International Congress Center, Japan, 2009.

[37] GEBERT, J.: *Adaptive Parametervariation bei Getriebesteuerungen zur Optimierung des Schaltkomforts*. VDI-Fortschritt-Berichte, Reihe 12, Nr. 424, ISBN 3-18-342412-6, 2000.

[38] GOETZ M., M. C. LEVESLEY, D. A. CROLLA: *Dynamic Modeling of a Twin Clutch Transmission for Controller Design*. Proceedings of the 5th International Conference on Modern Practice in Stress and Vibration Analysis, Glasgow, Scotland, 9-11 September 2003.

[39] GOBBI, M., I. HAQUE, P.Y. PAPALAMBROS, G. MASTINU: *Optimization and Integration of Ground Vehicle Systems*. Vehicle System Dynamics, Vol. 43, pp. 437–453, No. 6–7, June–July 2005.

[40] GOVINDSWAMY, M., T. D'ANNA et al.: *Understanding, Quantifying and Optimizing Vehicle Shift Quality*. In: 1st CTI Symposium Automotive Transmission North America, 2007.

[41] GRIFFIN, M. J.: *Discomfort from Feeling Vehicle Vibration*. Vehicle System Dynamics. Vol. 45, pp. 679–698, No. 7–8, July–August 2007.

[42] GUSTAVSSON, A.: *Development and Analysis of Synchronization Process Control Algorithms in a Dual Clutch Transmission*. Examensarbete utfört i Fordonssystem vid Tekniska högskolan i Linköping, 2009.

[43] HAGERODT, A.: *Automatisierte Optimierung des Schaltkomforts von Automatikgetrieben*. Dissertation, Institut für Fahrzeugtechnik der TU Braunschweig, 2003.

[44] HAGERODT, B.: *Untersuchungen zu Lastwechselreaktionen frontgetriebener Personenkraftwagen*. Dissertation, Institut für Kraftfahrwesen der TU Aachen, 1998.

[45] HAJ-FRAJ, A., F. PFEIFFER: *Dynamic Modeling and Analysis of Automatic Transmissions*. Proceedings of the 1999 EEW ASME International Conference on Advanced Intelligent Mechatronics, September 19-23, Atlanta, USA, 1999.

[46] HAJ-FRAJ, A., F. PFEIFFER: *Optimization of Gear Shift Operations in Automatic Transmissions*. 0-7803-5976-3/00©IEEE, AMC-Nagoya, pp. 469-473, 2000.

[47] HAJ-FRAJ, A.: *Dynamik und Regelung von Automatikgetrieben*. VDI-Fortschritt Berichte, Reihe 12, Nr. 489, 2002.

[48] HAN, K., W. RYU, I. G. JANG, J. JEON, H. KIM, S. H. HWANG: *Experimental Study on the Shift Control Characteristics of CVT Using Embedded System*. SICE-ICASE International Joint Conference 2006 October 18-21, in Bexco, Busan, Korea, 2006.

[49] HARRIS, W.: *How Dual-clutch Transmissions Work*. http://auto.howstuffworks.com /dual-clutch-transmission.htm, 2006.

[50] HEBBALE, K.: *Control of the Geared Neutral Point in a Traction Drive CVT*. 0-7803-7896-2/03/©IEEE, 2003.

[51] HENZE, R.: *Beurteilung von Fahrzeugen mit Hilfe eines Fahrermodells*. Dissertation, Institut für Fahrzeugtechnik der TU Braunschweig, 2004.

[52] HOEIJMAKERS, M. J.: *The Electrical Variable Transmission in a City Bus*. 2004 35th Annual IEEE Power Electronics Specialists Conference, Aachen Germany, 0-7803-8399-0/04©IEEE, pp. 2773-2778, 2004.

[53] HOLWAY, M., S. QUINN: *Using Modern Design Tool to Integrate the Systems Engineering and Software Engineering Process*. Proceedings of the IEEE International Symposium on Computer Aided Control System Design, Kohala Coast-Island of Hawaii, Hawaii, USA August 22-27, 1999.

[54] JIADING, G., Z. ZHIGUO, Y. ZHUOPING: *Development of the Power-train Control System for Four-Wheel Driven Hybrid Electric Vehicle*. 978-0-7695-3571-5/09©IEEE, Global Congress on Intelligent Systems, 2009.

[55] JIANGWEI, Y., G. YAHUI, L. ZHIYUAN: *Development of Automatic Transmission Dynamics Simulation System*. Proceedings of the 25th Chinese Control Conference 7-11 August 2006, Harbin, Heilongjiang, 2006.

[56] JOSHI, A. S., N. P. SHAH, C. MI: *Modeling and Simulation of a Dual Clutch Hybrid Vehicle Power-train*. 978-1-4244-2601-0/09©IEEE, 2009.

[57] JUN, Y., W. XUELIN, H. Y. IN, L. CHENGGANG: *Fuzzy Control and Simulation on Automatic Transmission of Tracked Vehicle in Complicated Driving Conditions*. 1-4244-0759-1/06/©IEEE, 2006.

[58] JÜRGENSOHN, T., W. MÜLLER et Al.: *Verbesserte Methoden zur Objektivierung von subjektiven Bewertungen des Fahrverhaltens*. Forschungsbericht Nr. 96-5, TU Berlin, 1996.

[59] KALININ, V., R. LOHR, A. LEIGH, G. BOWN: *Application of Passive SAW Resonant Sensors to Contactless Measurement of the Output Engine Torque in Passenger Cars*. 1-4244-0647-1/07©IEEE, 2007.

[60] KARMEL, A. M.: *Dynamic Modeling and Analysis of the Hydraulic System of Automotive Automatic Transmissions*. IEEE, WA9 - 11:30, 1986.

[61] KATSU, F., T. MATSUMURA: *Use of HILS and an Approach to MBCSD for AT and CVT Development*. Proceedings of the 2006 IEEE pp. 2111–2114, International Conference on Control Applications, Munich, Germany, October 4-6, 2006.

[62] KIM, W., G. VACHTSEVANOSS: *Fuzzy Logic Ratio Control for a CVT Hydraulic Module*. Proceedings of the 15th lEEE International Symposium on Intelligent Control (ISIC 2000) Rio, Patras, Greece 17-19 July 2000.

[63] KIM, K., J. KIM, K. S. HUH, K. YI, D. CHOA: *Real-Time Multi-Vehicle Simulator for Longitudinal Controller Design*. Vehicle System Dynamics Vol. 44, pp. 369–386, No. 5, May 2006.

[64] KIM, D., H. PENG, S. BAI, J. M. MAGUIRE: *Control of Integrated Power-train with Electronic Throttle and Automatic Transmission*. IEEE Transactions on Control Systems Technology, Vol. 15, No. 3, May 2007.

[65] KIM, J. H., D. I. D. CHO: *An Automatic Transmission Model for Vehicle Control*. 0-7803-4269-0/97©IEEE, 1998.

[66] KIM, J. H., B. Y. JEONG, D. I. D. CHO, H. KIM: *"Autotool", A PC-Based Object-Oriented Automotive Power-train Simulation Tool*. 0-7803-4269-0/97©IEEE, 1998.

[67] KIM, J., S. PARK, C. SEOK, H. SONG, D. SUNG, C. LIM, J. KIM, H. KIM: *Simulation of the Shift Force for a Manual Transmission.* Proceedings of the Institution of Mechanical Engineers, Part D: Journal of Automobile Engineering 2003 217: 573, 2003.

[68] KIRCHNER, E.: *Leistungsübertragung in Fahrzeuggetrieben*. Springer Verlag, ISBN 978-3-540-35288-4. 2007.

[69] KOHN, W.: *Statistik, Datenanalyse und Wahrscheinlichkeitsrechnung*. Springer Verlag Berlin Heidelberg, 2005.

[70] KREIK, S.: *Entwicklung einer Simulationsumgebung für eine pneumatische Achspositionierung*. Diplomarbeit, Hochschule Hamburg, 2008.

[71] KÜÇÜKAY, F., F. RENOTH: *Intelligente Steuerung von Automatikgetrieben durch den Einsatz der Elektronik*. ATZ Automobiltechnische Zeitschrift 96 No.4 pp. 228-235, 1994.

[72] KÜÇÜKAY, F., C. Bock: *Geregelte Wandlerkupplung für den neuen 7er von BMW*. ATZ 96, pp. 690-697, 1994.

[73] KÜÇÜKAY, F.: *Fahrzeugtechnik 1* – Antrieb und Bremsung, Vorlesungsumdruck, Institut für Fahrzeugtechnik, TU Braunschweig, 2007.

[74] KÜÇÜKAY, F.: *Auslegung und Betriebsstrategien von Automatikgetrieben*. Tagung Automatische Getriebe, Technische Akademie Esslingen, 2005.

[75] KÜÇÜKAY, F., T. Kassel, M. Eghtessad, H. Kollmer: *Requirement Engineering using the 3D method*. SAE International, TU Braunschweig, 2008.

[76] KULKARNI, M., T. SHIM, Y. ZHANG: *Shift Dynamics and Control of Dual Clutch Transmissions*. Mechanism and Machine Theory 42, 168-182, 2007.

[77] LI, C., H. CHEN, Y. LI, G. ZHENG*: Automatic Transmission Test Data Acquisition System Development Based on Virtual Instrument*. 978-1-4244-3864-8/09/©IEEE, 2009, The Ninth International Conference on Electronic Measurement & Instruments ICEMI, 2009.

[78] LIAO, C., H. CHEN, H. DING: *The Research of Improving Shift Quality through the Integrated Power-train Control*. 0-7803-5296-3/99©IEEE, pp. 395-397, 1999.

[79] LINDER, A.: *Statische Methoden*. Birkhäuser Verlag Basel und Stuttgart, 1957.

[80] LING, T. Q., W. P. LIN: *Research on Fuzzy Logical Control System of the Electronic Automatic Transmission of Automobile*. 0-7803-5296-3/99©IEEE, pp. 398-400, 1999.

[81] LIU, Y., D. QIN, H. JIANG, C. LIU, Y. ZHANG, Z. LEI*: Shift Schedule Optimization for Dual Clutch Transmission*, IEEE, 978-1-4244-2601-0, 2009.

[82] LOOMAN, J.: *Zahnradgetriebe*. ISBN 978-3-540-89459-9, Springer Verlag, 2009.

[83] LOVAS, L., D PLAY, J MARIALIGETI, J F RIGAL: *Modeling Indexing Phase of Borg Wagner Gearbox Synchromesh Mechanism*. International Conference Power Transmission, 2003.

[84] LOVAS, L., D PLAY, J MARIALIGETI, J F RIGAL: *Mechanical Performance Simulation for Synchromesh Mechanism Improvements*. Proceedings of the Institution of Mechanical Engineers, Part D: Journal of Automobile Engineering 2006 220: 919, 2006.

[85] MATSUMURA, T., S. ICHIKAWA, F. KATSU, M. SATO: *The Development of a Controller Confirmation System for Automatic Transmissions and its Applications*. Proceedings of the 2004, IEEE International Conference on Control Applications, Taipei, Taiwan, September 2-4, 2004.

[86] MICHALEWICZ, M.: *Modellierung und Simulation des Schaltprozesses eines Doppelkupplungsgetriebes mit Matlab-Simulink/Simscape*. Studienarbeit, Institut für Fahrzeugtechnik der TU Braunschweig, 2010.

[87] MIN, K. J., C. W. KANG, S. G. JUNG: *Refinement of the Interior Booming Noise Caused by the Lock-up Clutch in Automatic Transmission Vehicle*. 1-4244-0427-4/06©IEEE, 2006. 18-20 Oct. 2006 IFOST pp. 89-93, 2006.

[88] MINGZHU, Z.: *Speed Change and Range Shift Control Schedule of the Multi-Range Hydro-Mechanical CVT for Farm Tractors*. Proceedings of the 2006 IEEE International Conference on Mechatronics and Automation, June 25-28, 2006, Luoyang, China pp. 1970-1974, 1-4244-0466-5/06©IEEE, 2006.

[89] MORSELLI, R., R. ZANASI, A. VISCONTI: *Generation of Acceleration Profiles for Smooth Gear Shift Operations*. IECON 02, 5-8 Nov. 2002. ISBN: 0-7803-7474-6 pp. 1681–1686, IEEE, 2002

[90] MUSTAFA, R., T. KASSEL, G. ALVERMANN, F. KÜÇÜKAY: *Modelling and Analysis of the Electrohydraulic and Driveline Control of a Dual Clutch Transmission*. FISITA 2010.

[91] MUSTAFA, R., F. KÜÇÜKAY: Model-based *Estimation of Unknown Contact Forces Acting on a Piston in Dual Clutch Transmission*. SAE Technical Paper 2012-01-0110, 2012.

[92] NAUNHEIMER, H., B. BERTSCHE, G. LECHNER: *Fahrzeuggetriebe*. ISBN 978-3-540-30625-2, Springer Verlag, 2007.

[93] NI, C., T. LU, J. ZHANG: *Gearshift Control for Dry Dual-Clutch Transmissions*. WSEAS Transactions on Systems Issue 11, Volume 8, November 2009.

[94] N.N.: *Automotive Transmission Market, By Transmission Types [Continuously Variable (CVT), Dual Clutch (DCT)], Vehicle Types (Passenger, Commercial) & Geography: Global Trends and Forecast to 2018*. Research and Markets, press@researchandmarkets.com, 2014.

[95] N.N.: *Graziano Highlights the "Pre-Cog" Dual-Clutch Transmission in the McLaren MP4-12C*. Auto Blog, May 2011.

[96] N.N.: *Systeme für Doppelkupplungsgetriebe*. http://m.schaeffler.de/content.mobile.products/de/products/automotive/transmission/dct/dct_info.html, 2013.

[97] N.N.: *Automatic Transmission History and Evolution Time Line*. http://myautomatictransmission.com/automatic-transmission-history.htm, 2013.

[98] N.N.: *Smart Actuation – The Heart of Efficient Dual Clutch Transmissions.* http://www.getrag.com/media/media/press/english/2014_1/20141110_GETRAG_PR_Smart_Actuation.pdf, 2014.

[99] N.N.: *Automotive Group Powertrain*. http://www.continental-corporation.com/www/pressportal_com_en/themes/press_releases/3_automotive_groug/powertrain/press_releases/pr_2014_01_28_10_years_dct_en.html, 2014.

[100] N.N.: *Innovations of Great Value*, ZF Friedrichshafen AG, www.zf.com, 2008.

[101] N.N.: *Automatic Driving Pleasure*, ZF Friedrichshafen AG, www.zf.com, 2008.

[102] N.N.: *The Freedom to Exceed Limits*, ZF Friedrichshafen AG, www.zf.com, 2008.

[103] N.N.: *Development of Optimized Friction Systems for Vehicle Transmission*. Hörbiger Antriebstechknik GmbH, Hörbiger Engineering Report 34.

[104] N.N.: *Genetic Algorithm*. The MathWorks, Inc, 2007.

[105] N.N.: *Getrag DCT*. The Getrag GmbH, 2010.

[106] N.N.: *Bedienungsanleitung Mitsubishi Twin Clutch-Sportronic Shift Transmission (TC-SST) Model W6DGA*.

[107] N.N.: *DCT Training*. Institute of Automotive Engineering, TU-Braunschweig, 2009.

[108] N.N.: ISO 2631-1, *Mechanical Vibration and Shock – Evaluation of Human Exposure to Whole-body Vibration* – Part 1: General requirement. International Organization of Standardization, Second edition, 1997.

[109] N.N.: *Beurteilung der Einwirkung mechanischer Schwingungen auf den Menschen – Ganzkörperschwingungen*. VDI 2057, 1999.

[110] N.N.: *Ermittlung der Spontanitätskennzahl*. ZF Getriebe GmbH Friedrichshafen, 2001.

[111] PENNATI, M., M. GOBBI, G. MASTINU: *A Dummy for the Objective Ride Comfort Evaluation of Ground Vehicles*. Vehicle System Dynamics. Vol. 47, No. 3, pp. 343–362, March 2009.

[112] PESGENS, M., B. VROEMEN, B. STOUTEN, F. VELDPAUS, M. STEINBUCH: *Control of a Hydraulically Actuated Continuously Variable Transmission*. Vehicle System Dynamics, Vol. 44, No.5, pp. 387–406, May 2006.

[113] PIERSMA, D., D. de WAARD: *Shifting from Manual to Automatic Gear when Growing Old: Good Advice? Results from a Driving Simulator Study*. Traffic Phycology Group, University of Groningen, 2014.

[114] QIN, G., A. GE, J. J. LEE: *Knowledge-Based Gear-Position Decision*. IEEE Transactions on Intelligent Transportation Systems, Vol. 5, No. 2, June 2004 pp. 121-126. 2004.

[115] QIN, G., A. GE, H. LI: *On-Board Fault Diagnosis of Automated Manual Transmission Control System*. IEEE Transactions on Control Systems Technology, Vol. 12, No. 4, pp. 564-568, July 2004.

[116] RAZZACKI, S. T., J. E. HOTTENSTEIN: *Synchronizer Design and Development for Dual Clutch Transmission (DCT)*. SAE World Congress, Detroit, Michigan, April 16-19, 2007.

[117] RINDERKNECHT, S.: *Getrag Power 7DCI600-Dual Clutch Transmission for High Efficiency and Dynamics in Inline Powertrain*. 6th International CTI Symposium-Innovative Automotive Transmissions, pp. 235-424, Berlin, 2007.

[118] RINDERKNECHT, S.: *Getrag Powershift 7DCI600*. 6th CTI Symposium, Berlin, 2007.

[119] SAKAGUCHI, S., I. SAKAI, T. HAGA: *Application of Fuzzy Logic to Shift Scheduling Method for Automatic Transmission*. 0-78034614-7/93©IEEE, 1993.

[120] SASSE, C., J. SUDAU: *Wet Starting Clutch for Automatic Transmissions with Innovative Cooling Approach*. ATZ worldwide, Vol. 111, Issue 12, pp. 24-29, December 2009.

[121] SATOH, K., M. SHINTANI, S. AKAI, K. HIRAIWA: *Development of New Synchronizer with the Lever Mechanism*. JSAE 24 (2003), pp. 93-97, 2003.

[122] SCHULZT, J.: *New Disc Spring for Dual Clutch Transmission. 8th International* CTI Symposium, ISBN 978-3-00-028976-7, Vol. 2, 2009.

[123] SELANDER, H., I. BOLIN, T. FALKMER: *Does Automatic Transmission Improve Driving Performance in Older Drivers?*. Gerontology, DOI:10.1159/000329769, August 25, 2011

[124] SETLUR, P., J. R. WAGNER, D. M. DAWSON, B. *SAMUELS: Nonlinear Control of a Continuously Variable Transmission (CVT)*. IEEE Transactions on Control Systems Technology, Vol. 11, No. 1, January 2003, pp. 101-108. 2003.

[125] SETLUR, P., J. R. WAGNER, D. M. DAWSON, B. SAMUELS: *Nonlinear Control of a Continuously Variable Transmission (CVT) for Hybrid Vehicle Power-train*. Proceedings of the American Control Conference, Arlington, VA June 25-27, 2001.

[126] SHENA, S., J. ZHANGB, X. CHENA, Q. C. ZHONGC, R. THORNTON: *ISG Hybrid Power-train: A Rule-based Driver Modeling Cooperating Look-ahead Information*. Vehicle System Dynamics, pp. 1–37, 2009.

[127] SHENGXUE, H., F. XISHENG, Z. MEI, G. LE: *Investigation of the Torque Capacity of Automatic Transmission Fluids with Various Oil Additives*. J. Synthetic Lubrication 21-2, ISSN 0265-6582, July 2004.

[128] SHIJING, W., L. QUNLI, Z. ENYONG, Z. DAWEI, X. JING: *Dynamic Modeling and Simulation on Automatic Transmission of Tracked Vehicle Using Fuzzy Control*. Proceedings of the 27th Chinese Control Conference, July 16-18, Kunming, Yunnan, China, 2008.

[129] SHIYI, Z., L. GUANGHUI: *Modeling and Simulative Analysis of Shifting Schedule for the Automatic Transmission Vehicle*. 978-1-4244-2723-9/09©IEEE, 2009.

[130] SONG, X., L. JASON, S. DANIEL: *Simulation Study of Dual Clutch Transmission for Medium Duty Truck Applications*. SAE Commercial Vehicle Engineering Congress and Exhibition, Chicago, Illinois, November 1-3, 2005.

[131] SONG, X., Z. SUN: *Pressure-Based Clutch Control for Automotive Transmissions Using a Sliding-Mode Controller*. IEEE/ASME Transactions on Mechatronics, Vol. 17, No. 3, June 2012.

[132] SUTCLIFFE, S.: *The Death of the Manual Gearbox*. http://www.autocar.co.uk/car-news/industry/death-manual-gearbox, January 2014.

[133] SOMUAH, C. B., A. F. BURKE, B. K. BOSE, R. D. KING, M. A. POCOBELLOA: *Microcomputer-Controlled Power-train for a Hybrid Vehicle*. 0278-0046/83/0500-0126©IEEE, 1983.

[134] SZCZEPANIAK, C., A. KESY: *Damping Performance of Power Transmission System with Hydraulic Torque Converter*. Vehicle System Dynamics. 20 (1991), pp. 283-295, 0042-31 14/91/2005-0283©Sweb & Zeitlinger, 2005.

[135] TAKAHASHI, H., K. KURODA: *A Study on Automated Shifting and Shift Timing Using a Driver's Mental Model*. 0-7803-3652-6/96©IEEE, 1996.

[136] TANAKA, H., H. WADA: *Fuzzy Control of Clutch Engagement for Automated Manual Transmission*. Vehicle System Dynamics, pp. 365-376, 0042-31 14/95/2404-365S6©Swets & Zeitlinger, 1995.

[137] TING, T. L.: *Development of a Neural Network Based Virtual Sensor for Automatic Transmission Slip*. Proceedings of the 2002 IEEE International Symposium on Intelligent Control, Vancouver, Canada October 27-30, 2002.

[138] VÖRSMANN, P.: *Regelungstechnik 1*. Vorlesungsumdruck, Institut für Luft- und Raumfahrtsysteme, TU Braunschweig, 2007.

[139] WALKER, P. D., N. ZHANG, R. TAMBA: *Control of Gear Shifts in Dual Clutch Transmission Powertrains*. J. Mechanical Systems and Signal Processing 25 (2011) 1923-1936, 2011.

[140] WALKER, P.D., N. ZHANG, R. TAMBA, S. FITZGERALD: *Simulations of Drag Torque Affecting Synchronizers in A Dual Clutch Transmission*. Japan J. Industrial Application Mathematic (2011) 28:119–140, 2011.

[141] WALKER, P. D., N. ZHANG: *Engagement and Control of Synchronizer Mechanisms in Dual Clutch Transmissions*. J. Mechanical Systems and Signal Processing 26 (2012) 320-332, 2012.

[142] WALKER, P. D., N. ZHANG: *Investigation of Synchronizer Engagement in Dual Clutch Transmission Equipped Powertrains*. Journal of Sound and Vibration 331 (2012) 1398-1412, 2012.

[143] WANG, Y., M. KRASKA, W. ORTMANN: *Dynamic Modeling of a Variable Force Solenoid and a Clutch for Hydraulic Control in Vehicle Transmission System*. Proceedings of the American Control Conference Arlington, VA June 25-27, 2001.

[144] WATECHAGIT, S., K. SRINIVASAN: *Implementation of On-Line Clutch Pressure Estimation for Stepped Automatic Transmissions*. 2005 American Control Conference, June 8-10, Portland, OR, USA. 2005.

[145] WATECHAGIT, S., K. SRINIVASAN: *On-Line Estimation of Operating Variables for Stepped Automatic Transmissions*. 0-7803-7729-X/03©IEEE, pp. 279-284, 2003.

[146] WATTS, R.F., R.K. NIBERT, M. TANDON: *Anti-Shudder Durability of Automatic Transmission Fluids: Mechanism of the Loss of Shudder Control*. Tribotest Journal 4-1, September 1997.

[147] WEIL, H.-G., G. PROBST, F. GRAF: *Fuzzy Expert System for Automatic Transmission Control*. CH3000-7/92/0000-0716©IEEE, 1992.

[148] WENTAO, S., C. HUIYAN: *Research on Control Strategy and Integrated Power-train System as Shifting Progress. IEEE Vehicle Power and Propulsion Conference (VPPC)*, September 3-5, 2008, Harbin, China 978-1-4244-1849-7/08©IEEE, 2008.

[149] WU, D., Y. ZHANG, Y. P. CHANG: *Dynamic Analysis and Simulation of Drive Ability and Control of a Double Transition Shifting System*. 978-1-4244-2601-0/09©IEEE, 2009.

[150] WU, S., H. LU: *Fuzzy Neural Network Control in Automatic Transmission of Construction Vehicle*. Proceedings of the 6th World Congress on Intelligent Control and Automation, June 21 – 23, 2006, Dalian, China. 2006.

[151] WU, S., E. ZHU, Q. LI, J. XIE, X. PENG: *Study on Intelligent Shift Control Strategy of Automobile Based on Genetic-fuzzy Algorithm*. The 3rd International Conference on Innovative Computing Information and Control (ICICIC'08) 978-0-7695-3161-8/08©IEEE, 2008.

[152] XIAO W., Y. PAN: *Virtual Design and Test of Manual Gear Shifting Bench*. 2011 International Conference on Electronic & Mechanical Engineering and Information Technology, IEEE, 2011.

[153] XU, N., H. CHEN, Y. HU, H. LIU: *The Integrated Control System in Automatic Transmission*. Proceedings of the 2007 IEEE International Conference on Mechatronics and Automation. August 5 - 8, 2007, Harbin, China, 2007.

[154] XU, L. X., X. L. YANFANG: *Simulation of Gearshift Algorithm for Automatic Transmission Based on MATLAB*. 978-0-7695-3570-8/09©IEEE, IEEE 10.1109/WCSE.2009.198 World Congress on Software Engineering, pp. 476-480, 2009.

[155] YANG, W., G. WU: *Research and Development of Automatic Transmission Electronic Control System*. Proceedings of the 2007 IEEE International Conference on Integration Technology, March 20 - 24, 2007, Shenzhen, China pp. 442-445, 1-4244-1092-4/07©IEEE, 2007.

[156] YOON, A., P. KHARGONEKAR: *Design of Computer Experiments for Open-loop Control and Robustness Analysis of Clutch-to-Clutch Shifts in Automatic Transmissions*. Proceedings of the American Control Conference Albuquerque, New Mexico, June 1997. 0-7a03-3~32-41971©AACC, 1997.

[157] YU, W., N. LI: *Adaptive Fuzzy Shift Strategy in Automatic Transmission of Construction Vehicles*. Proceedings of the 2006 IEEE International Conference on Mechatronics and Automation, June 25 - 28, 2006, Luoyang, China. 2006.

[158] YULONG, L., L. XINGZHONG, L. H. WEIPENG: Hydraulic *System Optimization and Dynamic Characteristic Simulation of Double Clutch Transmission*. Procedia Environmental Sciences 10 (2011) 1065 – 1070, 2011.

[159] ZANASI, R., R. MORSELLI, A. VISCONTI, M. CAVANNA: *Head-Neck Model for the Evaluation of Passenger's Comfort*. Proceedings of the 2002 IEEE/RSJ International Conference on Intelligent Robots and Systems EPFL, Lausanne, Switzerland, October 2002.

[160] ZHANG, Y., Z. ZHOU: *Hybrid Modeling and Simulation of Shifting Process Involving Multigroup Clutches*. 1-4244-0759-1/06©IEEE, 2006.

[161] ZHANG, Z. Y.: *Study on Fuzzy Automatic Transmission Strategy of vehicles*. 978-1-4244-1674-5/08 ©IEEE, CIS 2008 pp. 1359-1363, 2008.

[162] ZHANG, Z. Y.: *Study on Three Parameters Fuzzy Automatic Transmission Schedule for Vehicle by PLC and HMI*. Proceedings of the 2009 IEEE International Conference on Mechatronics and Automation, August 9 - 12, Changchun, China 978-1-4244-2693-5/09©IEEE, pp. 4050-4054, 2009.

[163] ZHONG, Z., C. XIANG, M. ZHENG: *Drive Train Modeling and Model Analysis for Real-Time Application*. 0-7803-5296-3/99©IEEE, 1999.

A. Attachment

A.1 Specifications of the Test Vehicle

Table A.1: Specifications of the BMW M3 2 doors coupe (E92)

Description	Data
Wheel Drive	Rear Wheel Drive
Length	4615 mm
Width	1817 mm
Height	1418 mm
Wheel Base	2760 mm
Wheel Track	Front: 1538 mm Rear: 1539 mm
Min. Turning Circle	11.7 m
Weight	Curb: 1655 kg Max: 2080 kg
Engine Layout	Front longitudinal V8 engine
Engine Capacity	3999cm^3; Bore: 92 mm; Stroke:75 mm
Max Power	420 hp @ 8300 rpm
Max Torque	400 Nm @ 3900 rpm
Compression Ratio	12
Fuel System	Multi point injection
Emission Standard	EURO IV
Fuel Tank Volume	63 Litres
Tyre Size	Front: 245/40 R18 Rear: 265/40 ZR18
Wheel Rim Size	Front: 8yJ x 18; Rear: 9yJ x 18
1st Gear Ratio	1 : 4.811
2nd Gear Ratio	1 : 3.075
3rd Gear Ratio	1 : 2.167
4th Gear Ratio	1 : 1.688
5th Gear Ratio	1 : 1.399
6th Gear Ratio	1 : 1.230
7th Gear Ratio	1 : 1.000
Reverse Gear Ratio	1 : 4.483
Final Gear Ratio	1 : 3.154
Gear Spread	4.811

A.2 Picture of the Longitudinal 7-Speed Wet DCT with its Mechatronics Module

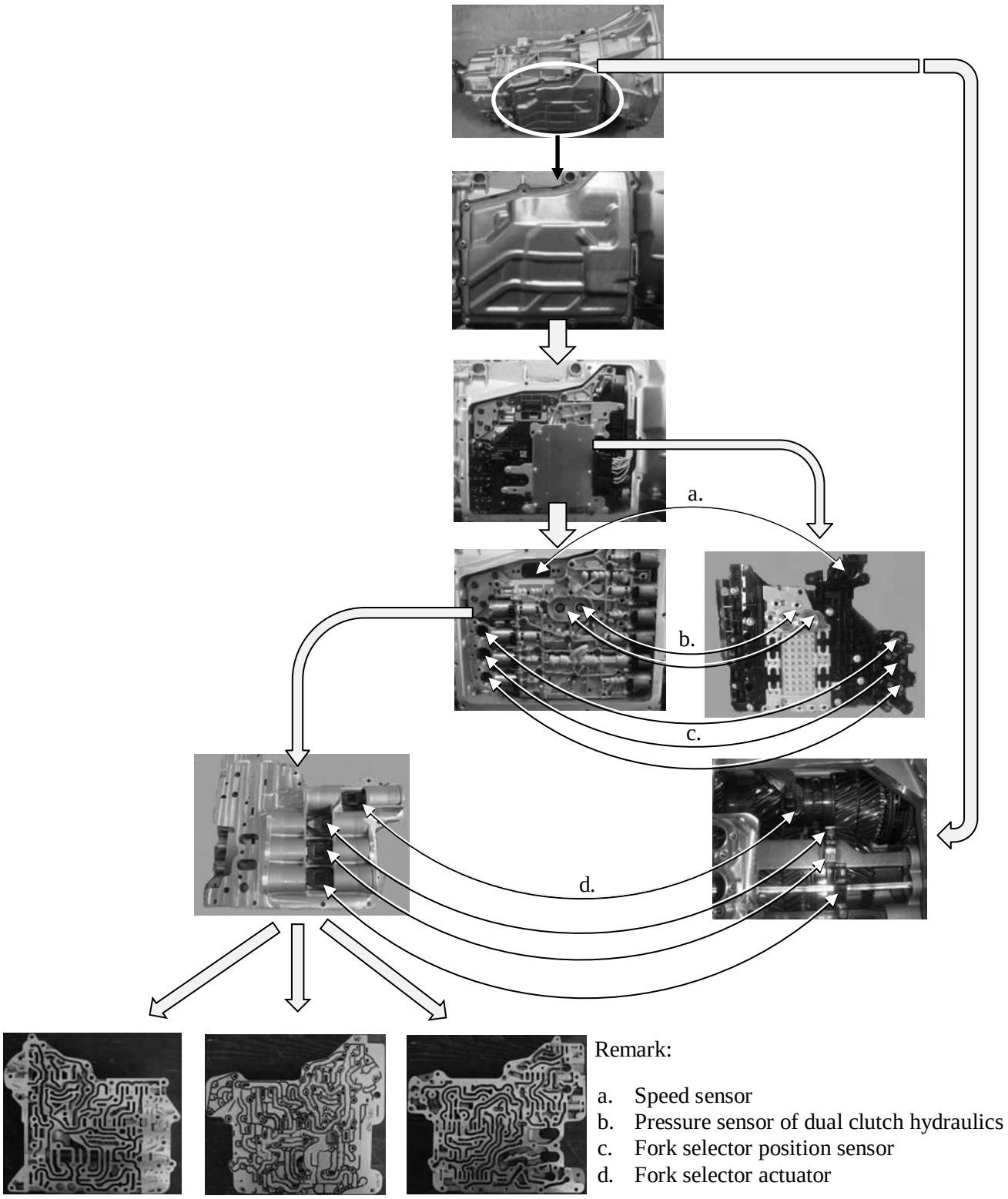

Figure A.1: Picture of the Getrag 7DCI600 with its mechatronics module.
(all pictures are taken from the right side)

A.3 Result of the Model Simulation

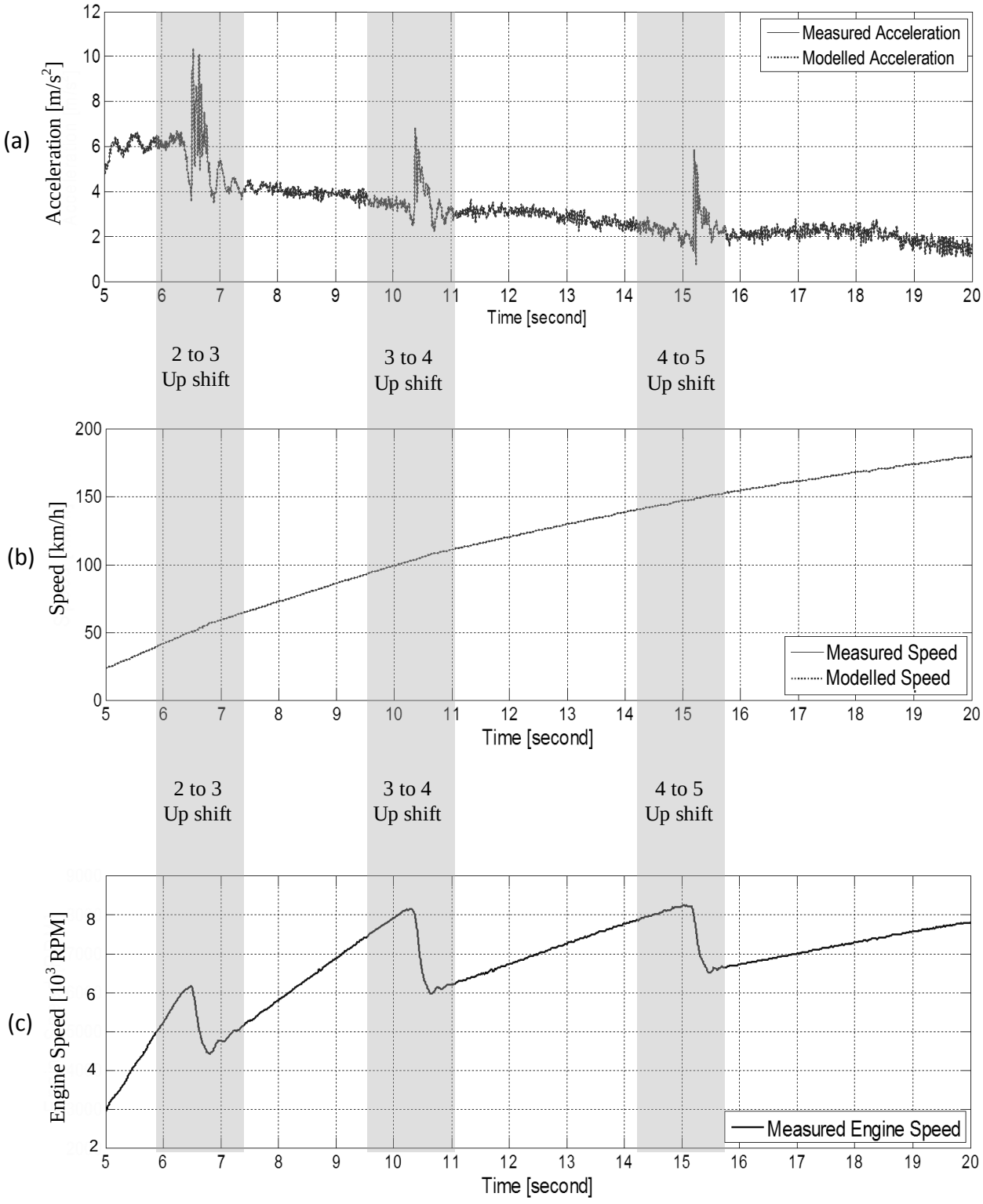

Figure A.2: Comparison between measured and modelled vehicle acceleration (a), and, vehicle speed (b), corresponding to the up shift that is shown by the engine speed in (c).

Lebenslauf

Name:	Mohammad Adhitya
Geburtsdatum:	2. März 1977
Geburtsort:	Jakarta
Staatsangehörigkeit:	Indonesien
Familienstand :	Verheiratet
Eltern:	Marsda TNI (Purn) Gaharudin Gunawan
	Enny Endang Widyanti
Ehepartner:	Nadilla Riani
Kinder:	Siti Salsabiila Maryam Adhitya
	Siti Assyifa Maryam Adhitya
	Muhammad Faza Athallah Adhitya

Schulausbildung:

1983 bis 1989	Grundschule in SDN 1 Saptorenggo, Pakis, Malang
1989 bis 1990	Mittelschule in SMPN 3 Malang
1990 bis 1992	Mittelschule in SMPN 115 Jakarta
1992 bis 1995	Oberschule in SMAN 8 Jakarta

Studium:

1995 bis 2000	Studium des Maschinenbau an der Universitas Indonesia, Abschluss: Bachelor
2001 bis 2004	Studium des Maschinenbau mit der Fachrichtung Fahrzeugtechnik an der FH-Offenburg, Abschluss: Master

Berufstätigkeit:

2004 bis 2007	Maschinenbau Dozent an der Universitas Darma Persada
seit Aug. 2007	Maschinenbau Dozent an der Universitas Indonesia